A STUDY ON THE TRANSPORT PROPERTIES OF ELECTROLYTES

SHEKH MAHIUDDIN

DEPARTMENT OF CHEMISTRY
SCHOOL OF PHYSICAL SCIENCES

SUBMITTED IN FULFILMENT OF THE REQUIREMENT OF THE DEGREE OF

DOCTOR OF PHILOSOPHY

To

THE NORTH-EASTERN HILL UNIVERSITY
SHILLONG - 793001
INDIA

JANUARY, 1983

Phone : 26593

Grams : NEHU-CHEM

NORTH EASTERN HILL UNIVERSITY
Department of Chemistry, School of Physical
Sciences, Shillong 793003 (Meghalaya) India

Dr. K. Ismail

I certify that the thesis entitled "A Study on the Transport Properties of Electrolytes ", submitted by Mr. Shekh Mahiuddin for the Degree of Doctor of Philosophy of the North-Eastern Hill University, Shillong, embodies the record of original investigation carried out by him under my supervision. He has been duly registered and the thesis presented is worthy of being considered for the award of the Ph.D. Degree. This work has not been submitted for any Degree of any other University.

PLace: Shillong;

Date : 14/1/83

Signature of the supervisor

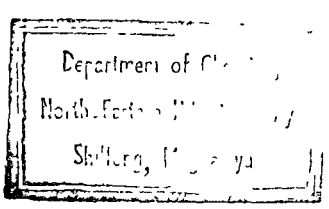

Department of Chemistry
School of Physical Sciences
North-Eastern Hill University
Mawkhrah, Shillong-793003.

phone : 6593
Grams : NEHU

This is to certify that Mr. S. Mahiuddin, JRF in the Department of Chemistry has completed satisfactorily the following four pre-Ph.D. courses:

1. CHEM - 541 Chemical Binding
2. CHEM - 544 Physical Methods in Chemistry
3. CHEM - 545 Advanced Concepts in Physical Chemistry
4. CHEM - 654 Chemistry of Molten Salts

T. S. B. Narasaraju
Professor & Head

A C K N O W L E D G E M E N T

It is a pleasure to express my deep sense of gratitude to Dr. K. Ismail for his useful advice, constant encouragement, and valuable suggestions throughout my Ph.D. programme. I am also thankful to Professor H. Junjappa and Professor T.S.B. Narasaraju, former and present Heads of the Chemistry Department, respectively for being kind enough to provide me the research facilities.

I am equally thankful to Dr. D.K. Ray, Adviser to Minerals, North-Eastern Council, Shillong and to Professor A.L. Verma, Head of the Physics Department, NEHU, Shillong for kindly allowing me to use their Micro Computers. I gratefully acknowledge the help rendered by Dr. Y.S.T. Rao, Reader, Physics Department, NEHU, Shillong and by Mr. S.S. Khatri, Pre-doctoral Fellow, Physics Department, NEHU, Shillong during the computational works.

I also acknowledge the financial assistance given to me from the University Grants Commission (New Delhi) during the course of this work. Lastly, I wish to express my thanks to Mr. Vijayan. T.R. for typing this manuscript.

(SHEKH MAHIUDDIN)

C O N T E N T S

PAGE

PAGE

APPENDICES

GENERAL INTRODUCTION

One of the major aims of physical chemistry since its earliest days has been to study the thermodynamic and transport properties of electrolyte solutions. Most of this effort for understanding the behaviour of electrolytes has been devoted to solutions containing water, solvent in general, in large excess. This is mainly because there are successful empirical, semi-empirical, and theoretical expressions for describing the properties of electrolytes in the dilute region. On the other hand, the attempt to interpret properties of electrolyte solutions at concentrations far from the very dilute region has not been very successful. The major handicap in interpreting the properties of electrolyte solutions at higher concentrations is due to the lack of a feasible analytical expression in this region to account quantitatively for the electrolyte property. Continuous efforts have been going on to overcome the above difficulty in extending the studies on electrolyte properties to concentrated solutions and the importance of this kind of study has been highlighted very recently by Pitzer.[1]

Among the equilibrium and non-equilibrium properties of electrolytes, their transport properties are relatively more difficult to deal with and have provided a most challenging field for experimental as well as theoretical research.

In the present work our main interest is to obtain an expression for describing quantitatively the behaviour of transport properties, viscosity and conductance in particular, of electrolyte solutions in the concentration region from dilute to saturation point. Before presenting the actual study made it would be worthwhile to review the existing models available for describing the viscosities and conductances of electrolyte solutions and molten salt systems.

Expressions for Viscosity of Electrolytes

The earliest equation used for describing the concentration dependence of viscosity, η is the Einstein's equation[2] originally developed for dilute suspensions based on the classical principles of hydrodynamics and is of the form

$$\eta = \eta_o (1+2.5\Theta) \qquad (0-1)$$

where η_o is the viscosity of the pure solvent and Θ is the volume fraction of one litre solution occupied by the solute. Θ can be written as $\Theta=c\Theta_s$, where Θ_s and c are the molar volume and molar concentration of the solute, respectively. Therefore, Eq(0-1) becomes

$$\eta = \eta_o (1+Bc) \qquad (0-2)$$

where $B = 2.5\ \theta_s$.

Falkenhagen and Dole[3] considered the viscosity of electrolyte solutions in terms of the interionic forces between the adjacent layers of an electrolyte solution. They proposed that the electrical forces between ions in the solution tend to establish and maintain a preferred rearrangement and thus to 'stiffen' the solution thereby causing its viscosity to increase. This resulted in a mathematical expression of the form

$$\eta = \eta_o (1+Ac^{1/2}) \qquad (O-3)$$

where A is a positive constant and depends on the solvent properties, ionic charges, ionic mobilities, and temperature. Eq (O-3) was found to be applicable only upto a very low concentration of electrolytes ($< 0.01M$) and practically this equation was of little use in calculating the viscosity.

The most widely used equation for describing the concentration dependence of viscosity in the dilute region is the empirical equation of Jones and Dole[4] which is essentially a hybrid equation of Eqs (O-2) and (O-3) and it is of the form

$$\eta = \eta_o \left[1+Ac^{1/2} + Bc\right] \qquad (O-4)$$

A and B are the same constants occurring in Eqs(O-3) and (O-2), respectively. A represents the ion-ion interaction and B supposedly represents the ion-solvent interaction. The B coefficient is found to be greater or less than zero depending on the salt and to have a characteristic value for a given electrolyte at a particular temperature. The B coefficients are also found to be fairly accurately additive properties of the constituent ions. Negative values for B are observed for ions which exert a 'structure-breaking' effect on the solution and the B values are found to be fairly large and positive for strongly hydrated ions (structure makers). The Jones-Dole equation is generally valid upto a few tenths of molar concentrations. Modified Jones-Dole equations by including higher terms of c have been tried.[5,6] However, no new interpretive information has been revealed by this approach.

Another theoretical expression employed to interpret the viscosity data in the dilute region is of Vand.[7] Vand's equation was developed by considering that the solvated solute particles distort the stream lines of flow of the solvent and it is generally written as

$$\ln(\eta/\eta_o) = k'c/(1-qc) \qquad (O-5)$$

where k' and q are constant parameters. q is proposed to be the hydrodynamic interaction parameter. Several alternative expressions[8-10] which are essentially based on Vand's equation have also been used for describing the viscous behaviour of electrolyte solutions. Vand's type equations have been found to be successful in describing the concentration dependence of viscosity at higher concentrations also. However, the theoretical concept based on which Vand's equation was derived cannot be expected to be valid at those higher concentrations due to the fact that in concentrated solutions solvated particle does not behave like a suspended particle in the solvent medium (amount of solvent is comparatively less). Consequently, the reason for the applicability of Vand's equation in the concentrated solutions must be of a different theoretical origin.

There are a few more other empirical equations[11,12] which have been employed to describe the viscous behaviour of concentrated solutions. Suryanarayana and Venkatesan[13,14] reported that an empirical equation of the type

$$\eta_p = A' \exp(B' X_p) \qquad (0\text{-}6)$$

adequately describes the variation of electrolyte viscosity throughout the high concentration range. In Eq (0-6),

A' and B' are empirical constants, η_p represents the ratio of the viscosity of the solution at a given concentration to that at saturation at the same temperature, and X_p is the ratio of the mole fraction of the solute at a given concentration to that at saturation at the same temperature.

Temperature dependence of viscosity has also been widely studied. Normally, at higher temperatures the temperature dependence of viscosity is explainable by the Andrade[15] or Arrhenius type equation

$$\eta = A'' \exp (B''/T) \qquad (0\text{-}7)$$

where A'' and B'' are constant parameters. T is the absolute temperature. Eq (0-7) was derived theoretically using the absolute rate theory approach[16] and the equation so obtained is of the form

$$\eta = (Nh/V) \exp (\Delta G^*/RT) \qquad (0\text{-}8)$$

where h is the Planck's constant, N Avogadro's number, V the molar volume of the hole in the liquid, ΔG^* the molar free energy of activation for creating this hole in the liquid, and R the gas constant.

Goldsack and Franchetto[17] by splitting V and ΔG^* terms into ionic and solvent contributions suggested another exponential relation between η and concentration which was found to explain the concentration dependence of η of alkali and ammonium halides in the range 1-10 molal. However, for electrolytes whose viscosity-temperature dependence is non-Arrhenius, which is true for all electrolytic systems at lower temperatures, the isothermal equation of Goldsack and Franchetto cannot be employed.

Expressions for Conductance of Electrolytes

The widely used expression for describing the electrical conductivity of electrolytes in the dilute region is the famous square-root law of Kohlrausch. The theoretical account of this square-root law was first given by Debye and Hückel[18] by employing basically the concept of primitive model in which aqueous solutions of simple salts were considered as a mixture of charged hard spheres in a continuous dielectric medium, the solvent water. The square-root law is written as

$$\Lambda = \Lambda_o - Sc^{1/2} \qquad (0\text{-}9)$$

where Λ is the molar conductance at concentration c moles

per litre, Λ_o the molar conductance at infinite dilution, and S is a constant which depends upon the viscosity (electrophoretic effect) and dielectric constant (relaxation effect) of the solvent. S is generally known as the limiting-law slope.

The range of validity of Eq (O-9) was extended by a considerable margin by introducing the ion-size parameter, a°, into both the electrophoretic and relaxation parts of the conductance. This extension was done by several workers[19-26] and the modified conductance equation for non-associating electrolytes is of the form

$$\Lambda = \Lambda_o - Sc^{1/2} + Ec\ln c + B_o c \qquad (O-10)$$

Similar to S, the E and B_o parameters are also dependent on viscosity and dielectric constant of the solvent. The modified conductance equation for associating electrolytes is of the form

$$\Lambda = \Lambda_o - S(\alpha c)^{1/2} + E(\alpha c)\ln(\alpha c) + B_o(\alpha c) - K_c(\alpha c)^2 f \qquad (O-11)$$

where α is the degree of dissociation, f the activity coefficient, and K_c the equilibrium constant for the association.

However, in spite of the improvement over the original square-root law of the conductance, the range of validity of Eq (0-10) or (0-11) has been found to be still confined to the dilute region.

In the concentrated region no theoretical expression is yet available to interpret the conductance data. The only semi-empirical expression which has made some success in describing the conductance data of concentrated electrolytic solutions is of Wishaw and Stokes[27]. This equation is of the form

$$\Lambda = (\eta_o/\eta)\left[(\Lambda_o - \alpha' c^{1/2})\,(1-\beta' c^{1/2})\right] \qquad (0\text{-}12)$$

where the parameters α' and β' depend upon the viscosity and dielectric constant of the solvent as well as on the temperature and concentration of the solution. Although, theoretical explanation to the success of Wishaw-Stokes equation is not available, a qualitative explanation has been proposed according to which the multiplication of the theoretical term inside the square-bracket of Eq (0-12) by the reciprocal of the relative solution viscosity might be accounting for the ion-solvent interaction which contributes significantly to the conductance of the electrolytic solution at higher concentrations.

Models for Transport Properties of Molten Salts

Normally, the temperature dependence of viscosity and conductance of fused salts at higher temperatures is found to be Arrhenius and is explainable by Eq (0-8) based on the transition state theory. When the temperature of viscosity or conductance measurement is lowered, it has been observed in the case of melts or liquids (this is true for electrolytes also) that there is always a change-over from Arrhenius type temperature dependence of transport property to a non-Arrhenius type dependence. Several theoretical models[28-32] have been advanced to account for the non-Arrhenius temperature dependence of transport property. Among the various expressions the Vogel-Tammann-Fulcher (VTF) equation[33] has been extensively employed for describing the non-Arrhenius behaviour of transport properties. The VTF equation is of the form

$$Y(\Lambda, \phi) = A_1 \exp\left[-B_1/(T-T_o)\right] \qquad (0\text{-}13)$$

where Y refers to either conductance, Λ or fludity ($\phi = 1/\eta$). A_1, B_1, and T_o are the three constant parameters. T_o is a significant parameter known as ideal glass transition

temperature. The VTF equation has been theoretically derived from the Cohen-Turnbull free volume model[28] as well as from the Adam-Gibbs configurational entropy model.[29]

As we have based our study on the Adam-Gibbs model (AGM), it would be worthwhile to review this theory here. Adam and Gibbs viewed that at low temperatures the transport property of a liquid is determined by the probabilities of cooperative rearrangements. In order to evaluate these transition probabilities, Adam and Gibbs defined a cooperatively rearranging region as a sub-system of the sample which, upon a sufficient fluctuation in energy, can rearrange into another configuration independently of its environment. Considering the probability of a cooperative rearrangement in a fixed subsystem as a function of its size, the expression for the average transition probability, $\bar{\omega}(T)$, was obtained as

$$\bar{\omega}(T) = \bar{A} \exp \left[-\Delta\mu s_c^* / kT\, S_c \right] \qquad (0\text{-}14)$$

where $\bar{A}$ is a frequency factor, $\Delta\mu$ the free energy barrier per mole of particles hindering the cooperative rearrangement, s_c^* the critical configurational entropy which a

region of the liquid must possess in order to undergo co-operative rearrangement, k the Boltzmann constant, and S_c the configurational entropy per mole of the liquid.

For obtaining the VTF equation from Eq(O-14), one equates T_o to the temperature at which the configurational entropy, S_c vanishes. S_c may then be evaluated as

$$S_c = \int_{T_o}^{T} \Delta C_p \, d\ln T \qquad (O-15)$$

where ΔC_p is the difference between the liquid and glass heat capacities. On assuming ΔC_p as constant, Eq(O-15) takes the form

$$S_c = \Delta C_p \ln(T/T_o) \qquad (O-16)$$

In the light of this result and realizing that the transport property, Y (Λ,ϕ), is proportional to $\bar{\omega}(T)$, Eq(O-14) becomes

$$Y(\Lambda,\phi) = A^* \exp\left[-B^*/T \ln(T/T_o)\right] \qquad (O-17)$$

where A^* and B^* ($=s_c^* \Delta\mu/k \Delta C_p$) are constant parameters. For temperatures T not too far above T_o, it may be shown that

$$T \ln(T/T_o) \approx T - T_o \qquad (O-18)$$

which on substitution into Eq (O-17) gives the VTF equation.

Temperature Dependence of Heat Capacity

As mentioned above Eq (O-17) has been derived from the Adam-Gibbs model[29] with the assumption that the configurational heat capacity, ΔC_p is independent of temperature. Strictly speaking, the heat capacity of a crystal, glass or liquid is always found to show an intricate dependence on temperature. Accounting for the temperature dependence of ΔC_p in Eq (O-14) is essential for obtaining an improved Adam-Gibbs equation for the transport property of liquids or glasses. Therefore, it would be relevant to review here the nature of the dependence shown by heat capacity on temperature.

The thermodynamic relation between the two heat capacity terms, C_p(at constant pressure) and C_v (at constant volume), is given as

$$C_p = C_v + (\alpha_o^2 / \kappa)\, TV \qquad (O\text{-}19)$$

where α_o is the coefficient of volume expansion and κ the compressibility. Einstein[34] calculated C_v for crystals by considering a crystal as an ensemble of independent and

distinguishable harmonic oscillators. A more successful theory of heat capacities of solids was formulated by Debye.[34] In this model also a crystal is pictured as a collection of harmonic oscillators, but the oscillations are considered to be due to the vibrations of the entire crystal and not due to the single atoms; a crystal is considered to be a 'huge molecule'. According to Debye's model C_v of crystals at low temperatures is proportional to the third power of temperature. At very high temperatures the value of C_v approaches 3R. At intermediate temperatures it is, however, difficult to precisely represent the temperature dependence of C_v by a simpler mathematical form. The contribution to crystal heat capacity due to electronic degree of freedom has also been calculated ($\approx 3RT/E_F$, where E_F is the Fermi energy) and it shows a linear dependence on temperature. This contribution becomes significant only at temperatures very near to 0°K.

In the case of amorphous materials theoretical description of the temperature dependence of heat capacity is more complicated. Even at low temperatures a departure from the Debye T-cube law was observed in these materials. A distinct feature of many amorphous substances is the 'super-Debye' excess heat capacity at low temperatures.

Recently, DiMarzio and Dowell[35] by taking into account the configurational (Gibbs-DiMarzio[36] configurational entropy model) as well as the vibrational (Einstein[34] model) degrees of freedom could predict the specific heat discontinuity at the glass transition to within 20%.

In liquids also since the exact evaluation of partition functions is hardly possible, a precise theoretical calculation of their heat capacities as a function of temperature is an extremely difficult task.

The Glass Transition Phenomenon

In describing the transport behaviours of melts, liquids, and electrolytic solutions since glass transition temperature has been considered as a more significant and important parameter, it would be worthwhile to give here a brief account of the glass transition phenomenon.

In the conventional sense the temperature range of the liquid state is usually considered to be from the normal boiling point (upper limit) to the equilibrium freezing point (lower limit). It is, however, possible to extend this normal temperature range of the liquid state by bypassing both the upper and lower limits. The upper limit may be extended by performing measurements at pressures higher

than the atmospheric pressure. In such cases the upper boundary for the liquid state is more appropriately taken as the critical temperature, T_c. The lower limit may like wise be bypassed by supercooling a liquid as liquids have a tendency to remain in a state of internal equilibrium even below their normal freezing points. In nature some of the liquids have inherent tendency to supercool whereas in rest of the liquids supercooling may be induced. The inherent tendency of some of the liquids to supercool is, in fact, due to their failure to crystallize at or below the equilibrium freezing point which may be understood interms of the model developed by Turnbull and Cohen[37] based on the kinetic considerations of crystallization. According to this model noticeable crystallization will not occur in the absence of foreign nucleating agents if $\gamma\beta^{1/3} \gtrsim 0.9$ and $\Delta G' \gg 0$, or if $\Delta G'$ or $\Delta G'' \gg 30(\Delta H_f/\beta) = 30\ RT_m$, where γ is the ratio of the molar liquid-solid interfacial tension to the heat of fusion (ΔH_f), β the ratio of the entropy of fusion to the gas constant, $\Delta G'$ the kinetic free energy barrier to nucleation, $\Delta G''$ the kinetic free energy barrier to the growth of the finite crystal, and T_m the equilibrium freezing point. In those liquids which do not have an inherent tendency to supercool, crystallization may be averted by the sudden quenching of the system during which process there may not be sufficient time for the crystal nuclei to form.

The extent to which a liquid may be supercooled and kept in the supercooled state for a long enough time to perform measurements on it varies considerably from system to system. If the properties of a supercooled liquid are measured at increasingly low temperatures without the onset of crystallization, a point is eventually reached at which equilibrium properties can no longer be determined for the liquid due to the intervention of a nonequilibrium process, the glass transition. The transition of supercooled liquid into glass is characterized by a more or less sudden decrease in the intensive thermodynamic properties like heat capacity, expansion coefficient, and compressibility from liquid-like values to values very close to, but generally greater than, those of the crystalline phase of the substance. In this sense the glass transition, although it is a non-equilibrium phenomenon, possesses many of the characteristics of a second order thermodynamic transition in that the transition occurs at constant volume and entropy and is marked by discontinuities in the second derivatives of the Gibbs free energy. In the temperature region where these changes occur, the viscosity increases rapidly, but not discontinuously, to values in the vicinity of 10^{13} P. It must be emphasized that changes in termodynamic properties do not occur merely because the viscosity becomes high, rather the changes must

occur in order to avert the occurrence of a thermodynamic catastrophe as pointed out by Kauzmann,[38] viz., the production of an amorphous phase of lower entropy than the crystalline phase of the same substance at the same temperature. It may be pointed out that the experimental glass transition temperature, T_g is generally $\sim$ 10-20°K higher than the ideal (reversible) glass transition temperature, T_o.

In the present work we have measured the viscosities and conductances of six aqueous electrolytic solutions as functions of temperature and concentration with a view to developing, as mentioned above, an expression for describing quantitatively the transport behaviour of electrolytic solutions and to examining the applicability of such an expression. This work has been presented in Part I of the thesis in the form of three chapters, viz., Chapters I, II, and III. In Part II of the thesis which contains two more chapters, viz., Chapters IV and V, we have extended our study to molten salt systems also.

References

1. K.S. Pitzer, J. Amer. Chem. Soc., 102, 2902 (1980).
2. A. Einstein, Ann. Physik., 19, 289 (1906); 34, 591 (1911).
3. H. Falkenhagen and M. Dole, Physik. Z., 30, 611 (1929).
4. G. Jones and M. Dole, J. Amer. Chem. Soc., 51, 2950 (1929).
5. J.E. Desnoyers and G. Perron, J. Solution Chem., 1, 199 (1972).
6. S.P. Moulik and A.K. Rakshit, J. Indian Chem. Soc., 12, 450 (1975).
7. V. Vand, J. Phys. Colloid Chem., 52, 277; 300; 314 (1948).
8. E. Mooney, J. Colloid Chem., 6, 163 (1951).
9. J. Padova, J. Chem. Phys., 38, 2635 (1963).
10. D.G. Thomas, J. Colloid Sci., 20, 267 (1965).
11. S.P. Moulik, J. Phys. Chem., 72, 4689 (1968).
12. E.C. Bingham, J. Phys. Chem., 45, 885 (1941).
13. C.V. Suryanarayana and V.K. Venkatesan, Nature, 178, 1461 (1956).
14. C.V. Suryanarayana and V.K. Venkatesan, Acta Chim. Acad. Sci. Hung., 16, 149; 338 (1958).
15. E.N. Andrade, Nature, 125, 309 (1930).

16. S. Glasstone, K. Laidler, and E. Eyring, 'The Theory of Rate Processes', McGraw-Hill, New York, 1941.

17. D.E. Goldsack and R. Franchetto, Can. J. Chem., 55, 1062 (1977).

18. P. Debye and E. Hückel, Physik. Z., 24, 305 (1923).

19. L. Onsager and R.M. Fuoss, J. Phys. Chem., 36, 2689 (1932).

20. S. Kaneko, J. Chem. Soc. Japan, 56, 793, 1320 (1935); 58, 985 (1937).

21. S. Kaneko, J. Electrochem. Soc. Japan, 18, 329 (1950).

22. H. Falkenhagen and G. Kelbg, Z. Elektrochem., 56, 834 (1952); 57, 609 (1953); 58, 653 (1954).

23. E. Pitts, Proc. Roy. Soc. London, A217, 43 (1953).

24. R.M. Fuoss and L. Onsager, Proc. Nat. Acad. Sci. USA., 41, 274 (1955).

25. R.M. Fuoss and L. Onsager, J. Phys. Chem., 61, 668 (1957); 66, 1722 (1962); 67, 621 (1963); 67, 628 (1963); 68, 1 (1964).

26. R.M. Fuoss, L. Onsager, and J.F. Skinner, J. Phys. Chem., 69, 2581 (1965).

27. B.F. Wishaw and R.H. Stokes, J. Amer. Chem. Soc., 76, 2065 (1954).

28. M.H. Cohen and D. Turnbull, J. Chem. Phys., 31, 1164 (1959).

29. G. Adam and J.H. Gibbs, J. Chem. Phys., 43, 139 (1965).

30. P.B. Macedo and T.A. Litovitz, J. Chem. Phys., 42, 245 (1965).

31. H. Eyring and M.S. Jhon, 'Significant Liquid Structure', John Wiley, New York, 1969.

32. J.H. Simmons and P.B. Macedo, J. Chem. Phys., 54, 1325 (1971).

33. (a) H. Vogel, Physik. Z., 22, 645 (1921);
(b) V.G. Tammann and W. Hesse, Z. Anorg. Allg. Chem., 156, 245 (1926);
(c) G.S. Fulcher, J. Amer. Ceram. Soc. 8, 339 (1925).

34. T.L. Hill, 'An Introduction to Statistical Thermodynamics', Addison-Wesley, Reading, Massachusetts, 1960.

35. E.A. DiMarzio and F. Dowell, J. Appl. Phys., 50, 6061 (1979).

36. J.H. Gibbs and E.A. DiMarzio, J. Chem. Phys., 28, 273 (1958).

37. D. Turnbull and M.H. Cohen, J. Chem. Phys., 29, 1049 (1958).

38. W. Kauzmann, Chem. Rev., 43, 219 (1948).

EXPERIMENTAL TECHNIQUES

Sample Preparation

E. Merck reagent grade calcium nitrate tetrahydrate and sodium thiosulfate pentahydrate, BDH analytical reagent grade magnesium nitrate hexahydrate and magnesium chloride hexahydrate, SD analytical reagent grade nickel chloride hexahydrate, and recrystallized (twice from double distilled water) sodium nitrate (BDH reagent grade) were used (each from single bottle) in preparing the solutions. The water used in preparing the solutions was double distilled from alkaline potassium permanganate in a quartz distilling unit. The specific conductance of this water was found to be less than 10^{-6} mho cm^{-1}. The exact concentrations of the solutions were volumetrically determined by the EDTA titration method. Erichrome Black T was used as an indicator in the cases of $Ca(NO_3)_2$-H_2O, $Mg(NO_3)_2$-H_2O, and $MgCl_2$-H_2O systems, whereas Murexide indicator was used in estimating Ni^{2+} in $NiCl_2$-H_2O systems. The exact concentrations of sodium thiosulfate solutions were determined by titrating against standard potassium dichromate solution. In the case of sodium nitrate solutions exact concentrations were calculated directly by weighing. All the titrations were carried out at 25°C.

Temperature Control

All the measurements were made in a thermostated water bath (Ultra-Thermostat Type NBE). The thermostat consists of an electronic relay (10 amps, 220 volts), an immersion heater of variable heating capacity (270, 400, 800, and 1200 watts), a circulating pressure pump cum stirrer, and a contact thermometer (0.03 amp, 250 volts). The bath temperature was measured with a calibrated check thermometer. The temperature of the thermostat remained stable to $\pm$ 0.02° during the course of density, viscosity, and conductance measurements.

Density Measurement

Density measurements of all the solutions were made in a glass dilatometer of $\sim$ 7.0 ml capacity with a stem of about 7 cm length and graduated to 0.01 ml divisions. Each mark on the stem of the dilatometer was calibrated using conductivity water as a reference liquid. For filling the dilatometer with test solutions a hypodermic syringe with a needle of $\sim$ 10 cm length was used.

Viscosity Measurement

The viscosities of all the electrolytic solutions

were measured using a Hoppler BH-2 falling sphere viscometer to 0.5%. This viscometer consists of a cylindrical tube of 15.936 mm inner diameter fixed at an inclination of 10° from the vertical axis. The cylindrical viscometer tube is jacketed with a larger tube through which water from the Ultra-Thermostat was circulated. The temperature of the circulated water in this outer jacket was measured with a Labortherm-N thermometer (GDR). In order to measure the viscosity of a solution, the viscometer tube was first filled with the test solution and a sphere of suitable dimension (depending on the viscosity of the test solution) was slid into this tube. The time required for the sphere to travel a path of 100 mm, which is designated by two marks on the cylindrical tube, was noted. This is repeated till constant value for the time of fall of the sphere was obtained. The viscosity of the solution was then calculated from the formula

$$\eta = t(\rho_1 - \rho_2)K$$

where η is the dynamic viscosity in cP, t the time of fall of the sphere in second, ρ_1 the density (g. cm^{-3}) of the sphere used, ρ_2 the density (g. cm^{-3}) of the solution, and

K(cP. $cm^3.g^{-1}.\ s^{-1}$) the constant factor characteristic of the sphere used. In this viscometer, since the solution is sealed, the condensation of water vapour at low temperatures and the loss of water at high temperatures are prevented.

In the case of molten salt systems viscosity measurements were made using Cannon-Ubbelohde suspended-level viscometers of viscometer constants 4.98×10^{-3} $cm^2.\ s^{-2}$ and 8.42×10^{-2} $cm^2.\ s^{-2}$.

Conductance Measurement

The conductances of all the electrolytic solutions were measured using a Philips PR 9500 conductivity bridge and a dip-type conductivity cell with platinized platinum electrodes of cell constant 1.081 cm^{-1}. For measuring the conductivity of molten salts a conventional conductivity bridge (ELICO CM 82T Type) and a dip-type conductivity cell of cell constant 1.198 cm^{-1} were used. In both the cases the accuracy of conductance measurements was found to be $\sim$ 0.1%.

For measuring conductance the sample ($\sim$ 20 ml) was taken in a 35 x 100 mm glass tube into which the conductivity

cell was properly fitted. The sample tube was then placed in the thermostat and the electrodes were connected to the conductance bridge.

All the measurements (density, viscosity, and conductance) were made in a descending order of temperature.

PART I

AQUEOUS ELECTROLYTES

CHAPTER I

TEMPERATURE AND CONCENTRATION DEPENDENCE OF VISCOSITY OF AQUEOUS ELECTROLYTES*

---

*Publications at present based on this study:

1. S. Mahiuddin and K. Ismail, Can. J. Chem., in press.
2. S. Mahiuddin and K. Ismail, revised manuscript submitted to J. Phys. Chem.

Introduction

In the previous section (General Introduction) we have highlighted the importance of obtaining a feasible expression for describing the concentration dependence of transport properties of electrolytic solutions in the concentration range from dilute to saturation point. In the recent years one of the approaches being used in glass-forming molten mixtures[1-3] to obtain such an isothermal expression is by substituting the concentration dependence of the three parameters of the VTF equation [Eq(0-13)]. The VTF equation for viscosity, η, is written as

$$\eta = A_\eta T^{1/2} \exp\left[B_\eta /(T-T_o)\right] \qquad (1-1)$$

where A_η, B_η, and T_o are constants. The preexponential $T^{1/2}$ term was not present in the original VTF equation, but it was incorporated on the basis of the free volume model.[4]

Since aqueous solutions also have a high tendency to form glasses (especially at high concentrations), Angell and Bressel[5] made an attempt to extend the above approach to electrolytic solutions and derived an isothermal equation from Eq(1-1) for describing the concentration dependence of fluidity of $Ca(NO_3)_2$-H_2O system. However, there is scope

for improving Angell and Bressels' isothermal equation by making more appropriate substitutions for the concentration dependence of the three constants of the VTF equation. In this chapter we have made an attempt to do this by measuring the viscosities of six electrolytic solutions, viz., $Ca(NO_3)_2$-H_2O, $Mg(NO_3)_2$-H_2O, $MgCl_2$-H_2O, $NiCl_2$-H_2O, $Na_2S_2O_3$-H_2O, and $NaNO_3$-H_2O, as functions of temperature and concentration.

Experimental Section

Methods of preparing solutions and of density and viscosity measurements are described in the preceding section (Experimental Techniques). Concentrations of all the solutions were varied from dilute up to almost the saturation point at the room temperature ($\sim$20°C).

Results and Discussion

The measured densities of all the solutions are found to be linear functions of both temperature (Tables 1-1) and molarity, c (Fig 1-1). The dependence of density on molality, m, however, does not exhibit such a linear relationship (Fig 1-1). From Fig 1-1 it may also be noted that the present density values of the different systems under study are in good agreement (within $\pm$ 0.3%) with the literature values.[6-10]

Table 1-1a: Least-Squares Fitted Values of the Density Equation, $\rho = a - bt(°C)$ for $Ca(NO_3)_2 - H_2O$ System.

m ($mol.kg^{-1}$)	a ($g.\ cm^{-3}$)	b x 10^4 ($g.\ cm^{-3}.°C^{-1}$)	Std. dev. in ρ σ x 10^4
0.1305	1.0261	4.4571	0.789
1.175	1.1375	4.9671	1.121
1.752	1.1958	5.8231	1.639
3.533	1.3442	6.8976	1.064
3.953	1.3743	6.7369	0.968
5.081	1.4402	6.6673	1.689
6.450	1.5112	7.1854	1.723
8.155	1.6014	7.2715	2.209
8.864	1.6267	7.9946	1.384
12.790	1.7450	7.3448	2.062

Table 1-1b: Least-Squares Fitted Values of the Density Equation, $\rho = a - bt(°C)$ for $Mg(NO_3)_2-H_2O$ system.

m (mol. kg^{-1})	a (g. cm^{-3})	b x 10^4 (g. cm^{-3}. $°C^{-1}$)	Std. Dev. in ρ σ x 10^4
0.0917	1.0214	4.6154	0.928
0.2297	1.0346	4.3443	0.716
0.4243	1.0559	4.5686	0.918
0.6753	1.0816	5.1671	0.769
1.0524	1.1170	5.2511	0.803
1.7055	1.1714	5.2673	1.533
2.0428	1.2047	5.4326	1.424
2.3300	1.2310	5.7854	1.665
3.1050	1.2884	5.9078	2.004
3.7251	1.3289	6.2154	1.030
4.6299	1.3828	6.0195	1.812
4.7091	1.3906	6.1908	1.857
4.8578	1.4002	5.8546	1.153
5.2393	1.4227	6.4114	1.318
6.0371	1.4671	8.0131	1.372
6.3682	1.4801	8.1530	1.313

Table 1-1c: Least-Squares Fitted Values of the Density Equation, $\rho = a - bt(°C)$ for $MgCl_2 - H_2O$ system.

m ($mol.kg^{-1}$)	a ($g.cm^{-3}$)	b x 10^4 ($g.cm^{-3}.°C^{-1}$)	Std. dev. in ρ σ x 10^4
0.1145	1.0199	4.2332	1.451
0.3597	1.0380	4.2719	4.246
0.5266	1.0518	4.4920	0.599
0.7336	1.0659	4.3372	0.475
1.5367	1.1246	5.5022	1.496
2.1294	1.1564	4.4234	0.772
2.8492	1.1997	4.0963	0.699
3.7490	1.2452	4.0361	0.963
4.2721	1.2721	3.9607	0.491
5.3787	1.3256	3.7530	0.548
5.9872	1.3513	3.7846	0.337

Table 1-1d: Least-Squares Fitted Values of the Density Equation, $\rho = a - bt(°C)$ for $NiCl_2 - H_2O$ system.

m ($mol.kg^{-1}$)	a ($g.\ cm^{-3}$)	b x 10^4 ($g.cm^{-3}.°C^{-1}$)	Std. dev. in ρ σ x 10^4
0.1736	1.0321	4.6060	0.803
0.7656	1.1011	4.7007	0.395
0.9962	1.1235	4.1625	0.375
1.1481	1.1397	4.1429	1.134
2.1643	1.2480	4.7598	0.535
2.7529	1.3037	4.5257	1.117
3.2131	1.3516	5.1025	0.773
3.7502	1.4012	4.9892	0.927
4.1787	1.4381	5.2248	0.389
4.7292	1.4784	5.2251	0.383
4.9901	1.5062	6.3566	1.410
5.6853	1.5581	5.2038	1.439

Table 1-1e: Least-Squares Fitted Values of the Density Equation, $\rho = a - bt(°C)$ for $Na_2S_2O_3 - H_2O$ system.

m ($mol.kg^{-1}$)	a ($g.\ cm^{-3}$)	b x 10^4 ($g.\ cm^{-3}.°C^{-1}$)	Std. dev. in ρ σ x 10^4
0.0934	1.0249	4.4220	0.790
0.5690	1.0806	5.0718	0.787
0.8714	1.119	4.9301	0.580
1.2120	1.1495	5.2443	0.708
1.7656	1.2054	5.5759	0.700
2.3472	1.2590	5.9842	0.903
2.8287	1.2983	6.2509	0.606
4.0214	1.3869	7.2897	1.920
4.6062	1.4189	6.5930	0.740
5.1026	1.4482	6.3982	5.390
6.2915	1.5153	7.2180	1.270
8.6109	1.6111	7.2415	0.510
9.8184	1.6542	7.0634	0.636

Table 1-1f: Least-Squares Fitted Values of the Density Equation, $\rho = a - bt(°C)$ for $NaNO_3 - H_2O$ system.

m ($mol.kg^{-1}$)	a ($g.\ cm^{-3}$)	b x 10^4 ($g.cm^{-3}.°C^{-1}$)	Std. dev. in ρ σ x 10^4
0.1113	1.0185	4.7547	1.120
0.5212	1.0401	4.7258	0.780
1.0532	1.0674	4.9553	0.734
1.8119	1.1038	5.4206	0.732
2.5441	1.1392	5.8859	0.730
3.3185	1.1711	5.9901	0.468
4.3956	1.2136	6.2521	0.415
5.3402	1.2502	6.9864	1.130
6.2532	1.2826	7.4778	0.722
7.3990	1.3175	7.4192	0.744
8.3060	1.3484	8.2895	1.220
9.8626	1.3858	7.5717	1.040

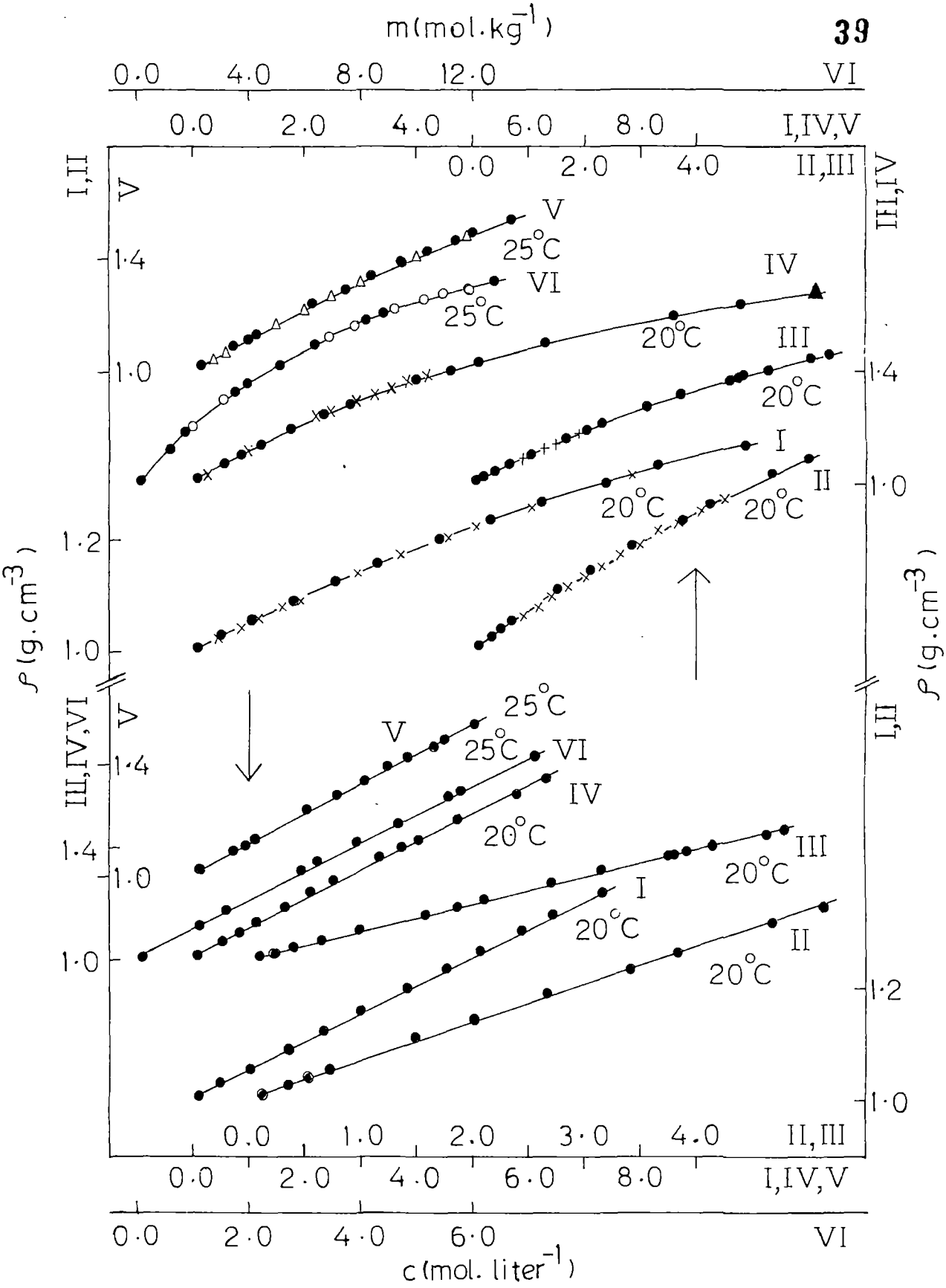

Fig 1-1. Plots of densities vs. concentration for aqueous electrolytes. I - $NaNO_3$, II - $MgCl_2$, III - $Mg(NO_3)_2$, IV - $Na_2S_2O_3$, V - $NiCl_2$, and VI - $Ca(NO_3)_2$ solutions (● - present data, o - ref. 6, + - ref. 7, Δ - ref. 8, ▲ - ref. 9, and x - ref. 10).

The measured viscosity values of all the electrolytic solutions are given in Tables 1-2. A comparison of the present viscosity data for the different systems with the reported values[5,10-12] is made by plotting η versus m isotherms (Fig 1-2) and they are found to be closely comparable ($< 2\%$). From the Arrhenius plots (Figs 1-3) it is apparent that viscosities of all the solutions under investigation show a non-Arrhenius temperature dependence. However, for some of the solutions, especially for those of low concentrations, as expected the non-Arrhenius behaviour was found to be less pronounced. For these solutions non-Arrhenius behaviour of viscosity may be considered to become prominent only at still lower temperatures.

We have, therefore, least-squares fitted the viscosity data of all the electrolytic solutions to Eq (1-1). The computed values of the A_η, B_η, and T_o parameters are listed in Tables 1-3. In the case of $Ca(NO_3)_2$-H_2O system the computed values of A_η, B_η, and T_o are found to be comparable with those reported by Angell and Bressel.[5] The reported[1] T_o values of a few concentrated $Mg(NO_3)_2$-H_2O systems based on their equivalent conductance data are also in agreement within $\pm$ 5°K with the values of T_o (Table 1-3b) obtained after

Table 1-2a: Viscosities of $Ca(NO_3)_2$ - H_2O System as Functions of Concentration and Temperature.

T(K)	η(cP)	T(K)	η(cP)	T(K)	η(cP)
0.1305 m		1.175 m		1.752 m	
291.0	1.0767	290.0	1.4487	291.0	1.7083
292.8	1.0329	292.1	1.3806	293.1	1.6130
298.0	0.9188	298.0	1.2115	298.0	1.4450
303.1	0.8218	302.9	1.0933	303.0	1.3082
308.0	0.7447	308.0	0.9908	308.0	1.1899
313.0	0.6782	313.0	0.9080	313.0	1.0852
318.0	0.6237	323.0	0.7700	323.0	0.9176
323.0	0.5745	333.0	0.6649	333.0	0.7858
328.0	0.5346	343.0	0.5817	343.0	0.6872
333.0	0.4986				
338.0	0.4667				
343.0	0.4374				

Continued.

Table 1-2a: (Continued)

T(K)	η(cP)	T(K)	η(cP)	T(K)	η(cP)
3.533 m		3.953 m		5.081 m	
290.5	3.1913	291.0	3.7781	291.0	5.7874
294.7	2.8817	293.6	3.5408	293.8	5.3349
298.0	2.6409	298.0	3.1691	298.0	4.7423
303.0	2.3655	303.0	2.8269	303.0	4.1556
308.0	2.1200	308.0	2.5209	308.0	3.6872
313.0	1.9363	313.0	2.2745	313.0	3.3095
317.9	1.7752	318.3	2.0502	318.0	2.9799
323.0	1.6451	323.0	1.8934	323.0	2.6917
328.0	1.5302	328.0	1.7593	328.0	2.4453
333.0	1.4305	333.0	1.6243	333.0	2.2411
338.0	1.3544	338.0	1.5276	338.0	2.0648
343.0	1.2859	343.0	1.4381	343.0	1.9095

Continued.

Table 1-2a: (Continued)

T(K)	η(cP)	T(K)	η(cP)	T(K)	η(cP)
6.450m		8.155m		8.864m	
291.0	10.1321	298.0	19.8033	291.0	36.7110
293.3	9.3897	303.0	16.3759	293.3	33.2088
298.0	8.0632	308.0	13.7503	298.0	26.6782
303.0	6.9282	313.0	11.7375	303.0	21.7392
308.0	6.0250	323.0	8.8377	308.0	18.0738
313.0	5.2960	333.0	6.8356	313.0	15.2841
318.2	4.6697	338.0	6.1030	317.9	13.1313
323.0	4.1927	343.0	5.4883	323.0	11.3769
328.0	3.7874	12.790m		328.0	9.9408
333.0	3.4198	291.0	335.6539	333.0	8.8238
338.0	3.1247	293.7	275.5320	338.0	7.8660
343.0	2.8615	298.0	203.3613	343.0	7.0676
		303.0	145.4488		
		308.0	106.5767		
		313.0	82.9930		
		318.0	63.4126		
		323.0	49.8526		
		328.0	40.8118		
		333.0	34.0292		
		338.0	31.0220		
		343.0	24.2261		

Table 1-2b: Viscosities of $Mg(NO_3)_2$ - H_2O System as Functions of Concentration and Temperature.

T(K)	η(cP)	T(K)	η(cP)	T(K)	η(cP)
0.0917m		0.2297m		0.4243m	
289.4	1.1136	292.5	0.3701	290.0	1.2202
290.0	1.0936	293.3	0.3833	291.3	1.1839
292.5	1.0338	295.0	0.4018	294.5	1.0956
295.9	0.9566	298.0	0.4351	295.3	1.0762
298.0	0.9086	303.0	0.4534	298.0	1.0165
301.4	0.8446	308.0	0.4799	303.4	0.9061
304.5	0.7914	313.0	0.5183	308.0	0.8254
308.0	0.7366	317.9	0.5540	312.7	0.7552
313.7	0.6632	323.0	0.5950	318.1	0.6862
318.3	0.6139	327.8	0.6452	323.0	0.6368
323.0	0.5692	332.3	0.7034	327.9	0.5900
327.6	0.5318	337.8	0.7722	332.9	0.5509
333.1	0.4897	342.3	0.8527	338.0	0.5158
338.4	0.4549	348.0	0.9418	343.0	0.4832
342.9	0.4322	353.5	1.0178	347.0	0.4610
346.4	0.4149	358.2	1.0573	352.0	0.4349
351.5	0.3936	362.0	1.0771	357.0	0.4128
357.0	0.3667			362.0	0.3946
362.0	0.3576				

Continued.

Table 1-2b: (Continued)

T(K)	η(cP)	T(K)	η(cP)	T(K)	η(cP)
0.6753m		1.0524m		1.7055m	
291.0	1.2784	288.5	1.5358	290.6	1.8678
294.1	1.1882	290.2	1.4703	292.0	1.8055
294.7	1.1704	292.2	1.4061	293.8	1.7342
298.0	1.0870	294.6	1.3319	295.6	1.6992
302.8	0.9859	298.0	1.2328	298.0	1.6008
308.0	0.8878	303.6	1.0954	303.6	1.3522
313.1	0.8088	308.0	1.0050	308.0	1.2396
317.8	0.7411	313.9	0.9046	313.6	1.1160
323.0	0.6838	318.2	0.8401	317.9	1.0353
328.3	0.6302	323.0	0.7768	323.0	0.9508
333.2	0.5880	327.8	0.7196	328.5	0.8772
338.4	0.5524	332.3	0.6723	333.4	0.8152
343.0	0.5191	337.8	0.6264	338.0	0.7591
348.0	0.4884	342.3	0.5903	343.2	0.7090
352.5	0.4641	347.9	0.5543	347.8	0.6684
357.5	0.4398	353.0	0.5206	352.7	0.6315
362.0	0.4206	357.4	0.4957	357.0	0.6004
		362.0	0.4694	362.0	0.5706

Continued.

Table 1-2b: (Continued)

T(K)	η(cP)	T(K)	η(cP)	T(K)	η(cP)
2.0428m		2.3300m		3.1050m	
291.9	2.0398	291.2	2.3068	290.0	3.2615
294.3	1.9271	293.4	2.1882	291.3	3.1486
296.4	1.8493	294.7	2.1290	293.3	2.9875
298.0	1.7886	298.0	1.9852	296.3	2.7945
303.7	1.5174	303.6	1.6936	298.0	2.5763
308.0	1.4332	308.0	1.5578	303.6	2.2688
313.0	1.2720	313.6	1.3684	308.0	2.0759
318.0	1.1628	317.9	1.3074	313.0	1.8664
323.0	1.0590	323.0	1.1545	317.8	1.7026
328.2	0.9696	328.5	1.0742	323.0	1.5849
333.4	0.9074	333.4	1.0095	333.2	1.3372
340.0	0.8321	343.2	0.8786	342.6	1.1746
345.5	0.7825	347.8	0.8406	353.0	1.0344
351.0	0.7291	357.0	0.7652	362.0	0.9384
356.5	0.6988	362.0	0.7254		
362.0	0.6593				

Continued.

Table 1-2b: (Continued)

T(K)	η(cP)	T(K)	η(cP)	T(K)	η(cP)
3.7251m		4.6299m		4.7091m	
289.4	4.1106	290.0	5.9148	292.7	5.8214
293.7	3.6999	293.6	5.3768	293.5	5.7044
296.3	3.4666	296.2	5.0149	296.6	5.2726
298.0	3.3274	298.0	4.8009	298.0	5.0744
303.7	2.9047	303.6	4.1642	302.8	4.4868
308.0	2.6656	308.0	3.7642	308.0	3.9798
313.0	2.3453	313.0	3.4091	313.0	3.5828
318.0	2.1429	317.8	3.0897	318.4	3.2144
323.0	1.9503	323.0	2.7998	323.0	2.9489
328.2	1.7799	327.7	2.5843	327.9	2.7053
333.4	1.6342	333.2	2.3533	332.6	2.4982
345.5	1.3961	337.5	2.1966	337.0	2.3281
351.0	1.3068	342.6	2.0479	342.1	2.1578
362.0	1.1655	347.6	1.9059	346.8	2.0170
		353.0	1.7869	353.0	1.8692
		358.0	1.6746	357.0	1.7802
		362.0	1.6156	362.0	1.6763

Continued.

Table 1-2b: (Continued)

T(K)	η(cP)	T(K)	η(cP)	T(K)	η(cP)
4.8578m		5.2393m		6.0371m	
291.8	6.5818	308.0	5.1554	323.0	4.7324
293.6	6.2477	313.4	4.5633	328.2	4.2876
295.9	5.8775	317.2	4.1840	333.0	3.9234
298.0	5.5503	323.0	3.7263	336.1	3.7100
303.7	4.8082	327.5	3.4551	340.1	3.4836
308.0	4.3418	332.1	3.1678	344.4	3.2482
313.0	3.9046	338.8	2.8526	348.8	3.0420
318.0	3.5250	345.4	2.5570	354.5	2.8083
323.0	3.2034	351.0	2.3854		
328.2	2.9180	356.5	2.2124	6.3682 m	
333.4	2.6840	362.0	2.0608	323.0	5.3209
340.0	2.3972	366.5	1.9374	328.8	4.7167
345.5	2.2214			333.5	4.3164
351.0	2.0522			337.7	3.9946
356.5	1.9279			343.6	3.6087
362.0	1.7875			350.3	3.2356
				353.0	3.1250
				358.4	2.8955
				362.0	2.7447

Table 1-2c: Viscosities of $MgCl_2$ - H_2O System as Functions of Concentration and Temperature.

T(K)	η(cP)	T(K)	η(cP)	T(K)	η(cP)
0.1145m		0.3597m		0.5266m	
293.0	1.0710	293.0	1.1771	293.0	1.2515
298.0	0.9590	298.0	1.0508	298.0	1.1094
308.0	0.7740	308.0	0.8504	308.0	0.9061
314.6	0.6852	313.6	0.7674	314.9	0.7925
323.0	0.5983	323.0	0.6553	323.0	0.6906
332.9	0.5140	332.8	0.5614	332.9	0.5939
0.7336m		1.5367m		2.1294m	
293.0	1.3492	293.0	1.8266	293.0	2.3448
298.0	1.1983	298.0	1.6300	298.0	2.0695
308.0	0.9725	308.0	1.3083	308.0	1.6604
313.9	0.8691	314.4	1.1553	316.4	1.4087
323.0	0.7398	323.0	0.9935	323.0	1.2532
332.9	0.6337	333.2	0.8451	332.8	1.0672

Continued.

Table 1-2c: (Continued)

T(K)	η(cP)	T(K)	η(cP)	T(K)	η(cP)
2.8492m		3.7490m		4.2721m	
293.0	3.1778	293.0	4.6336	293.0	6.0814
298.0	2.7842	298.0	4.0444	298.0	5.2586
308.0	2.2153	308.0	3.1851	308.0	4.0726
315.0	1.9263	314.2	2.7628	313.8	3.5781
323.0	1.6900	323.0	2.3324	323.0	2.9506
332.0	1.4623	333.5	1.9521	333.0	2.4547
5.3787m		5.9872m			
293.0	11.5068	308.0	10.3689		
298.0	9.8200	313.7	8.8545		
308.0	7.4004	323.0	7.0616		
314.4	6.2672	328.0	6.3131		
323.0	5.1448	333.3	5.6510		
333.0	4.1543	338.0	5.1542		
		343.0	4.6992		

Table 1-2d: Viscosities of $NiCl_2$ - H_2O System as Functions of Concentration and Temperature.

T(K)	η(cP)	T(K)	η(cP)	T(K)	η(cP)
0.1736m		0.7656m		0.9962m	
288.0	1.2445	288.0	1.5313	288.0	1.6981
293.0	1.0962	293.0	1.3566	293.0	1.4933
298.0	0.9757	298.0	1.1984	298.0	1.3356
302.7	0.8883	303.4	1.0640	303.3	1.1862
308.0	0.7929	308.0	0.9724	308.0	1.0825
315.8	0.6762	315.8	0.8391	316.1	0.9242
323.0	0.5994	323.0	0.7415	323.0	0.8215
1.1481m		2.1643m		2.7529m	
288.0	1.7726	288.0	2.6327	288.0	3.4176
293.0	1.5584	293.0	2.3696	293.0	2.9956
298.0	1.3835	298.0	2.1056	298.0	2.6367
303.2	1.2442	303.0	1.8752	300.0	2.5171
308.0	1.1246	308.0	1.6788	303.1	2.3332
315.3	0.9731	315.8	1.4447	308.0	2.1098
323.0	0.8560	323.0	1.2912	315.4	1.8301
				323.0	1.6105

Continued.

Table 1-2d: (Continued)

T(K)	η(cP)	T(K)	η(cP)	T(K)	η(cP)
3.2131m		3.7502m		4.1787m	
288.0	4.4167	288.0	5.8378	288.0	7.0824
293.0	3.8383	293.0	5.0469	293.0	6.0686
298.0	3.3966	298.0	4.4076	298.0	5.2706
303.2	2.9844	303.3	3.8400	303.4	4.5337
308.0	2.6710	308.0	3.4318	308.0	4.0207
314.5	2.3112	315.4	2.9138	314.9	3.4194
323.0	1.9626	323.0	2.4897	323.0	2.8517
4.7292m		4.9901m		5.6853m	
288.0	9.1666	288.0	10.4344	293.0	13.4724
293.0	7.7757	293.0	8.8179	293.0	11.2404
298.0	6.6816	298.0	7.5297	303.2	9.4981
303.8	5.6391	303.3	6.4268	308.0	8.2280
308.0	5.0258	308.0	5.6294	315.2	6.7132
316.0	4.1078	315.4	4.6736	323.0	5.4990
323.0	3.4917	323.0	3.9052		

Table 1-2e: Viscosities of $Na_2S_2O_3$-H_2O system as Functions of Concentration and Temperature.

T(K)	η (cP)				
	0.0934m	0.5690m	0.8714m	1.2120m	1.7656m
285.0	1.2977	1.5549	1.7506	2.1281	2.6210
288.0	1.1975	1.4353	1.6178	1.9472	2.4078
293.0	1.0526	1.2751	1.4214	1.6937	2.0991
298.0	0.9424	1.1370	1.2648	1.4994	1.8583
303.0	0.8446	1.0199	1.1349	1.3416	1.6489
308.0	0.7608	0.9208	1.0226	1.2143	1.4761
313.0	0.6923	0.8382	0.9282	1.0863	1.3313
318.0	0.6336	0.7664	0.8481	0.9839	1.2076
323.0	0.5799	0.7038	0.7762	0.9009	1.1016

Table 1-2e: (Continued)

T(K)	η(cP)			
	2.8287m	4.0214m	4.6062m	5.1026m
285.0	4.1274	7.6644	9.6060	12.6544
288.0	3.7356	6.8556	8.4202	11.1048
293.0	3.1993	5.6982	6.8752	8.9339
298.0	2.7827	4.7893	5.7361	7.3367
303.0	2.4507	4.1312	4.8899	6.1587
308.0	2.1604	3.5831	4.1631	5.1982
313.0	1.9365	3.1290	3.6299	4.4742
318.0	1.7504	2.7656	3.2058	3.8821
323.0	1.5745	2.4561	2.8027	3.4047

Continued.

Table 1-2e: (Continued)

T(K)	η (cP)		
	6.2915m	8.6109m	9.8184m
285.0	22.5746	61.3310	87.783
288.0	19.3972	50.4127	72.445
293.0	15.0758	37.5567	52.512
298.0	11.9688	28.3152	41.256
303.0	9.7929	22.0590	31.642
308.0	8.0319	17.4636	25.198
313.0	6.7855	14.2523	20.4673
318.0	5.7576	11.7880	16.8927
323.0	5.0249	9.9241	14.1114

Table 1-2f: Viscosities of $NaNO_3$ - H_2O System as Functions of Concentration and Temperature.

T(K)	η(cP)	T(K)	η(cP)	T(K)	η(cP)
0.1113m		0.5212m		1.0532m	
293.0	1.0202	293.0	1.0563	293.0	1.0982
298.0	0.9067	298.0	0.9433	298.0	0.9825
302.2	0.8252	303.1	0.8394	303.4	0.8770
308.0	0.7317	308.0	0.7591	308.0	0.7957
315.2	0.6421	314.3	0.6756	314.3	0.7107
323.0	0.5618	323.0	0.5867	323.0	0.6179
327.9	0.5230	327.8	0.5473	328.2	0.5728
1.8119m		2.5441m		3.3185m	
293.0	1.2396	293.0	1.2811	293.0	1.4109
298.0	1.1045	298.0	1.1376	298.0	1.2703
303.3	0.9870	303.4	1.0211	304.2	1.1115
308.0	0.9051	308.0	0.9273	308.0	1.0297
315.0	0.7852	315.2	0.8134	315.2	0.9051
323.0	0.6887	323.0	0.7166	323.0	0.7971
328.0	0.6320	328.2	0.6616	328.0	0.7345

Continued.

Table 1-2f: (Continued)

T(K)	η(cP)	T(K)	η(cP)	T(K)	η(cP)
4.3956m		5.3402m		6.2532m	
293.0	1.5449	293.0	1.7306	293.0	1.9229
298.0	1.3783	298.0	1.5564	298.0	1.7192
304.3	1.2162	303.2	1.3950	303.4	1.5346
308.0	1.1328	308.0	1.2768	308.0	1.4014
314.5	0.9940	315.2	1.1148	315.2	1.2214
323.0	0.8651	323.0	0.9818	323.0	1.0681
327.4	0.8059	327.7	0.9186	328.3	0.9895
7.3990m		8.3060m		9.8526m	
293.0	2.2463	293.0	2.3955	293.0	2.8349
298.0	1.9778	298.0	2.1325	298.0	2.4894
303.7	1.7403	303.6	1.8884	303.1	2.2140
308.0	1.5781	308.0	1.7245	308.0	1.9894
314.8	1.3980	315.4	1.4934	315.2	1.7509
323.0	1.2064	323.0	1.3116	323.0	1.5450
328.4	1.1037	328.0	1.2058	327.5	1.4534

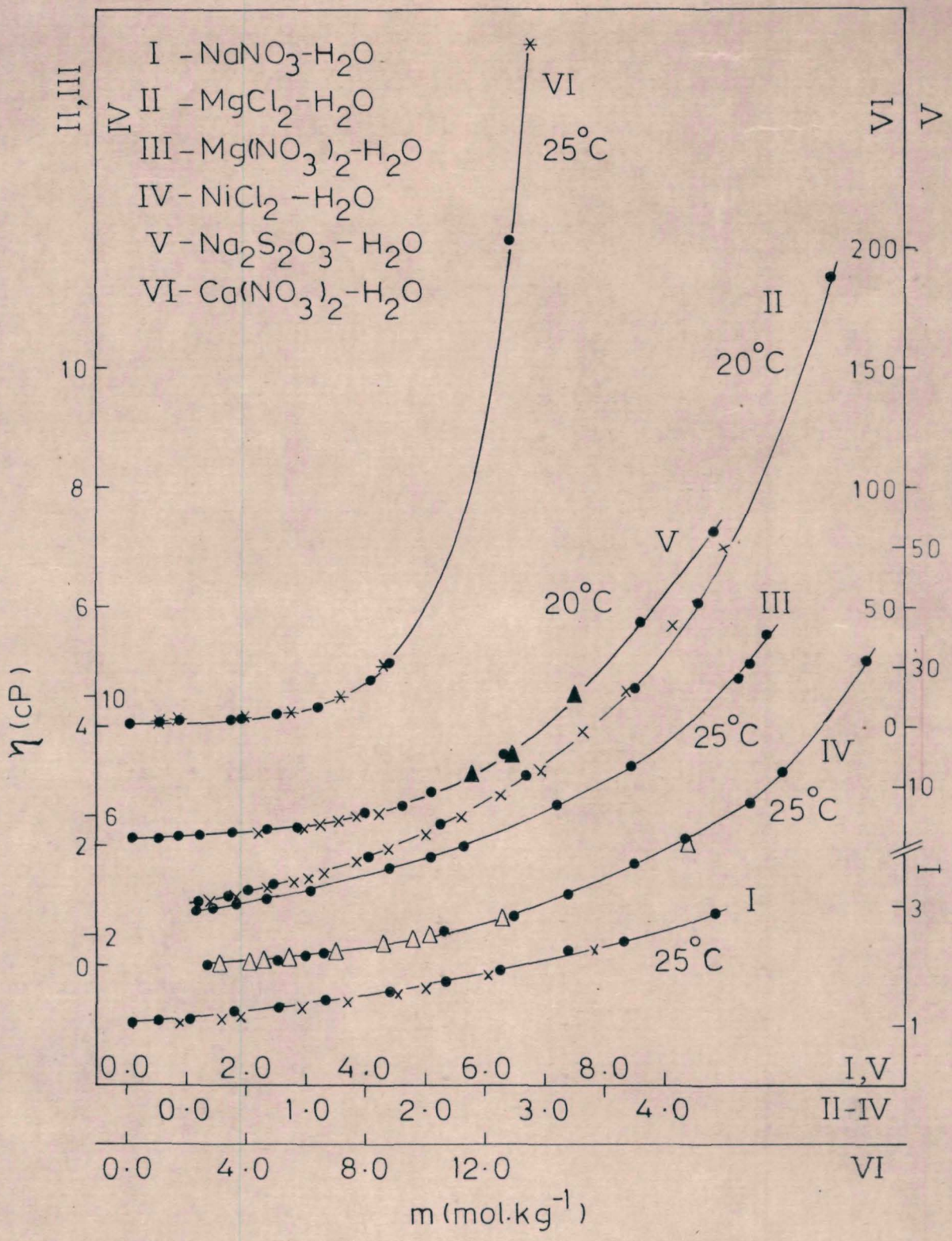

Fig 1-2. Viscosity vs. molality isotherms for aqueous electrolytes (● - present data, * - ref. 5, x - ref. 10, ▲ - ref. 11, and Δ - ref. 12).

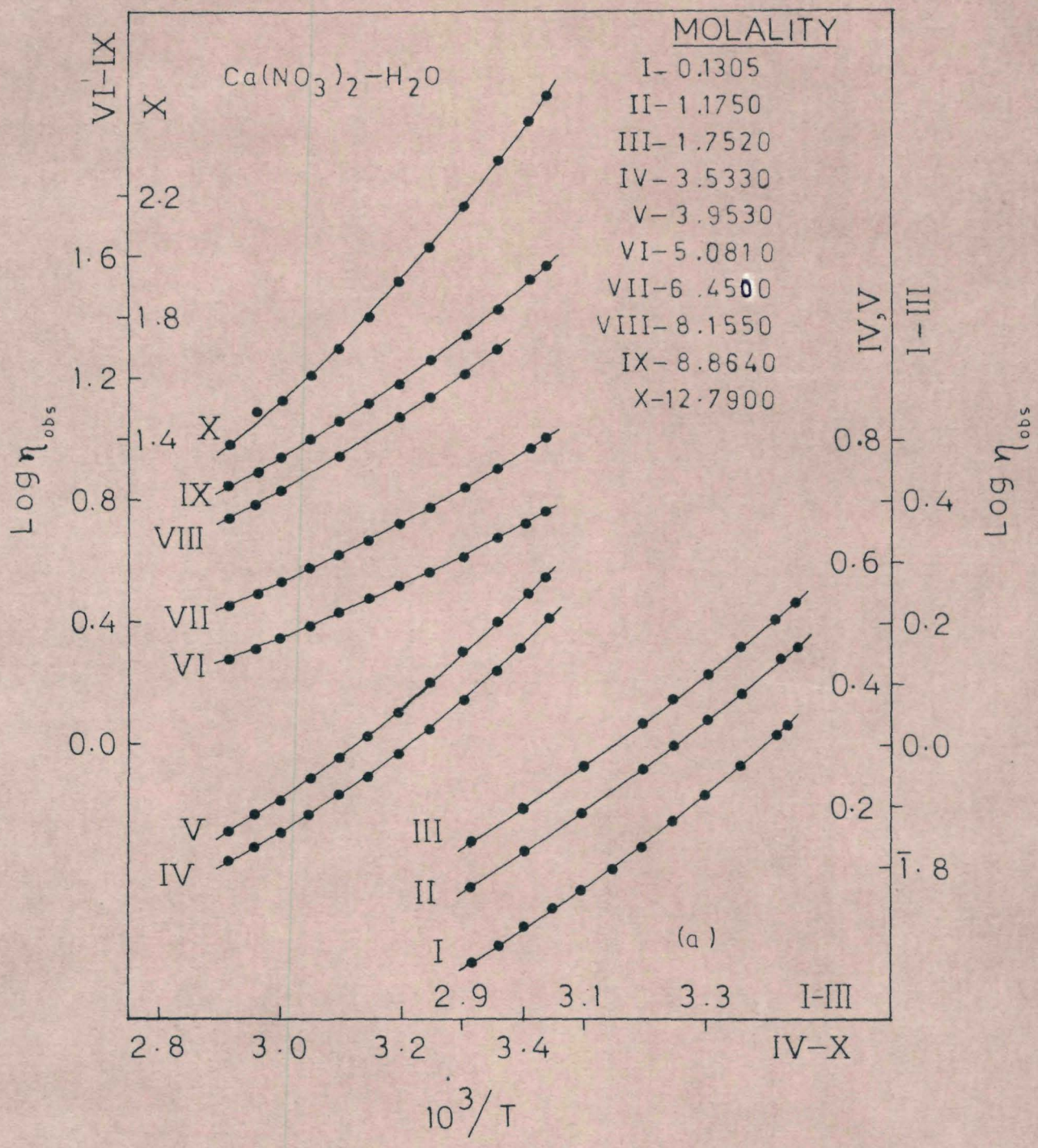

Fig 1-3a. Arrhenius plots for viscosity of $Ca(NO_3)_2$ - H_2O systems.

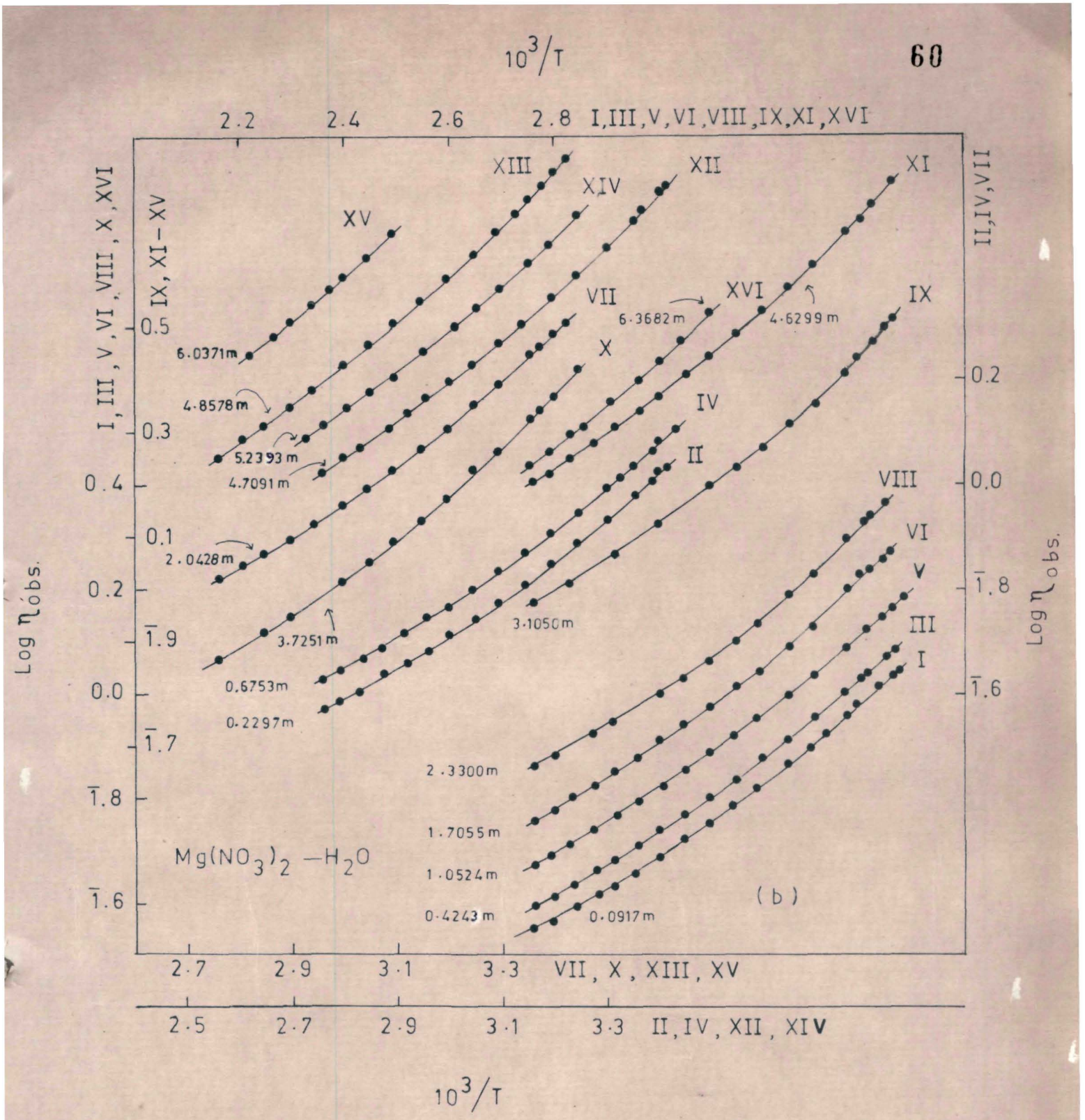

Fig 1-3b. Arrhenius plots for viscosity of $Mg(NO_3)_2$ - H_2O systems.

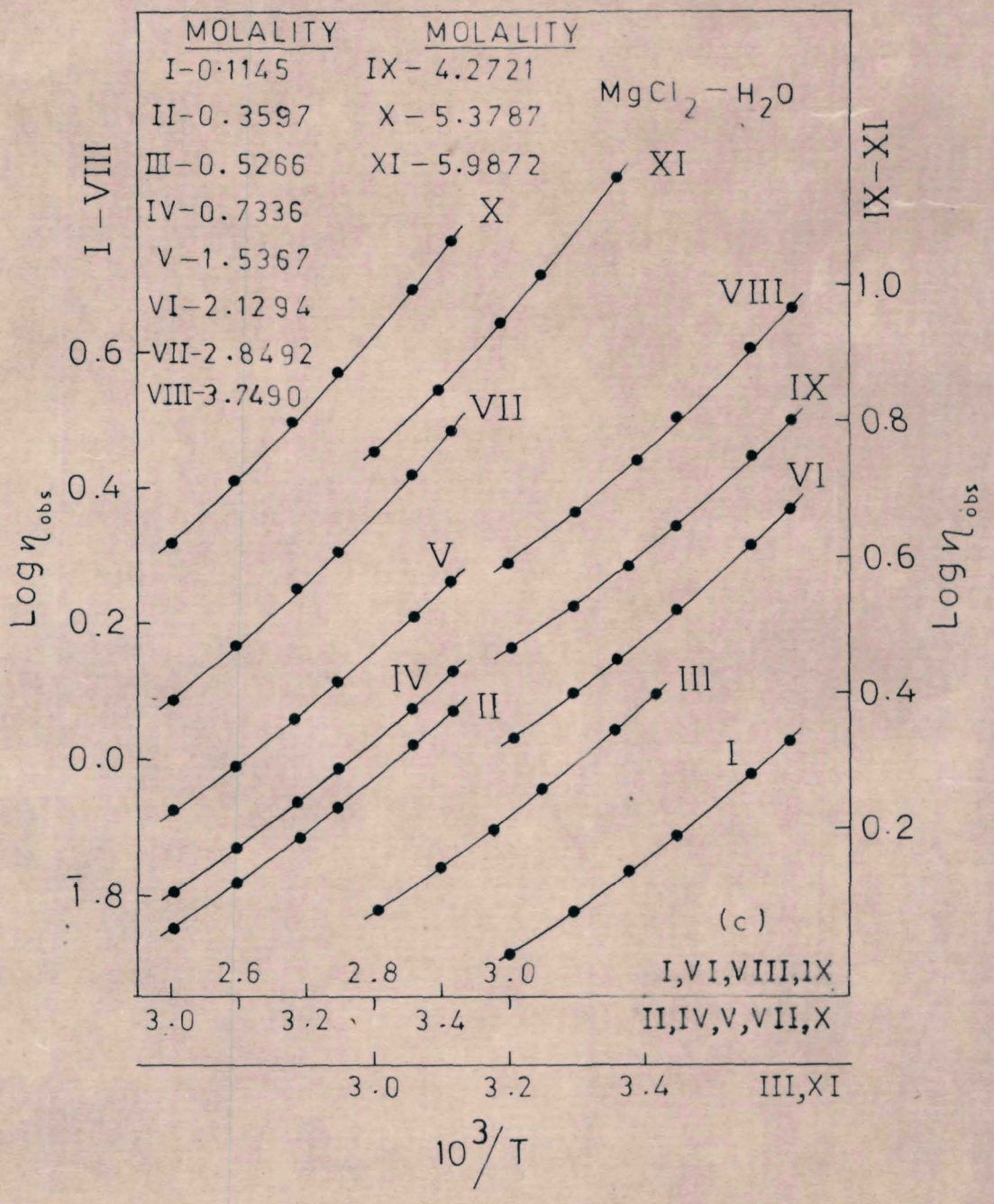

Fig 1-3c. Arrhenius plots for viscosity of $MgCl_2$ - H_2O systems.

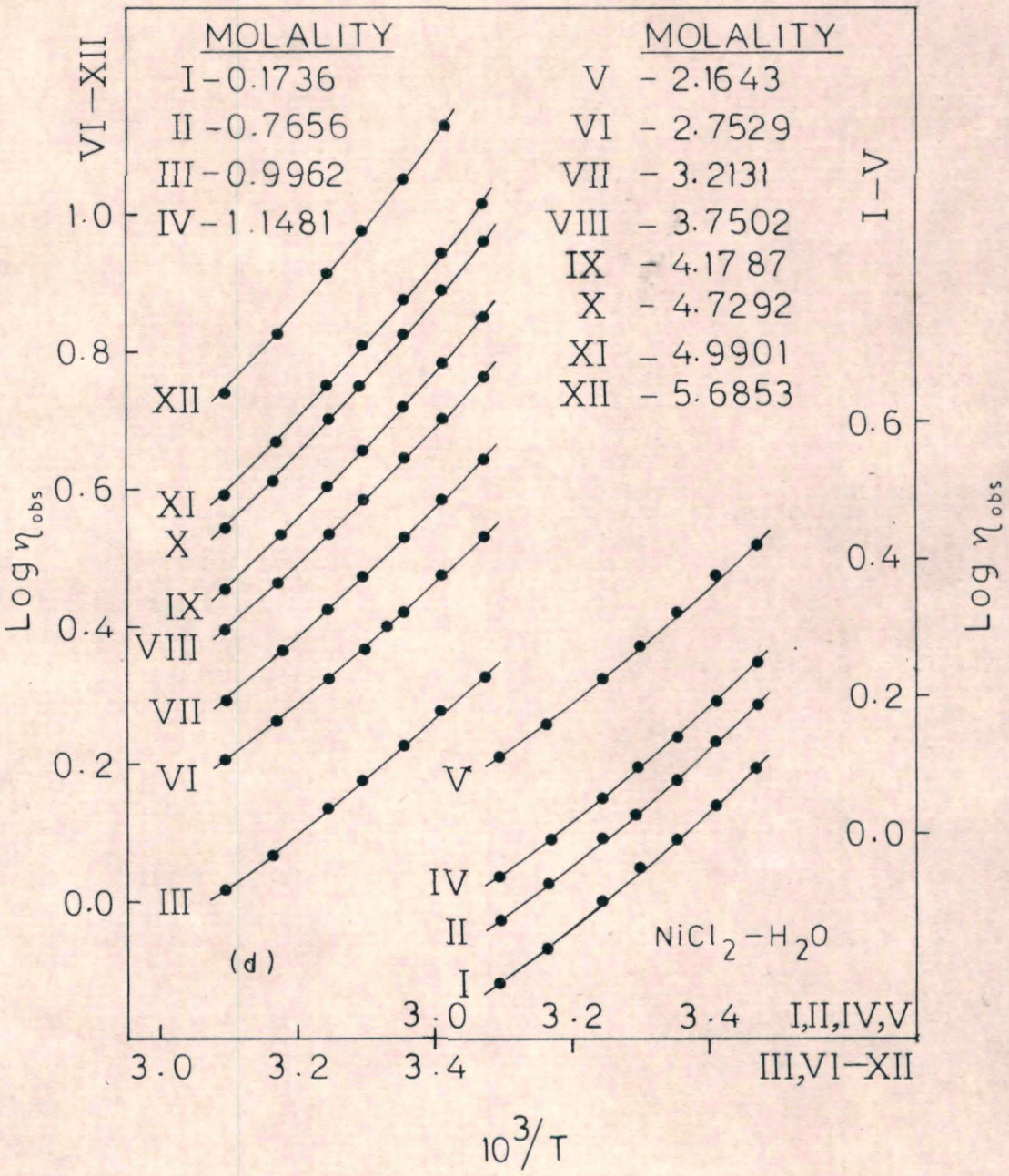

Fig 1-3d. Arrhenius plots for viscosity of $NiCl_2$ - H_2O systems.

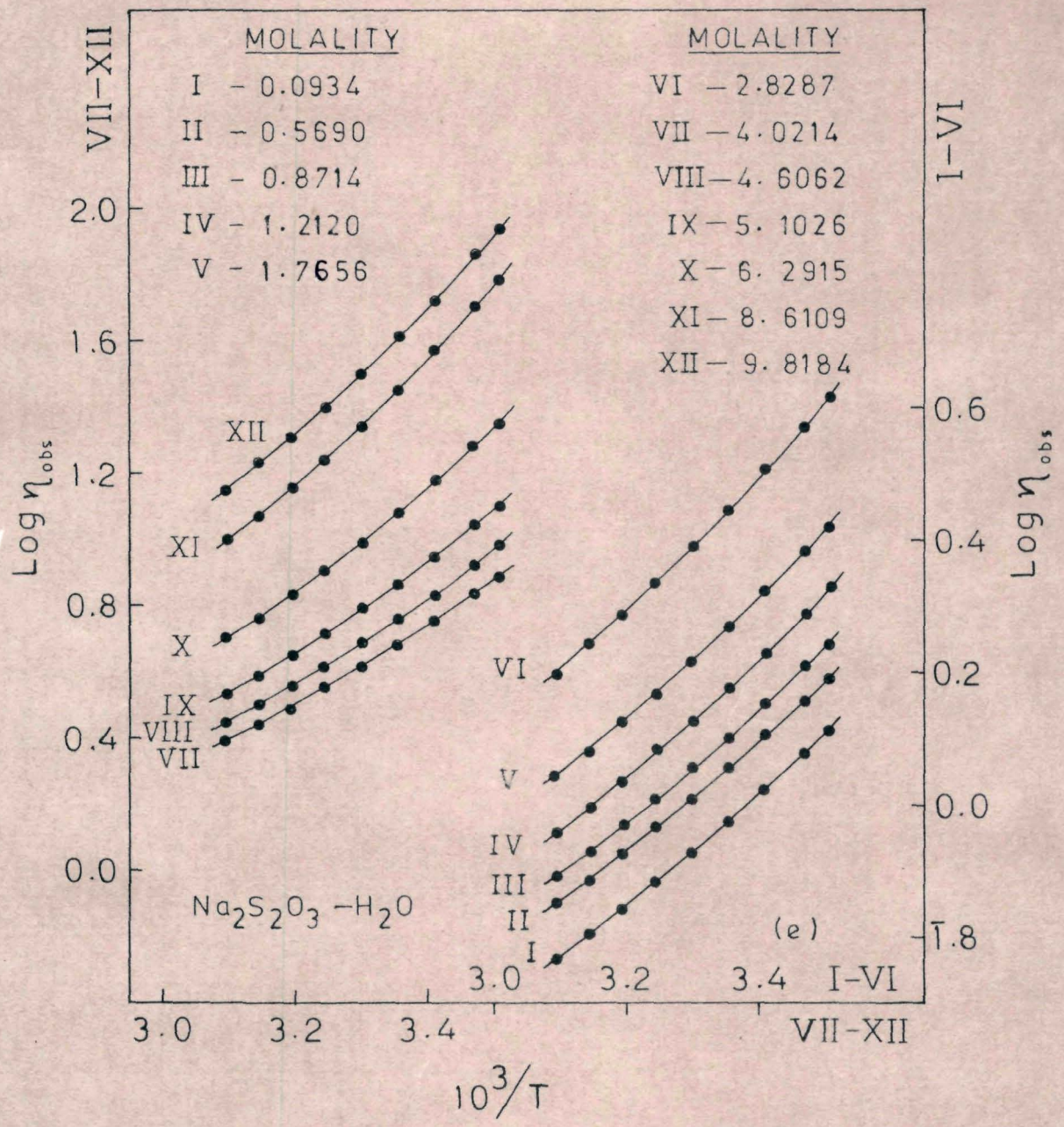

Fig 1-3e. Arrhenius plots for viscosity of $Na_2S_2O_3 - H_2O$ systems.

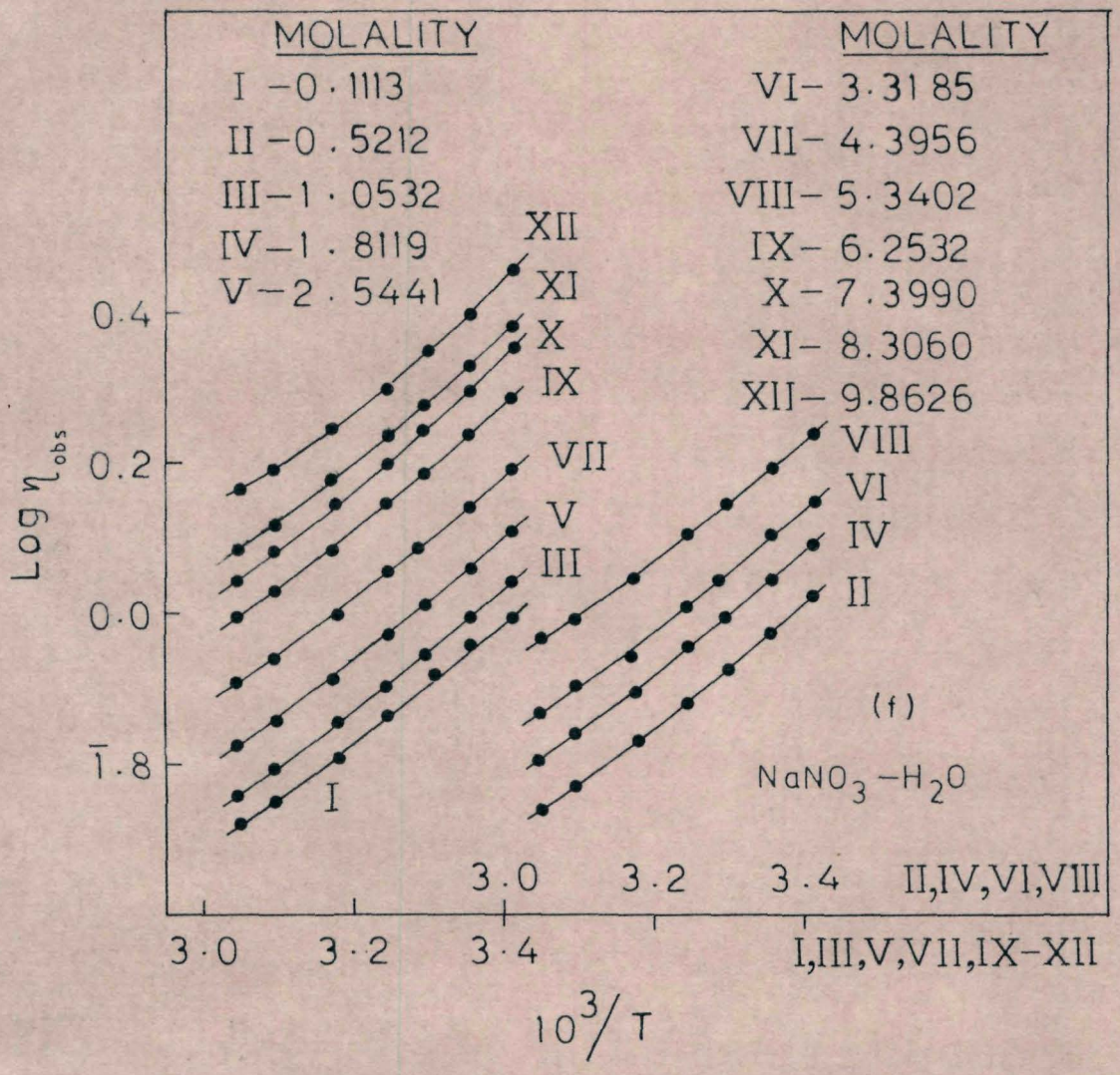

Fig 1-3f. Arrhenius plots for viscosity of $NaNO_3$ - H_2O systems.

Table 1-3a: Least-Squares Fitted Values of the Parameters of Eq(1-1) for the viscosity of $Ca(NO_3)_2$ - H_2O System.

m (mol. kg^{-1})	$A_\eta \times 10^3$	B_η	T_o(K)	Std. dev. in $\ln\eta$
0.1305	1.1840	626.74	133.2	0.0005
1.175	1.7431	598.71	136.0	0.0001
1.752	2.2905	555.02	144.0	0.0003
3.533	4.5869	522.61	149.0	0.0014
3.953	4.5896	534.52	153.0	0.0008
5.081	5.1343	550.20	159.8	0.0003
6.450	6.0522	573.60	166.0	0.0001
8.155	8.2586	588.42	178.8	0.0002
8.864	9.7186	593.42	181.0	0.0007
12.790	13.7111	640.61	203.0	0.0026

Table 1-3b: Least-Squares Fitted Values of the Parameters of Eq(1-1) for the Viscosity of $Mg(NO_3)_2$-H_2O System.

m (mol.kg^{-1})	$A_\eta \times 10^3$	B_η	T_o(K)	Std. dev. in ln η
0.0917	1.2263	614.62	134.5	0.0013
0.2297	1.3246	607.00	135.0	0.0012
0.4243	1.4194	602.99	136.0	0.0008
0.6753	1.5474	596.77	137.0	0.0005
1.0524	1.7865	585.42	139.3	0.0003
1.7055	2.0927	574.02	145.7	0.0015
2.0428	2.4980	561.54	146.5	0.0019
2.3300	2.7977	554.24	148.0	0.0020
3.1050	3.7373	533.81	154.0	0.0016
3.7251	4.7852	516.49	158.0	0.0011
4.6299	7.0307	492.38	164.0	0.0004
4.7091	7.2028	495.05	164.5	0.0003
4.8578	7.4559	500.90	165.0	0.0005
5.2393	7.9671	508.96	167.0	0.0004
6.0371	8.1115	530.15	171.5	0.0009
6.3682	7.9414	542.63	174.0	0.0012

Continued

Table 1-3b: (Continued)

m ($mol.kg^{-1}$)	$A_\eta \times 10^3$	B_η	T_o(K)	Std. dev. in ln η
8.56	-	-	192.0* (195.0)	
10.93	-	-	205.4* (210.0)	
14.14	-	-	214.2* (218.0)	

* These values are obtained by extrapolating the plot of T_o vs. m. The values within the parentheses are the reported values (ref. 1).

Table 1-3c: Least-Squares Fitted Values of the Parameters of Eq(1-1) for the Viscosity of $MgCl_2$ - H_2O System.

m (mol. kg^{-1})	$A_\eta \times 10^3$	B_η	T_o(K)	Std. dev. in ln η
0.1145	1.1352	642.22	132.8	0.0002
0.3597	1.2511	636.26	134.2	0.0004
0.5266	1.3240	633.48	135.0	0.0001
0.7336	1.4031	630.06	136.6	0.0001
1.5367	2.0193	597.11	142.6	0.0002
2.1294	2.5656	583.10	146.4	0.0001
2.8492	3.7133	565.80	148.0	0.0007
3.7490	4.3222	576.72	153.6	0.0003
4.2721	4.8842	586.39	156.2	0.0005
5.3787	6.6896	606.20	161.6	0.0008
5.9872	7.9763	617.34	164.6	0.0005

Table 1-3d: Least-Squares Fitted Values of the Parameters of Eq(1-1) for the Viscosity of $NiCl_2$ - H_2O System.

m (mol. kg^{-1})	$A_\eta \times 10^3$	B_η	T_o(K)	Std. dev. in ln η
0.1736	1.0140	663.85	133.0	0.0003
0.7656	1.3683	636.72	136.0	0.0002
0.9962	1.5392	633.24	136.3	0.0002
1.1481	1.6428	622.68	138.0	0.0002
2.1643	2.6427	600.40	141.0	0.0006
2.7529	3.1401	598.59	144.0	0.0004
3.2131	3.2906	616.89	147.0	0.0003
3.7502	3.7536	628.48	149.0	0.0002
4.1787	3.7032	644.33	151.8	0.0003
4.7292	3.9037	660.43	154.2	0.0003
4.9901	4.1728	664.60	155.0	0.0002
5.6853	4.5490	690.47	159.0	0.0001

Table 1-3e: Least-Squares Fitted Values of the Parameters of Eq(1-1) for the Viscosity of $Na_2S_2O_3$-H_2O System.

m (mol.kg^{-1})	$A_\eta \times 10^3$	B_η	T_o(K)	Std. dev. in ln η
0.0934	1.0519	645.11	134.6	0.0020
0.5690	1.3434	634.18	135.0	0.0013
0.8714	1.4474	630.44	137.4	0.0011
1.2120	1.6063	621.55	142.4	0.0047
1.7656	1.9658	612.42	145.0	0.0028
2.8287	2.3634	622.87	150.6	0.0003
4.0214	2.7091	635.58	160.9	0.0002
4.6062	2.7218	638.01	165.4	0.0005
5.1026	2.8498	644.15	169.4	0.0002
6.2915	3.4881	647.88	175.6	0.0016
8.6109	3.7198	661.68	189.5	0.0026
9.8184	3.8434	666.88	194.5	0.0091

Table 1-3f: Least-Squares Fitted Values of the Parameters of Eq(1-1) for the Viscosity of $NaNO_3$ - H_2O System.

m ($mol.kg^{-1}$)	$A_\eta \times 10^3$	B_η	T_o(K)	Std. dev. in $\ln \eta$
0.1113	1.0664	637.01	134.5	0.0038
0.5212	1.1733	623.42	135.5	0.0056
1.0532	1.2468	617.12	136.6	0.0067
1.8119	1.3797	616.11	137.5	0.0040
2.5441	1.5720	596.33	138.5	0.0028
3.3185	1.8051	586.99	139.5	0.0026
4.3956	2.1173	570.22	140.8	0.0071
5.3402	2.4735	560.66	142.0	0.0027
6.2532	2.6189	560.16	144.0	0.0045
7.3990	2.8223	563.44	145.6	0.0096
8.3060	2.9478	567.82	146.0	0.0018
9.8626	3.1307	576.64	148.0	0.0184

extrapolating the plot of T_o versus m (Fig 1-4) to the corresponding concentrations. Furthermore, the T_o value (205.7°K) of $Na_2S_2O_3 \cdot 5H_2O$ (11.1 m) obtained by a similar extrapolation of the computed T_o values of sodium thiosulfate solutions is found to be in agreement with the value 203°K reported by Moynihan.[9] The T_o values of $Ca(NO_3)_2$-H_2O, $Mg(NO_3)_2$-H_2O, $MgCl_2$-H_2O, and $NiCl_2$-H_2O systems are also seen to be comparable within $\sim$ 10-15°K with their reported[13] T_g values. The above comparisons, therefore, appear to justify our data analysis.

Concentration dependence of A_η , B_η , and T_o parameters

Initially, in order to know the empirical nature of the concentration dependence of T_o, A_η , and B_η parameters we plotted (Figs 1-4 to 1-6) their values against molality of the solute. In all the systems studied here T_o increases linearly with m, A_η increases non-linearly with m, and B_η decreases linearly with m up to a particular concentration and then starts increasing linearly. The concentration limit, m_c (critical concentration) beyond which B_η increases with m is found to have a value characteristic of the electrolytic solution, viz., 3.2 m, 4.63 m, 2.85 m, 2.4 m, 2.5 m, and 5.7 m for $Ca(NO_3)_2$-H_2O, $Mg(NO_3)_2$-H_2O, $MgCl_2$-H_2O, $NiCl_2$-H_2O,

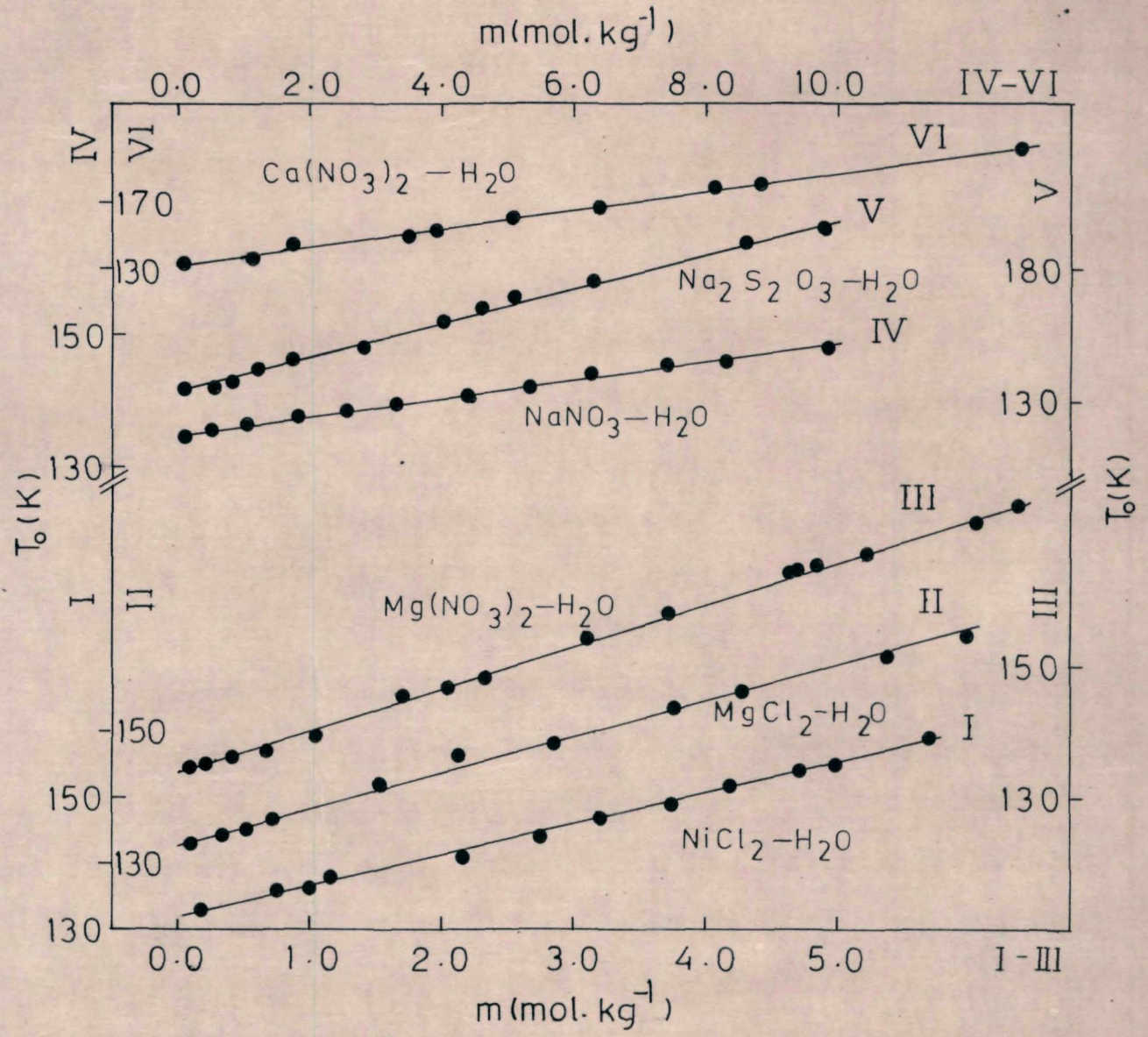

Fig 1-4. Plots of T_o vs. molality for aqueous electrolytes.

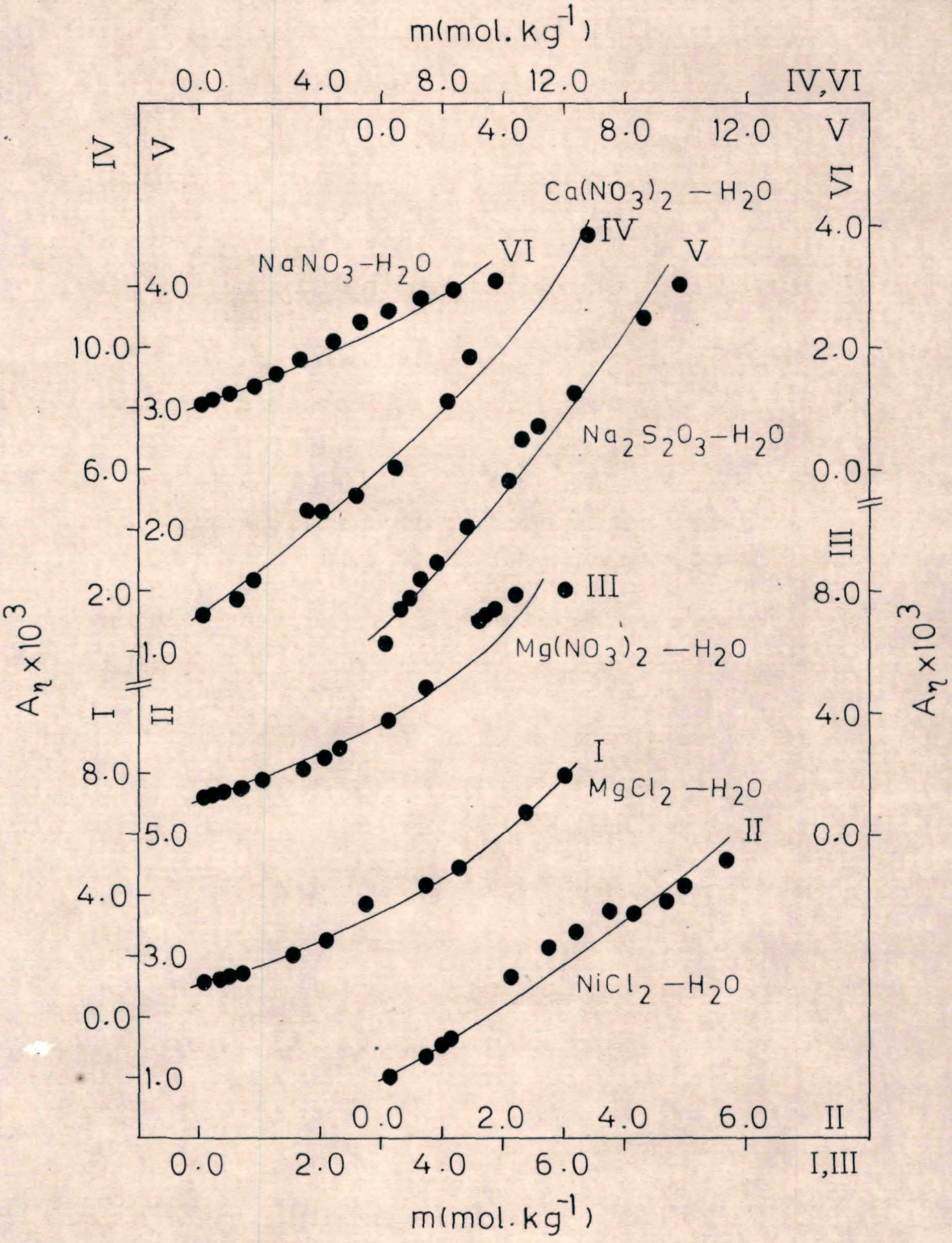

Fig 1-5: Plots of A_η vs. molality for aqueous electrolytes.

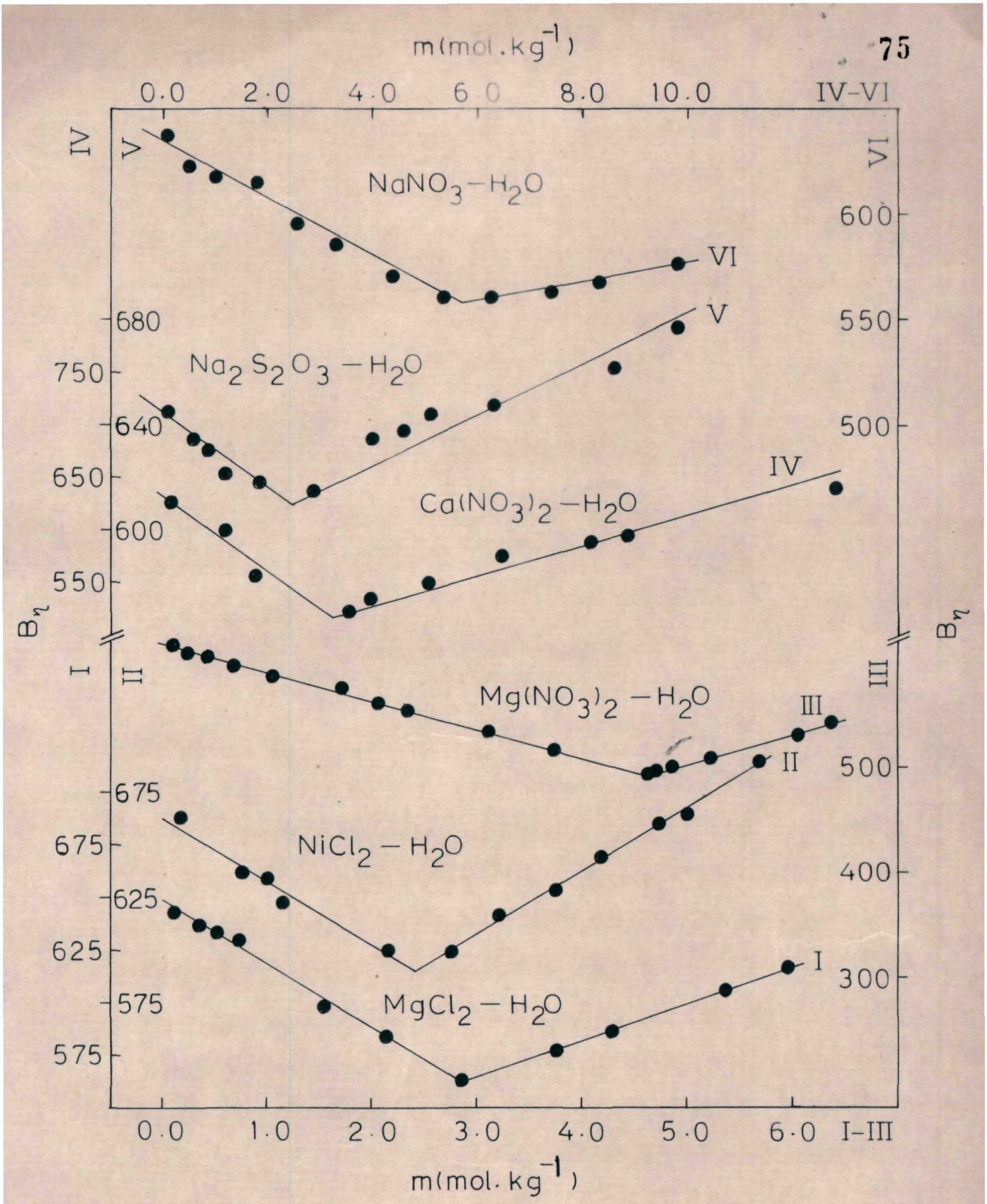

Fig 1-6. Plots of B_η vs. molality for aqueous electrolytes.

$Na_2S_2O_3$-H_2O, and $NaNO_3$-H_2O systems, respectively.

The linear increase of T_o with m may be described in terms of the interactions taking place in the electrolytic system. Since contribution to viscosity from the ion-ion interaction is relatively significant only at very low concentrations, in the experimental range of concentration contribution due to the ion-solvent interaction may be considered to dominate. The ion-solvent interaction causes solvation of solute particles which, in turn, causes the system to lose some of its configurational degrees of freedom thereby resulting in a decrease of the configurational entropy of the electrolytic solution. The configurational entropy must therefore decrease with increasing concentration. On the other hand, T_o which is defined as the temperature at which configurational entropy becomes zero must increase with increase in concentration. Thus T_o may be related to the hydration phenomenon in terms of the probability, p, of finding a solvent particle in the hydration shells of the solute particles. p is equal to $nm/55.51$, where n is the total hydration number of the solute molecule, and the linearity of the plot of T_o versus m (Fig 1-4) therefore appears to envisage a direct correlation between T_o and p. Quantitatively the concentration dependence of T_o may be written as

$$T_o = T_o(o) + Qm \qquad (1\text{-}2)$$

where $T_o(o)$ is the T_o of pure water and Q is the slope. The value of $T_o(o)$ in the cases of all the systems studied here is found to be 132 $\pm$ 1K which is in agreement with the reported[14] glass transition temperature (139°K) for amorphous water. The least squares fitted values of Q for the $Ca(NO_3)_2$-H_2O, $Mg(NO_3)_2$-H_2O, $MgCl_2$-H_2O, $NiCl_2$-H_2O, $Na_2S_2O_3$-H_2O, and $NaNO_3$-H_2O systems are 5.60, 6.44, 5.41, 4.66, 6.50, and 1.37 K. mol^{-1}. kg, respectively.

In the light of the correlation made above between T_o and p it is apparent that Q must be proportional to the total hydration number of the solute particle. Although obtaining the value of n from the knowledge of Q alone may not be possible, the ratio of the hydration numbers of the different solutes may be estimated from the ratio of the respective Q values with the assumption that the proportionality constant for the dependence of Q on n is the same for all the electrolytes studied here. The values of Q ratios calculated for the different pairs of electrolytes are listed in Table 1-4. An approximate estimation of the ratios of hydration numbers of the electrolytes under interest may be done using the reported values of the ionic hydration numbers for Ca^{2+} (=4),[1,15-17] Mg^{2+} (=6),[1,18-21] Ni^{2+} (=6),[19,22,23] Na^{+} (=4),[24-26] Cl^{-} (=6),[19,27] and NO_3^{-} (=9)[28] and the values

Table 1-4: Values of Q, n, and m_c Ratios for Different Pairs of Electrolytes.

System	Q ratio	n ratio	m_c ratio
$Ca(NO_3)_2/Mg(NO_3)_2$	0.87	0.91	0.69
$Ca(NO_3)_2/MgCl_2$	1.03	1.22	1.12
$Ca(NO_3)_2/NiCl_2$	1.20	1.22	1.33
$Mg(NO_3)_2/MgCl_2$	1.19	1.33	1.62
$Mg(NO_3)_2/NiCl_2$	1.38	1.33	1.93
$MgCl_2/NiCl_2$	1.16	1.00	1.19
$Ca(NO_3)_2/NaNO_3$	4.07	1.69	0.56
$Mg(NO_3)_2/NaNO_3$	4.69	1.84	0.81
$Ca(NO_3)_2/Na_2S_2O_3$	0.86	-	1.28
$Mg(NO_3)_2/Na_2S_2O_3$	0.99	-	1.85

obtained thus are also given in Table 1-4 for comparison. In view of the facts that the second hydration number of the solute also contributes to the T_o value of the solution and secondly the total hydration number of the solute may not be exactly additive of its ionic hydration numbers, the agreement found between the Q and the corresponding n ratios for the different pairs of 2-1-valent electrolytes seems to be quite reasonable. A large difference has, however, been observed between the Q and n ratios when the pair of electrolytes considered are of different valence type, e.g., $Ca(NO_3)_2$ and $NaNO_3$ or $Mg(NO_3)_2$ and $NaNO_3$. This may be attributed to the fact that the value of the proportionality constant for the dependence of Q on n in the case of a 2-1-valent electrolyte may be very much different from that for a 1-1-valent electrolyte. Furthermore, it is interesting to find that the values of the Q ratios are also comparable with those of the corresponding critical concentration ratios (m_c ratio) which are also included in Table 1-4. The critical concentration may be considered as the concentration at which Gurney's cospheres[5,13,29] of solute particles begin to overlap. Consequently, the value of the critical concentration seems to be proportional to the total hydration number of the solute particle and hence the critical concentration ratio may be related to the ratio of the corresponding hydration numbers. Such a probable

correlation between the ratios of hydration numbers and of critical concentrations therefore appears to account for the observed agreement between the Q ratios and the latter. However, the agreement between Q and m_c ratios is not very much striking as apparent from Table 1 - 4. This may be due to the fact that the critical concentration value of an electrolyte, besides having dependence on n, is likely to be governed by the structural behaviour of the electrolyte and hence must be considered more appropriately as a structural factor rather than considering it simply as a concentration at which Gurney's cosphere overlap (cf. latter part of this chapter).

The foregoing discussion thus establishes the proposed linear relationship between T_o and p. It may be cited that a close dependence of T_o on the hydration number of the solute was also revealed earlier by the attempt made by Angell and Sare[13] to correlate T_o parameter with the viscosity B coefficient (B parameter of the Jones-Dole equation[30]) as well as with the pK_a of the conjugate acid of the anion of the solute.

In order to describe the concentration dependences of A_η and B_η parameters (Figs 1-5 and 1-6) in the light

of Adam-Gibbs model, we first made an attempt to account for the temperature dependence of configurational heat capacity, ΔC_p, in Eq(0-15) for S_c. The difficulty in accounting theoretically for the temperature dependence of heat capacity has been highlighted in the earlier section (General Introduction). In the absence of a rigorous theoretical description for the variation of heat capacity of electrolytic solutions with temperature, an alternative approach to account for the temperature dependence of ΔC_p in Eq(0-15) would be to take into cognizance the general trend in the empirical behaviour of C_p with temperature. Similar alternative approaches were adopted by others also.[5,31]

From the recent studies made by Angell and Tucker[32] on the heat capacities of electrolytic solutions it is apparent that their heat capacities vary almost linearly before and after the glass transition (a sharp change in C_p occurs around T_g only) over a considerable range of temperature. Accordingly ΔC_p may be written as

$$\Delta C_p = C_{ol} + C_{1l}\,(T-T_o) - C_{og} - C_{1g}\,(T-T_o)$$

$$= \Delta C_o + \Delta C_1\,(T-T_o) \qquad (1\text{-}3)$$

where C_{ol} is the extrapolated heat capacity of the solution at T_o, C_{1l} is the slope of the linear variation of solution heat capacity with temperature, C_{og} is the heat capacity of the corresponding glass at T_o, C_{1g} is the slope of the linear variation of glass heat capacity with temperature, $\Delta C_o = C_{ol} - C_{og}$, and $\Delta C_1 = C_{1l} - C_{1g}$. It may be noted that Eq (1-3) is similar to one of the heat capacity functions considered by Privalko.[31] On introducing such a temperature dependence of ΔC_p in Eq(0-15), we get

$$S_c = \Delta C_2 \ln(T/T_o) + C_1(T-T_o) \qquad (1\text{-}4)$$

where $\Delta C_2 = \Delta C_o - \Delta C_1 T_o$. Substitution of this result for S_c in the Adam-Gibbs equation for transport property [Eq (0-14)] provides for η an expression of the form

$$\eta = AT^{1/2} \exp\left\{ B/\left[T\,\Delta C_2 \ln(T/T_o) + T\,\Delta C_1 (T-T_o) \right] \right\} \qquad (1\text{-}5)$$

where A and B are constants for a particular system. It may be noted that the pre-exponential $T^{1/2}$ term has been incorporated in the original Adam-Gibbs equation for the sake of comparison with Eq(1-1). This is possible because the

temperature dependence of η is almost entirely governed by the exponential part of Eq(1-5). Eq(1-5) may be approximated (Appendix I) to a simpler equation of the type

$$\eta = AT^{1/2} \exp\left\{B'/\left[T(T-T_o)\right]\right\} \qquad (1\text{-}6)$$

where $B' = BT_o(1-\Delta C_1 T_o/\Delta C_2)/\Delta C_2$. Furthermore, from Eq (1-6) the VTF equation may be derived by approximating $1/T$ to $\left[1-(T-T_o)/T_o\right]/T_o$ and thus we obtain

$$\eta = A_1 T^{1/2} \exp(-B_1/T_o)\exp\left\{\left[B_1(1-\Delta C_1 T_o/\Delta C_2)\right]/(T-T_o)\right\} \qquad (1\text{-}7)$$

where $A_1 = A \exp(B_1 \Delta C_1/\Delta C_2)$ and $B_1 = B/\Delta C_2$

Comparing Eqs(1-1) and (1-7) it may be seen that

$$B_\eta = B_1\left[1-(\Delta C_1/\Delta C_2)T_o\right] \qquad (1\text{-}8)$$

The concentration dependence of B_η may now be examined in the light of Eq(1-8) by plotting the values of B_η for the different solutions versus T_o (Fig 1-7). From the plot it is apparent that in all the solutions B_η first decreases linearly with increase in T_o up to the critical concentration which is

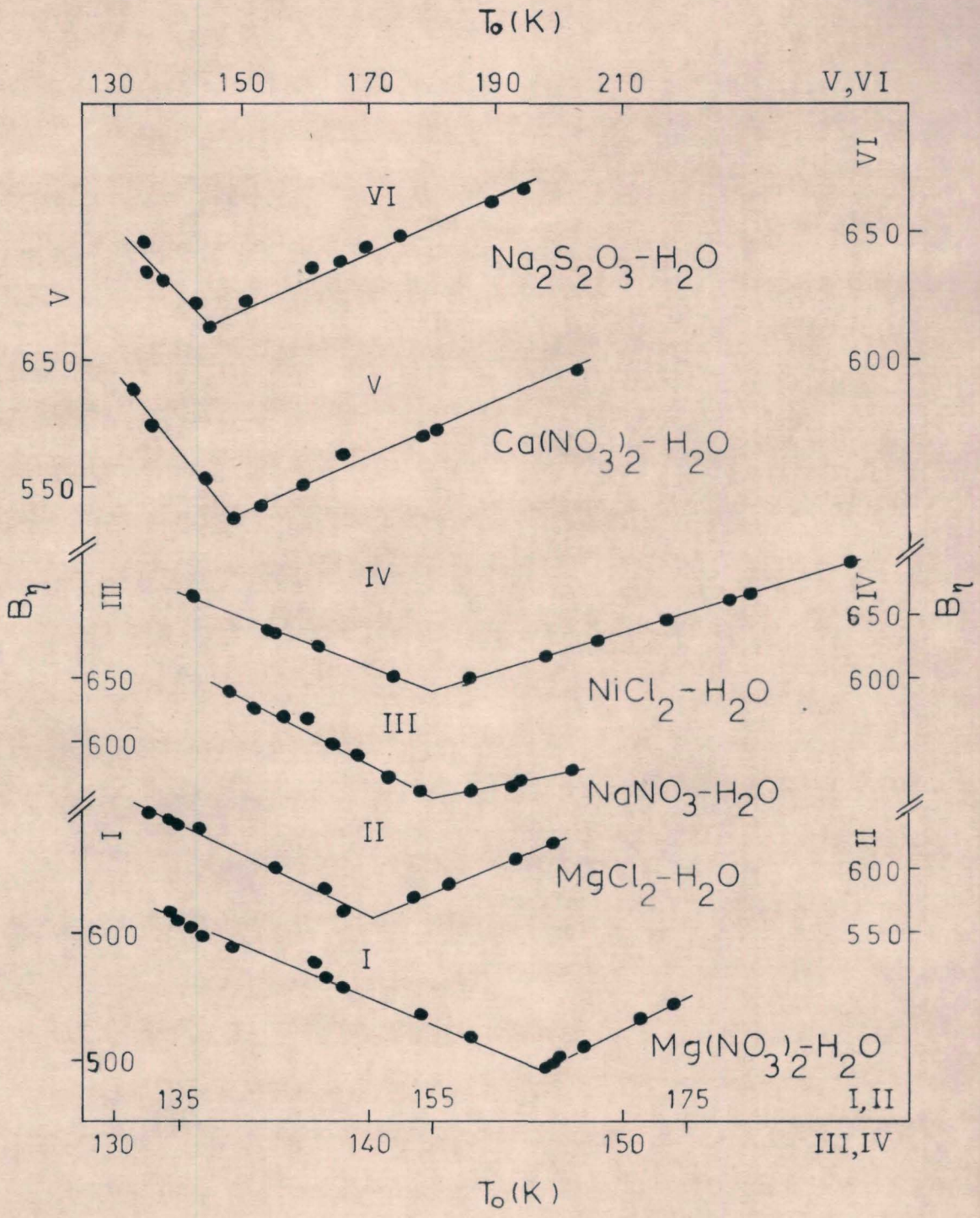

Fig 1-7. Plots of B_η vs. T_o for aqueous electrolytes.

consistent with Eq(1-8). This, in turn, explains the linear decrease of B_η with increase in m (Fig 1-5) as we have already seen that T_o is a linear function of m. The linear decrease of B_η also implies that up to the critical concentration $\Delta C_1/\Delta C_2$ remains almost independent of m in all the systems studied which is probably due to the same rates of decrease of ΔC_1 and ΔC_2 with concentration. However, it is evident from Fig 1-5 that above the critical concentration B_η increases linearly with T_o. It may be cited that a similar kind of behaviour of B_η(or B_ϕ) was earlier observed by others[5] in the case of $Ca(NO_3)_2$-H_2O system. In the light of Eq(1-8) we speculate that the increase of B_η with T_o above m_c is perhaps due to the linear increase of $\Delta C_1/\Delta C_2$ with $1/T_o$. In order to verify this we estimated, for instance, the values of $\Delta C_1/\Delta C_2$ for $Ca(NO_3)_2$-H_2O systems from its reported[31] heat capacity data and, in fact, found that $\Delta C_1/\Delta C_2$ varies linearly with $1/T_o$ at concentrations lying above the critical concentration value with negative intercept and positive slope. Eq(1-8) after substituting for such variation in $\Delta C_1/\Delta C_2$ above the critical concentration, therefore, satisfactorily accounts for the observed linear increase of B_η with T_o.

Comparison of Eqs(1-1) and (1-7) further provides

$$A_\eta = A_1 \exp(-B_1/T_o) \qquad (1\text{-}9)$$

In order to describe in the light of Eq(1-9) the concentration dependence of A_η, illustrated in Fig 1-6, we plotted $\ln A_\eta$ versus $1/T_o$ and interestingly a linear plot with a negative slope (Fig 1-8) was obtained. This emphasizes the success of Eq(1-9) in explaining quantitatively the concentration dependence of A_η. The linearity of the plot of $\ln A_\eta$ versus $1/T_o$ further envisages that for a particular solution B_1 remains a constant throughout the experimental concentration range as it was revealed above from the concentration dependence of B_η parameter also. The value of B_1 obtainable from the least-squares fitting of A_η values to Eq(1-9) is found to be significantly lower than its value obtainable, on the other hand, from the least-squares fitting of B_η values below the critical concentration to Eq(1-8). For instance, in the case of $Ca(NO_3)_2$-H_2O system the least-squares fitted values of B_1 derived from Eqs(1-8) and (1-9) are found to be 1465.0 and 907.3, respectively. Similar differences in the values of B_1 are observed in the cases of other systems under study also. Such a difference in the two values of B_1 appears to be attributable to the fact that in Eq(1-9) A_1 term includes the $\exp[B_1(\Delta C_1/\Delta C_2)]$ term which, in turn, is proportional to $\exp(\text{constant}/T_o)$ due to the linear increase of $\Delta C_1/\Delta C_2$ with $1/T_o$ above m_c. Consequently, the slope of $\ln A_\eta$ versus $1/T_o$ may be anticipated to be less

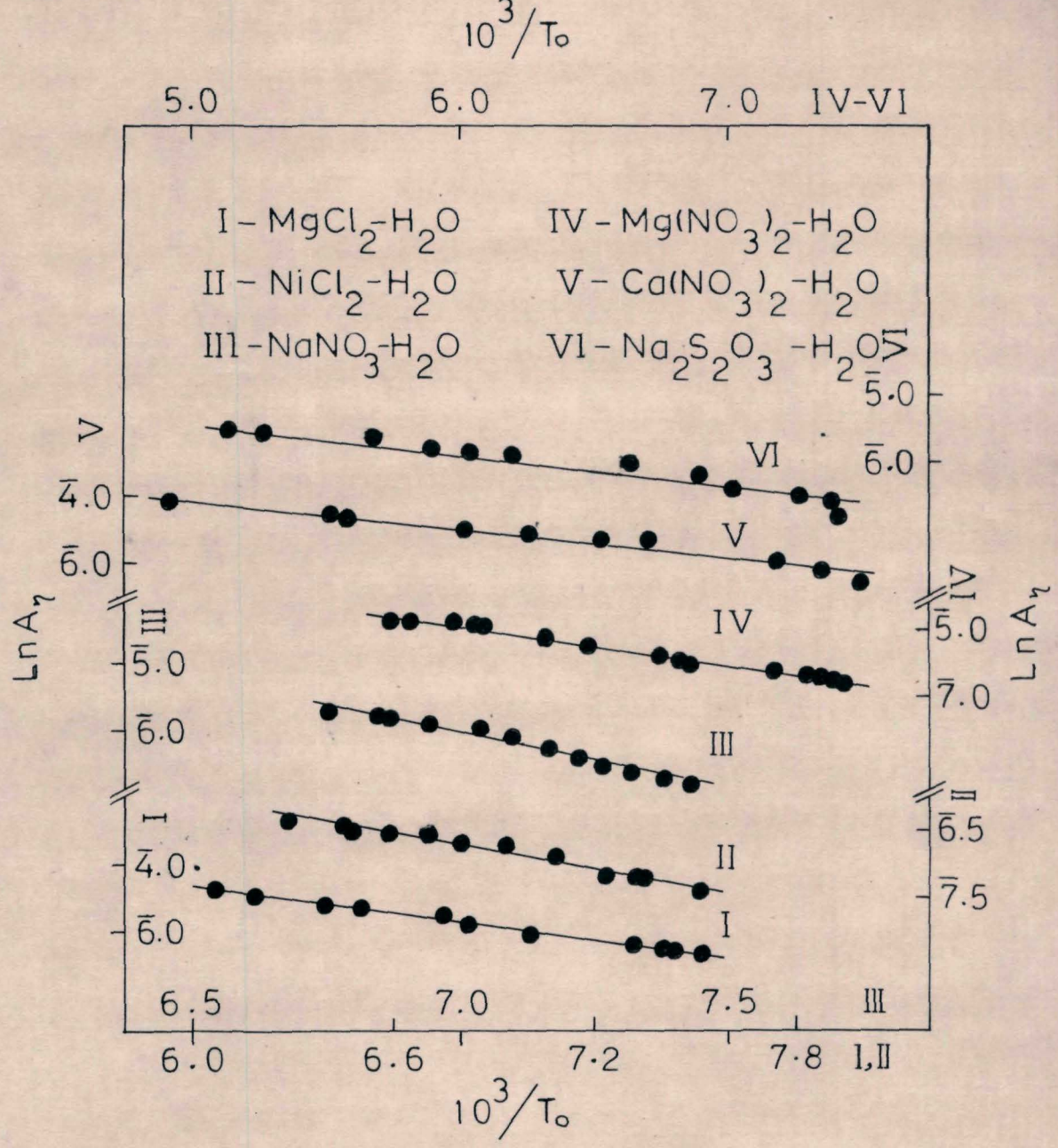

Fig 1-8. Plots of ln A_η vs. $1/T_o$ for aqueous electrolytes.

than B_1. In the light of this empirical finding, Eq(1-9) may be modified to

$$A_\eta = A' \exp(-B^*/T_o) \qquad (1\text{-}10)$$

where A' and B^* are constant terms and $B^* < B_1$.

Concentration Dependence of η

Substitution of Eqs(1-2), (1-8), and (1-10) in Eq (1-1) provides an isothermal expression for describing the overall concentration dependence of viscosity which is of the form

$$\eta = A^* \exp\left\{\left[-B^*/(T_o(o)+\Omega m)\right] + \left[B_1+\Omega_1(T_o(o)+\Omega m)\right]/\left[T-T_o(o)-\Omega m\right]\right\} \qquad (1\text{-}11)$$

where $A^* = A' T^{1/2}$ and Ω_1 is the slope of the linear plot of B_η versus T_o. B_1 and Ω_1, in fact, have different values below and above the critical concentration. It is worthwhile to note that the concentration dependence of viscosity is completely governed by that of the ideal glass transition temperature. Eq(1-11) may be approximated (Appendix II) to a simpler isothermal equation of the type

$$\eta = a_{o\eta} \exp(b_{o\eta} m + c_{o\eta} m^2) \qquad (1\text{-}12)$$

where $a_{o\eta}$, $b_{o\eta}$, and $c_{o\eta}$ are constant parameters. Separate least-squares fittings are done in the three regions of concentration at different temperatures and the values of $a_{o\eta}$, $b_{o\eta}$, and $c_{o\eta}$ obtained thus are listed in Tables 1-5. From Tables 1-5 it is apparent that Eq(1-12) satisfactorily describes the concentration dependence of η in the entire experimental range of concentration in spite of the fact that in this entire range of concentration the nature of the concentration dependence of B_η is not the same throughout. This is due to the adjustable tendency of the $a_{o\eta}$, $b_{o\eta}$, and $c_{o\eta}$ parameters so as to give a best-fitting. The success of Eq(1-12) in describing the concentration dependence of η is also envisaged by the linearity of the plots of $\log\eta$ versus $b_{o\eta}m+c_{o\eta}m^2$ (Fig 1-9) in the cases of all the electrolytic solutions under study.

It may be seen from Tables 1-5 that $c_{o\eta}$ takes up a very low value compared to $b_{o\eta}$. Therefore, at very low concentrations $c_{o\eta}m^2$ term may be neglected and Eq(1-12) becomes similar to the Einstein[33] equation or the Jones-Dole[30] equation without the ion-ion interaction term (at low concentrations, $\exp(b_{o\eta}m) \approx 1+b_{o\eta}m$ and $m \approx c$). Accordingly, the product of $a_{o\eta}$ and $b_{o\eta}$ terms must be equivalent to the viscosity B coefficient of the Jones-Dole equation. The

Table 1-5a: Least-Squares Fitted Values of the Parameters of Eq(1-12) for Viscosity of $Ca(NO_3)_2$-H_2O System.

T(K)	Concentration range in m (mol. kg^{-1})	$a_{o\eta}$	$b_{o\eta}$	$c_{o\eta} \times 10^3$	Std. dev. in ln η
298.0	0.1305 - 3.533	0.8891	0.2441	18.1228	0.002
	3.533 - 12.79	0.7754	0.3102	9.8511	0.040
	0.1305 - 12.79	0.8611	0.2813	11.5559	0.037
308.0	0.1305 - 3.533	0.7182	0.2646	11.8640	0.004
	3.533 - 12.79	0.6266	0.3201	6.4399	0.039
	0.1305 - 12.79	0.7001	0.2898	8.2131	0.036
343.0	0.1305 - 3.533	0.4241	0.2415	20.4688	0.003
	3.533 - 12.79	0.4323	0.2923	18.6951	0.048
	0.1305 - 12.79	0.4127	0.3035	1.2603	0.041

Table 1-5b: Least-Squares Fitted Values of the Parameters of Eq(1-12) for Viscosity of $Mg(NO_3)_2$ - H_2O System.

T(K)	Concentration range in m ($mol.kg^{-1}$)	$a_{o\eta}$	$b_{o\eta}$	$c_{o\eta} \times 10^3$	Std. dev. in ln η
298	0.0917 - 4.6299	0.8775	0.3284	8.1356	0.0114
	4.6299 - 4.8578	0.8749	0.3273	10.5142	0.0098
	0.0917 - 4.8578	0.8820	0.3166	11.6670	0.0015
308	0.0917 - 4.6299	0.7180	0.3106	10.4715	0.0076
	4.6299 - 5.2393	0.7143	0.3042	12.2315	0.0012
	0.0917 - 5.2393	0.7225	0.2967	14.3718	0.0124
323	0.0917 - 4.6299	0.5581	0.2911	12.4280	0.0103
	4.6299 - 6.3682	0.5498	0.3125	10.6928	0.0140
	0.0917 - 6.3682	0.5476	0.3218	6.5556	0.0271

Table 1-5c: Least-Squares Fitted Values of the Parameters of Eq(1-12) for Viscosity of $MgCl_2$ - H_2O System.

T(K)	Concentration range in m (mol. kg_{g}^{-1})	$a_{o\eta}$	$b_{o\eta}$	$c_{o\eta} \times 10^3$	Std. dev. in ln η
293	0.1145 - 2.8492	1.0326	0.3516	15.1027	0.003
	2.8492 - 5.3787	1.6177	0.0918	50.7708	0.004
	0.1145 - 5.3787	1.0480	0.3210	22.3947	0.018
308	0.1145 - 2.8492	0.7466	0.3526	10.1909	0.003
	2.8492 - 5.9872	1.0023	0.1733	36.4306	0.008
	0.1145 - 5.9872	0.7609	0.3126	20.2845	0.017
323	0.1145 - 2.8492	0.5786	0.3244	18.1105	0.003
	2.8492 - 5.9872	0.8653	0.1254	37.8289	0.010
	0.1145 - 5.9872	0.5831	0.3163	16.3528	0.018

Table 1-5d: Least-Squares Fitted Values of the Parameters of Eq(1-12) for Viscosity of $NiCl_2$ - H_2O system.

T(K)	Concentration range in m (mol. kg^{-1})	$a_{o\eta}$	$b_{o\eta}$	$c_{o\eta} \times 10^3$	Std. dev. in ln η
288	0.1736 - 2.1643	1.1682	0.3562	8.8936	0.006
	2.7529 - 4.9901	0.6250	0.6874	-24.975	0.007
	0.1736 - 4.9901	1.1617	0.3506	18.6401	0.020
308	0.1736 - 2.1643	0.7450	0.3502	11.6776	0.008
	2.7529 - 5.6853	0.7291	0.3685	9.4503	0.026
	0.1736 - 5.6853	0.7408	0.3581	10.8796	0.020
323	0.1736 - 2.1643	0.5571	0.4129	11.4230	0.031
	2.7529 - 5.6853	0.6459	0.3051	12.0026	0.022
	0.1736 - 5.6853	0.5596	0.3751	3.8780	0.018

Table 1-5e: Least-Squares Fitted Values of the Parameters of Eq(1-12) for Viscosity of $Na_2S_2O_3$ - H_2O system.

T(K)	Concentration range in m (mol. kg^{-1})	$a_{o\eta}$	$b_{o\eta}$	$c_{o\eta} \times 10^3$	Std. dev. in $\ln \eta$
288.0	0.0934 - 2.8287	1.1418	0.4226	-1.7852	0.0148
	4.0214 - 9.8184	0.6406	0.6452	-16.4704	0.0328
	0.0934 - 9.8184	1.0887	0.4672	-3.3316	0.0472
308.0	0.0934 - 2.8287	0.7278	0.4248	-14.2424	0.0111
	4.0214 - 9.8184	0.6931	0.4256	-6.0133	0.0228
	0.0934 - 9.8184	0.7288	0.4067	-4.5310	0.0433
323.0	0.0934 - 2.8287	0.5564	0.4131	-15.3133	0.0081
	4.0214 - 9.8184	0.6080	0.3563	-3.6741	0.0200
	0.0934 - 9.8184	0.5664	0.3799	-5.4060	0.0158

Table 1-5f: Least-Squares Fitted Values of the Parameters of Eq(1-12) for Viscosity of $NaNO_3$ - H_2O System.

T(K)	Concentration range in m ($mol.kg^{-1}$)	$a_{o\eta}$	$b_{o\eta}$	$c_{o\eta} \times 10^3$	Std. dev. in ln η
293.0	0.1113 - 5.3402	1.0051	0.1001	0.1038	0.0144
	6.2532 - 9.8626	1.3064	0.1753	-4.3541	0.0138
	0.1113 - 9.8626	1.0033	0.0997	0.6655	0.0160
308.0	0.1113 - 5.3402	0.7216	0.1060	-0.1123	0.0169
	6.2532 - 9.8626	0.6504	0.1391	-2.6077	0.0001
	0.1113 - 9.8626	0.7191	0.1097	-0.5960	0.0141
323.0	0.1113 - 5.3402	0.5560	0.1062	-0.3007	0.0138
	6.2532 - 9.8626	0.5740	0.0982	0.2165	0.0036
	0.1113 - 9.8626	0.5561	0.1061	-0.2626	0.0112

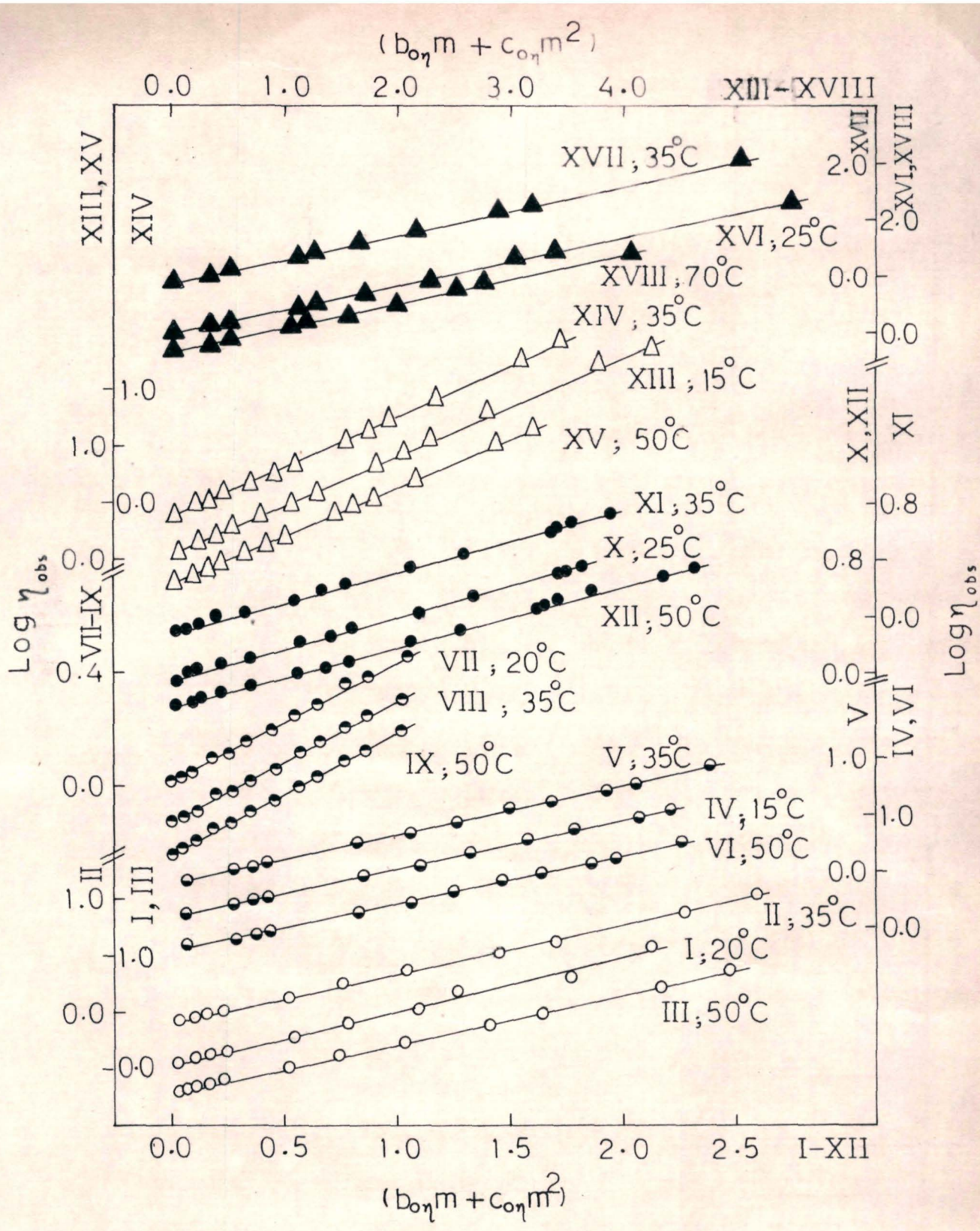

Fig 1-9. Plots of log η_{obs} vs. $b_{o\eta}\,m+c_{o\eta}\,m^2$ for aqueous electrolytes (o - $MgCl_2$, ⊖ - $NiCl_2$, ⊜ - $NaNO_3$, ● - $Mg(NO_3)_2$, Δ - $Na_2S_2O_3$, and ▲ - $Ca(NO_3)_2$ solutions).

values of B coefficients at 25°C calculated in this manner using the least-squares fitted values of $a_{o\eta}$ and $b_{o\eta}$ below the critical concentrations for $Ca(NO_3)_2$, $Mg(NO_3)_2$, $MgCl_2$, $NiCl_2$, and $NaNO_3$ aqueous solutions are 0.217, 0.288, 0.324, 0.315, and 0.052, respectively which are in good agreement with the literature values.[34] Moreover, using the relationship between m and c and neglecting the $c_{o\eta}$ term, Eq(1-12) may be reduced (Appendix III) to the Vand's equation[35] thereby providing a description for the success of Vand's equation at higher concentrations. Similarly, Eq(1-12) may be brought to the form of Angell and Bressels' equation[5] using the relationship between m and mole fraction, x(Appendix IV). Another noteworthy point is that the reduced form of Eq(1-12) at low concentrations, i.e. $a_{o\eta} \exp(b_{o\eta}c)$, is similar to the Arrhenius isothermal equation[36] employed to describe the concentration dependence of viscosity at relatively low concentrations.[11,37] Therefore, Eq(1-12) provides a basis to the Arrhenius isothermal equation as well as to a similar equation suggested by Carbonell.[38] Furthermore, Suryanarayana and Venkatesans' empirical equation[39] [Eq(0-6)] which was found to describe the concentration dependence of viscosity of electrolytic solutions from dilute region up to saturation point may

also be shown (Appendix V) to be an approximate form of Eq(1-12). The above correlations made between Eq(1-12) and other isothermal expressions proposed in the literature thus strongly emphasize the suitability of Eq(1-12) for describing the dependence of viscosity on concentration.

Finally, it is worthwhile to make an attempt to provide a structural interpretation to the observed minimum in the B_η versus m or T_o plot. The sudden change in the nature of concentration dependence of B_η envisages some kind of structural transition at the critical concentration. In the case of $Ca(NO_3)_2$-H_2O system a structural transition may therefore be expected to occur around 3.2 m which is in accordance with the observation of Angell and Bressel.[5] They suggested that this transition is probably due to the incompatibility of the net work water structure with an ionic liquid structure involving anions and hydrated cations leading to liquid-liquid phase separation at sufficiently low temperature. In the case of $NiCl_2$ solution Maisano et.al.[40] suggested a structural transition around 2m which is comparable with the critical concentration of $NiCl_2$-H_2O system observed in the present study. Furthermore, in the light of the attempts made by others[41,42] to correlate viscosity isotherms with the melting point curves of binary systems containing organic salts, it is interesting to find in the present

study that the critical concentration values of the $Ca(NO_3)_2$-H_2O, $Mg(NO_3)_2$-H_2O, $MgCl_2$-H_2O, and $NiCl_2$-H_2O systems are comparable with their respective first eutectic points.[13] Therefore, although it may not be possible in the absence of an intensive structural study to know the exact nature of the structural transition occurring around the critical concentration, a transition to a quasi-crystalline or lattice like structure[43] may, however, be anticipated in view of the above consideration.

References

1. C.A. Angell, J. Phys. Chem., 70, 3988 (1966).
2. N. Islam and K. Ismail, J. Phys. Chem., 80, 1929 (1976).
3. N. Islam, K.P. Singh, and S. Kumar, J.C.S. Faraday Trans. I, 75, 1312 (1979) and references therein.
4. M.H. Cohen and D. Turnbull, J. Chem. Phys., 31, 1164 (1959).
5. C.A. Angell and R.D. Bressel, J. Phys. Chem., 76, 3244 (1972).
6. W.W. Ewing and R.J. Mikovsky, J. Amer. Chem. Soc., 72, 1390 (1950).
7. J.A. Dean, ed., 'Lange's Handbook of Chemistry', 11th Ed., McGraw Hill, New York, 1973.
8. J.N. Pearce and H.C. Eckstrom, J. Phys. Chem., 41, 563 (1937).
9. C.T. Moynihan, J. Phys. Chem., 70, 3399 (1966).
10. R.C. Weast, ed., 'Handbook of Chemistry and Physics', 58th Ed., CRC Press, Ohio, 1977.
11. I.K. Taimni, J. Phys. Chem., 33, 52 (1929).
12. S. Phang, Aust. J. Chem., 32, 1149 (1979).
13. C.A. Angell and E.J. Sare, J. Chem. Phys., 52, 1058 (1970).
14. J.A. McMillan and S.C. Los, Nature, 206, 806 (1965).
15. C.A. Angell, J. Phys. Chem., 69, 2137 (1965).
16. T.J. Swift and W.G. Sayre, J. Chem. Phys., 44, 3567 (1966).
17. J.F. Hinton and E.S. Amis, Chem. Rev., 71, 627 (1971).

18. A. Fratiello, R.E. Lee, V.M. Nishida, and R.E. Schuster, J. Chem. Phys., 48, 3705 (1968).

19. H.G. Hertz, Angew. Chem. Internat. Ed., 9, 124 (1970).

20. A. Fratiello, D.D. Davis, S. Peak, and R.E. Schuster, Inorg. Chem., 10, 1627 (1971).

21. S.F. Lincoln, Coord. Chem. Rev., 6, 309 (1971).

22. R.E. Connick and D. Fiat, J. Chem. Phys., 44, 4103 (1966).

23. T.J. Swift and G.P. Weinberger, J. Amer. Chem. Soc., 90, 2023 (1968).

24. B.E. Conway and J.O'M. Bockris, 'Modern Aspects of Electrochemistry', Vol I, J. O M. Bockris, ed., Butterworths, 1954.

25. D.S. Allam and W.H. Lee, J. Chem. Soc. A, 5, 426 (1966).

26. J. O'M. Bockris and P.P.S. Saluja, J. Phys. Chem., 76, 2298 (1972).

27. A.H. Narten, J. Phys. Chem., 74, 765 (1970).

28. R. Caminiti, G. Licheri, G. Piccaluga, and G. Pinna, J. Chem. Phys., 68, 1967 (1978).

29. R.W. Gurney, 'Ionic Processes in Solutions', Dover Publications, New York, 1953.

30. G. Jones and M. Dole, J. Amer. Chem. Soc., 51, 2950 (1929).

31. V.P. Privalko, J. Phys. Chem., 84, 3307 (1980).

32. C.A. Angell and J.C. Tucker, J. Phys. Chem., 84, 268 (1980).

33. A. Einstein, Ann. Physik, 19, 289 (1906); 34, 591 (1911).

34. B. Breslau and I. Miller, J. Phys. Chem., 74, 1056 (1970).

35. V. Vand, J. Phys. Colloid Chem., 52, 277; 300; 314 (1948).

36. S. Arrhenius, Z. Physik. Chem., 1, 285 (1887).

37. J.N. Sugden, J. Chem. Soc., 129, 174 (1926).

38. J. Carbonell, Afinidad, 25, 451 (1968).

39. C.V. Suryanarayana and V.K. Venkatesan, Nature, 178, 1461 (1956); Acta Chim. Acad. Sci. Hung., 16, 149; 338 (1958).

40. G. Maisano, P. Migliardo, F. Wanderlingh, and M.P. Fontana, J. Chem. Phys., 68, 5594 (1978).

41. N.S. Kurnakov, D. Krotkov, M. Oksmann, I. Beketov, S. Perelmutter, F. Kanov, and I. Finkal, Z. Anorg. Allg. Chem., 135, 81 (1924).

42. R.H. Ewell, J. Chem. Phys., 5, 967 (1937).

43. H.P. Bennetto and J.J. Spitzer, J. Chem. Soc. Faraday Trans. I, 74, 2385 (1978).

CHAPTER II

TEMPERATURE AND CONCENTRATION DEPENDENCE OF CONDUCTANCE OF AQUEOUS ELECTROLYTES

Introduction

In the preceding chapter we have obtained based on the Adam-Gibbs model[1] an isothermal equation to describe the concentration dependence of viscosity of electrolytic solutions. Obtaining an expression for describing the concentration dependence of conductance is also equally important. Since Adam-Gibbs model has been employed to describe the temperature dependences of both viscosities and conductances of liquid systems, the isothermal equation derived from this model for explaining the concentration dependence of viscosity of electrolytic solutions may also be expected to hold good in the case of conductance. Accordingly in this chapter we have measured the conductances of the six electrolytic solutions cited in Chapter I as functions of temperature and concentration.

Experimental Section

Conductivity measurements were made as described under the Experimental Techniques.

Results and Discussion

The equivalent conductance values of all the systems under study are listed in Tables 2-1. These values are

Table 2-1a: Equivalent Conductance of $Ca(NO_3)_2 - H_2O$ System as Functions of Concentration and Temperature.

T(K)	Λ (mho cm^2 $equiv^{-1}$)	T(K)	Λ (mho cm^2 $equiv^{-1}$)
0.1305m		0.8116m*	
291.0	70.899	290.6	42.879
292.8	74.221	292.8	45.176
298.0	80.898	298.0	49.444
303.1	88.458	303.2	54.569
308.0	96.000	308.0	60.006
313.0	103.765	313.0	64.618
318.0	112.708	318.6	69.995
323.0	120.226	323.0	74.971
1.175m		1.752m	
290.0	35.001	291.0	26.754
292.1	36.575	293.1	28.005
298.0	41.229	298.0	30.940
302.9	45.182	303.0	34.127
308.0	49.107	308.0	37.352
313.0	53.726	313.0	40.698
318.1	58.816	317.6	43.775
323.0	62.598	323.0	47.518

Continued.

* Density of this solution is given by, $\rho = 1.1024 - 4.6995 \times 10^{-4} \theta(°C)$

Table 3-1a: (Continued)

T(K)	Λ (mho cm^2 $equiv^{-1}$)	T(K)	Λ (mho cm^2 $equiv^{-1}$)
3.533m		3.953m	
290.5	12.714	291.0	11.112
294.7	14.207	293.6	11.840
298.0	15.400	298.0	13.067
303.0	17.243	303.0	14.576
308.0	19.225	308.0	16.235
313.0	21.277	313.0	17.765
317.9	23.334	318.3	19.450
323.0	25.577	323.0	21.277
5.081m		6.450m	
291.0	7.5138	291.0	4.6154
293.8	8.0207	293.3	4.9392
298.0	8.9668	298.0	5.6081
303.0	9.8143	303.0	6.3674
308.0	10.973	308.0	7.0712
313.0	11.915	313.0	7.8589
318.0	13.029	318.2	8.7334
328.0	14.130	323.0	9.4356

Continued.

Table 2-1a: (Continued)

T(K)	Λ (mho cm^2 $equiv^{-1}$)	T(K)	Λ (mho cm^2 $equiv^{-1}$)
8.155m		8.864m	
290.0	2.0691	291.0	1.6727
293.3	2.3353	293.3	1.8168
298.0	2.7534	298.0	2.2018
303.0	3.2270	303.0	2.5800
308.0	3.7275	308.0	3.0154
313.0	4.2846	313.0	3.4728
317.9	4.8739	317.9	3.9786
323.0	5.4475	323.0	4.4762
11.428m*		12.790m	
290.9	0.6564	291.0	0.3009
293.4	0.7386	293.7	0.3558
298.0	0.9206	298.0	0.4715
303.0	1.1520	303.0	0.6048
308.0	1.3981	308.0	0.7699
313.0	1.6771	313.0	0.9625
318.2	2.0111	318.0	1.1722
323.0	2.3051	323.0	1.4033

* Density of this solution is given by, $\rho = 1.6798 - 4.0688 \times 10^{-4} t(^{\circ}C)$

Table 2-1b: Equivalent Conductance of $Mg(NO_3)_2$ - H_2O System as Functions of Concentration and Temperature.

T(K)	Λ (mho cm^2 $equiv^{-1}$)	T(K)	Λ (mho cm^2 $equiv^{-1}$)
0.2297m		0.4243m	
292.5	60.804	290.0	51.676
293.3	61.612	291.3	52.978
295.0	64.160	294.5	56.282
298.0	67.914	295.3	57.548
303.0	74.430	298.0	60.584
308.0	80.098	303.4	66.639
313.0	86.986	308.0	72.346
317.9	94.004	312.7	76.756
323.0	100.10	318.1	84.388
0.6753m		323.0	87.386
291.0	45.072		
294.1	47.810		
294.7	48.391		
298.0	51.465		
300.6	53.868		
302.8	55.802		
308.0	61.000		
313.1	65.956		
317.8	70.620		
323.0	75.820		

Continued.

Table 2-1b: (Continued)

T(K)	Λ (mho cm^2 $equiv^{-1}$)	T(K)	Λ (mho cm^2 $equiv^{-1}$)
1.0524m		1.7055m	
288.5	34.770	290.6	29.194
290.2	35.965	292.0	29.972
292.2	37.776	293.8	31.008
294.6	38.914	295.6	32.003
298.0	41.378	298.0	33.612
303.6	46.095	303.6	36.958
308.0	49.131	308.0	39.585
313.9	53.131	313.6	42.104
318.2	58.398	317.9	44.348
323.0	61.855	323.0	48.162
2.0428m		2.3300m	
291.9	26.239	291.2	22.633
294.3	28.054	294.7	24.105
296.4	28.922	298.0	25.657
298.0	29.549	303.7	28.586
303.6	32.603	308.0	30.438
308.0	34.614	312.2	32.698
313.4	37.365	316.9	34.987
318.7	40.582	323.0	37.092
323.0	43.053		

Continued.

Table 2-1b: (Continued)

T(K)	Λ_2 (mho cm^2 $equiv^{-1}$)	T(K)	Λ_2 (mho $cm^2 equiv^{-1}$)
3.1050m		3.7251m	
290.0	16.854	289.4	13.345
291.3	17.454	293.7	14.629
293.5	18.107	296.3	15.302
296.3	18.995	298.0	15.735
298.0	19.569	303.8	17.548
303.4	21.751	308.0	18.667
308.0	23.049	313.3	20.087
313.5	25.131	317.8	21.374
318.1	26.864	323.0	22.839
323.0	28.049		
4.6299m		4.7091m	
290.0	9.457	292.7	9.3412
293.6	10.262	293.5	9.5042
296.2	10.825	296.6	10.147
298.0	11.225	298.0	10.438
303.6	12.508	302.8	11.456
308.0	13.530	308.0	12.577
313.0	14.691	313.0	13.669
317.8	15.844	318.4	14.859
323.0	17.084	323.0	15.878

Continued.

Table 2-1b: (Continued)

T(K)	Λ (mho cm^2 $equiv^{-1}$)	T(K)	Λ (mho cm^2 $equiv^{-1}$)
4.8578m		5.2393m	
291.8	8.5714	308.0	10.071
293.0	8.8023	313.4	11.218
295.9	9.3606	317.2	11.951
298.0	9.7711	323.0	13.183
300.8	10.326	327.5	14.144
303.7	10.903	332.0	15.110
308.0	11.758	338.8	16.578
313.0	12.774	345.5	18.029
318.0	13.821		
323.0	14.855		

Table 2-1c: Equivalent Conductance of $MgCl_2$ - H_2O System as Functions of Concentration and Temperature.

T(K)	Λ_2 (mho cm^2 $equiv^{-1}$)	T(K)	Λ_2 (mho cm^2 $equiv^{-1}$)
0.1145m		0.3597m	
288.0	74.072	288.0	58.838
293.0	83.133	293.0	66.105
298.0	91.189	298.0	73.008
303.0	100.05	303.0	80.554
308.0	109.13	308.0	87.337
313.4	118.01	313.1	96.607
317.6	127.76	318.3	105.39
323.0	138.02	323.0	113.17
330.4	152.34		
0.7336m		1.5367m	
288.0	50.301	288.0	35.874
293.0	53.963	293.0	39.424
298.0	61.587	298.0	44.880
303.0	66.272	303.0	49.537
308.0	72.835	308.0	53.480
313.5	80.435	313.4	59.087
318.3	85.831	318.7	64.847
323.0	92.054	323.0	68.427
329.4	101.62	331.0	77.749

Continued.

Table 2-1c: (Continued)

T(K)	Λ (mho cm^2 $equiv^{-1}$)	T(K)	Λ (mho cm^2 $equiv^{-1}$)
2.1294m		2.8492m	
288.0	28.564	288.0	22.455
293.0	31.567	293.0	23.852
298.0	34.259	298.0	26.453
303.0	37.690	303.0	28.188
308.0	40.852	308.0	30.732
313.5	43.236	313.4	33.215
318.3	46.359	318.3	36.180
323.0	49.754	323.0	38.357
328.0	51.577	328.0	40.329
3.7490m		4.2721m	
288.0	14.884	288.0	12.505
293.0	17.687	293.0	14.071
298.0	19.390	298.0	15.872
303.0	20.186	303.0	17.550
308.0	22.268	308.0	18.015
313.5	24.271	313.3	19.959
318.3	25.983	317.9	21.591
323.0	28.228	323.0	23.469
328.3	30.141	328.2	25.512

Continued.

Table 2-1c: (Continued)

T(K)	Λ (mho cm^2 $equiv^{-1}$)	T(K)	Λ (mho $cm^2 equiv^{-1}$)
5.3787m		5.9872m	
288.0	6.9940	293.0	6.1217
293.0	7.9907	298.0	6.9611
298.0	9.6235	303.0	7.9117
303.0	10.444	308.0	8.8354
308.0	12.021	313.4	9.9370
313.2	13.332	318.1	10.316
318.3	14.728	323.0	11.465
323.0	14.954	328.1	12.622
328.0	16.321	333.5	13.825
		338.4	14.972

Table 2-1d: Equivalent Conductance of $NiCl_2$ - H_2O System as Functions of Concentration and Temperature.

T(K)	Λ (mho cm^2 $equiv^{-1}$)	T(K)	Λ (mho cm^2 $equiv^{-1}$)
0.1736m		0.7656m	
288.0	73.251	288.0	55.354
293.0	81.166	293.0	61.592
298.0	89.383	298.0	66.629
303.0	97.909	303.0	71.339
308.0	106.37	308.0	77.519
313.4	116.38	313.8	83.109
318.3	124.45	318.1	88.650
323.0	134.86	323.0	93.059
328.8	144.76	328.7	99.747
1.1481m		2.1643m	
288.0	44.615	288.0	26.571
293.0	50.168	293.0	30.063
298.0	55.125	298.0	32.816
303.0	59.573	303.0	35.619
308.0	67.296	308.0	38.578
313.2	73.543	313.2	41.612
318.3	79.807	318.3	44.389
323.0	84.816	323.0	47.185
328.9	93.346	328.7	50.533

Continued.

Table 2-1d: (Continued)

T(K)	Λ (mho cm^2 $equiv^{-1}$)	T(K)	Λ (mho cm^2 $equiv^{-1}$)
2.7529m		3.2131m	
293.0	23.314	293.0	19.479
298.0	25.400	298.0	21.321
303.0	27.792	303.0	23.565
308.0	30.345	308.0	25.808
313.1	32.589	313.4	28.602
318.3	34.969	318.5	30.859
323.0	37.350	323.0	32.532
328.4	39.942	329.0	34.655
3.7502m		4.1787m	
288.0	13.841	288.0	11.974
293.0	15.912	293.0	13.052
298.0	17.599	298.0	14.781
303.0	19.205	303.0	16.386
308.0	21.838	308.0	17.676
313.4	23.968	313.0	20.338
318.3	26.132	318.4	22.132
323.0	27.918	323.0	23.972
328.4	30.553	328.2	25.739

Continued.

Table 2-1d: (Continued)

T(K)	Λ (mho cm^2 $equiv^{-1}$)	T(K)	Λ (mho cm^2 $equiv^{-1}$)
4.7292m		4.9901m	
288.0	9.3358	288.0	7.7639
293.0	10.989	293.0	8.6897
298.0	11.900	298.0	10.178
303.0	13.412	303.0	11.143
308.0	14.852	308.0	12.403
313.0	16.044	313.4	13.771
318.1	18.460	318.4	14.878
323.0	19.927	323.0	16.792
328.2	21.614	328.6	18.363

Table 2-1e: Equivalent Conductance of $Na_2S_2O_3$ - H_2O System as Functions of Concentration and Temperature.

T(K)	Λ (mho cm^2 $equiv^{-1}$)	T(K)	Λ (mho cm^2 $equiv^{-1}$)
0.0823m*		0.5690m	
285.0	137.47	285.0	93.40
288.0	148.17	288.0	100.25
293.0	166.16	293.0	113.18
298.0	185.71	298.0	125.92
308.0	223.46	308.0	150.63
318.0	259.30	318.0	176.57
323.0	282.81	323.0	191.78
0.8714m		1.2120m	
285.0	82.871	285.0	72.743
288.0	89.225	288.0	78.520
293.0	99.853	293.0	87.820
298.0	111.14	298.0	98.409
308.0	135.05	308.0	120.03
318.0	161.75	318.0	144.24
323.0	174.55	323.0	155.91

Continued.

* Density of this solution is given by, $\rho = 1.0201 - 4.3042 \times 10^{-4} t(°C)$

Table 2-1e: (Continued)

T(K)	Λ (mho cm^2 $equiv^{-1}$)	T(K)	Λ (mho $cm^2 equiv^{-1}$)
1.7656m		2.3472m	
285.0	58.911	285.0	48.175
288.0	63.418	288.0	52.914
293.0	73.427	293.0	59.793
298.0	81.092	298.0	68.544
308.0	101.28	308.0	85.038
318.0	122.11	318.0	103.41
323.0	133.28	323.0	113.29
2.8287m		4.0214m	
285.0	41.532	285.0	26.064
288.0	46.681	288.0	28.823
293.0	53.721	293.0	34.564
298.0	61.644	298.0	40.121
308.0	79.093	308.0	52.909
318.0	98.851	318.0	67.949
323.0	109.22	323.0	75.666

Continued.

Table 2-1e: (Continued)

T(K)	Λ (mho cm^2 $equiv^{-1}$)	T(K)	Λ (mho cm^2 $equiv^{-1}$)
4.6062m		5.1026m	
285.0	23.492	285.0	19.106
288.0	25.963	288.0	21.326
293.0	30.223	293.0	25.640
298.0	35.563	298.0	30.138
308.0	45.472	308.0	40.039
318.0	57.597	318.0	51.465
323.0	63.549	323.0	57.501
6.2915m		8.6109m	
288.0	14.504	293.0	8.202
293.0	17.447	298.0	10.418
298.0	21.238	303.0	13.024
308.0	29.075	308.0	15.767
313.0	33.275	313.0	19.436
318.0	38.026	318.0	23.027
323.0	42.990	323.0	27.160

Continued.

Table 2-1e: (Continued)

T(K)	Λ (mho cm^2 $equiv^{-1}$)
9.8184m	
288.0	3.845
293.0	5.298
298.0	7.018
308.0	11.359
313.0	14.029
318.0	17.042
323.0	20.325

Table 2-1f: Equivalent Conductance of $NaNO_3$ - H_2O System as Functions of Concentration and Temperature.

T(K)	Λ (mho cm^2 $equiv^{-1}$)	T(K)	Λ (mho $cm^2 equiv^{-1}$)
0.1113m		1.0532m	
288.0	83.263	288.0	60.040
293.0	96.609	293.0	64.252
298.0	106.48	298.0	71.855
303.2	117.32	303.0	78.091
308.0	134.91	308.0	86.141
313.3	147.54	313.1	92.301
318.3	160.92	323.0	105.16
323.0	176.74	328.2	111.17
328.4	190.85		
1.8119m		2.5441m	
288.0	49.135	288.0	44.392
293.0	54.428	293.0	48.997
298.0	59.449	298.0	54.942
303.0	65.105	303.2	59.771
308.0	70.228	308.0	65.865
313.6	76.224	313.4	71.704
318.4	81.807	318.4	76.713
323.0	86.204	323.0	82.494
328.9	93.398	327.9	88.101

Continued.

Table 2-1f: (Continued)

T(K)	Λ (mho cm^2 $equiv^{-1}$)	T(K)	Λ (mho cm^2 $equiv^{-1}$)
3.3185m		4.3956m	
288.0	39.906	288.0	34.442
293.0	43.417	293.0	38.832
298.0	45.340	298.0	42.463
303.0	49.968	303.4	46.698
308.0	53.882	308.0	50.598
313.4	58.496	313.1	54.488
318.3	63.264	318.3	58.981
323.0	66.309	323.0	62.729
328.7	70.925	328.5	67.684
6.2532m		7.3990m	
288.0	26.021	288.0	23.250
293.0	29.105	293.0	25.746
298.0	31.818	298.0	28.308
303.0	34.885	303.5	31.155
308.0	37.799	308.0	33.460
313.4	40.543	313.4	36.337
317.9	42.978	318.2	38.880
323.0	46.258	323.0	41.426

Continued.

Table 2-1f: (Continued)

T(K)	Λ (mho cm^2 $equiv^{-1}$)	T(K)	Λ (mho cm^2 $equiv^{-1}$)
8.3060m		9.8626m	
288.0	20.928	288.0	18.285
293.0	23.495	293.0	20.563
298.0	25.816	298.0	22.635
303.6	28.606	303.6	25.133
308.0	30.713	308.0	26.999
313.3	33.296	313.5	29.366
318.5	35.790	318.2	31.357
323.0	38.004	323.0	33.485

compared with the reported data by plotting Λ versus normality, N (Fig 2-1). It is apparent from Fig 2-1 that the measured equivalent conductance data are comparable within about $\pm$ 2% with the reported values.[2-4]

In order to analyze the temperature dependence of Λ first we plotted $\ln \Lambda$ of each system versus 1/T (Figs 2-2). These plots reveal a deviation from Arrhenius behaviour in the cases of all the electrolytic solutions under study. However, the non-Arrhenius behaviour is not very much prominent due to relatively higher temperature range of measurement. The conductance data were therefore analyzed by least-squares fitting the measured values to the VTF equation which may be written for Λ as

$$\Lambda = A_\Lambda \; T^{-1/2} \exp\left[-B_\Lambda /(T-T_o)\right] \qquad (2\text{-}1)$$

where A_Λ , B_Λ , and T_o are constant parameters. The least-squares fitted values of A_Λ , B_Λ , and T_o are given in Tables 2-2. It may be noted that the computed values of T_o for the different systems are comparable with those obtained in Chapter I based on their viscosity data. Such an agreement between $T_o(\Lambda)$ and $T_o(\eta)$ of a particular

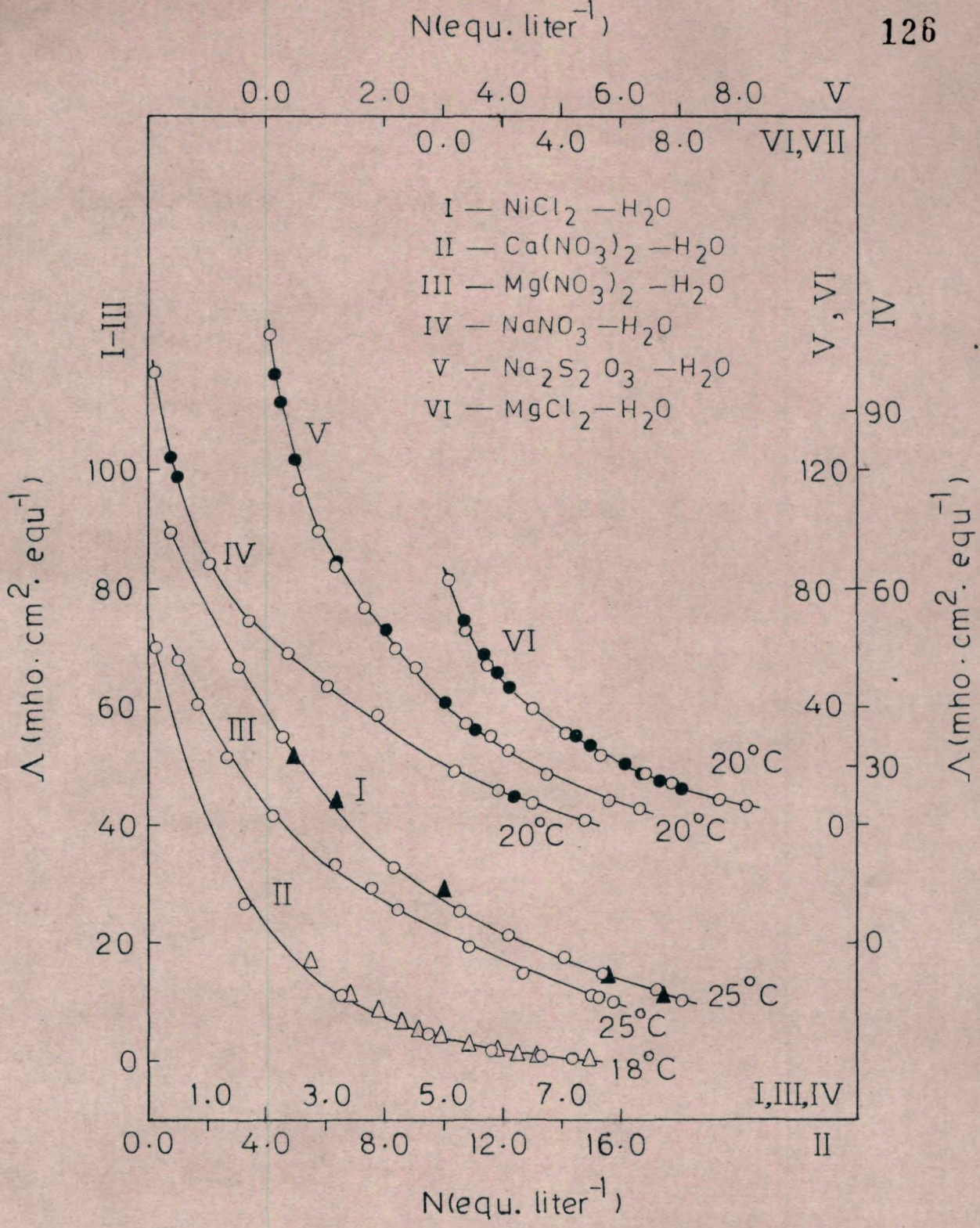

Fig 2-1: Equivalent conductance vs. normality isotherms for aqueous electrolytes (O - present data, ▲- ref. 2, Δ - ref. 3, and ● - ref. 4).

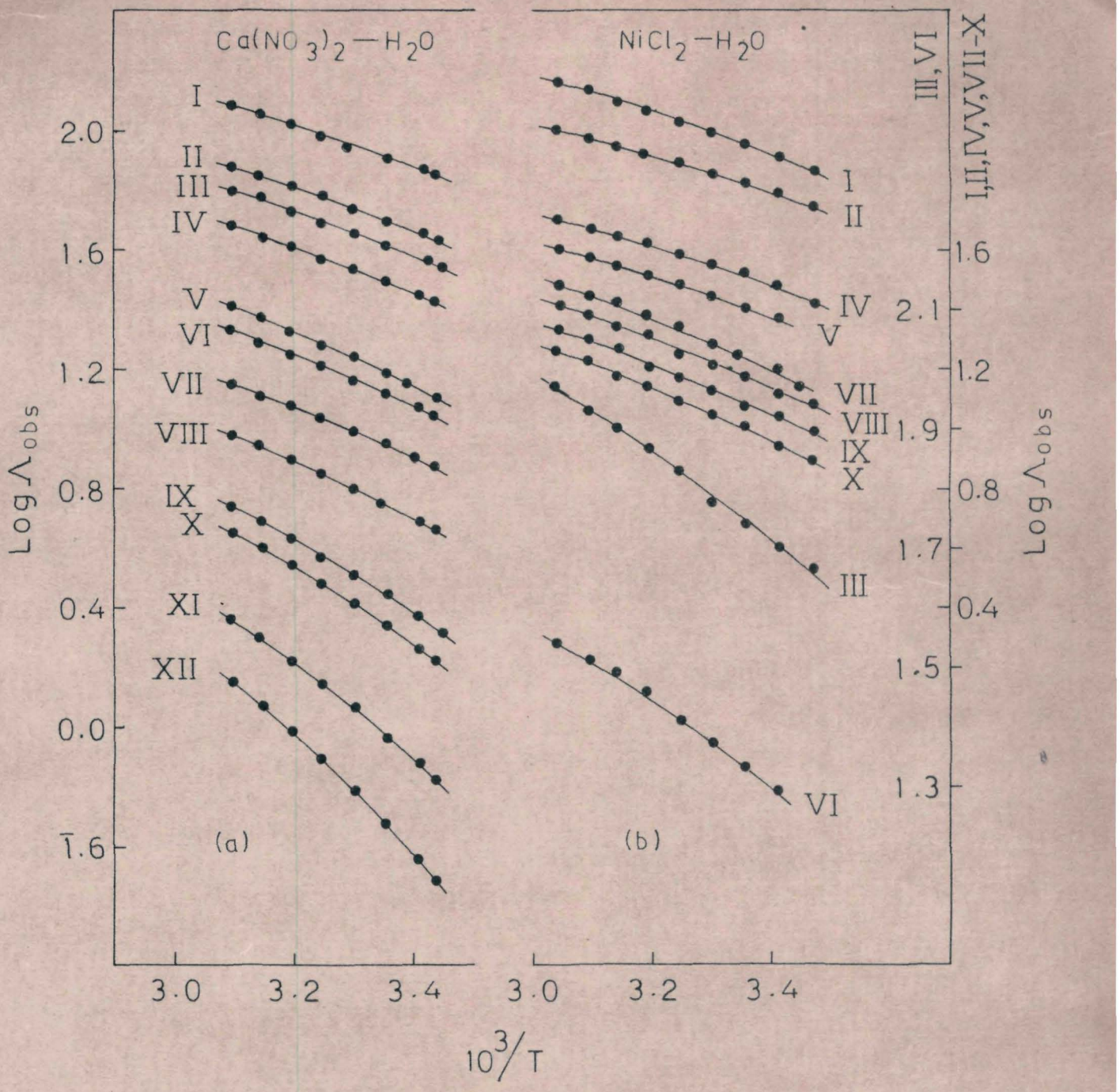

Fig 2-2a. Arrhenius plots for Λ of $Ca(NO_3)_2$-H_2O (the concentrations of the twelve solutions, I-XII, are in the same increasing order as given in Table 2-1a) and $NiCl_2$-H_2O(the concentrations of the ten solutions, I-X, are in the same increasing order as given in Table 2-1d) systems.

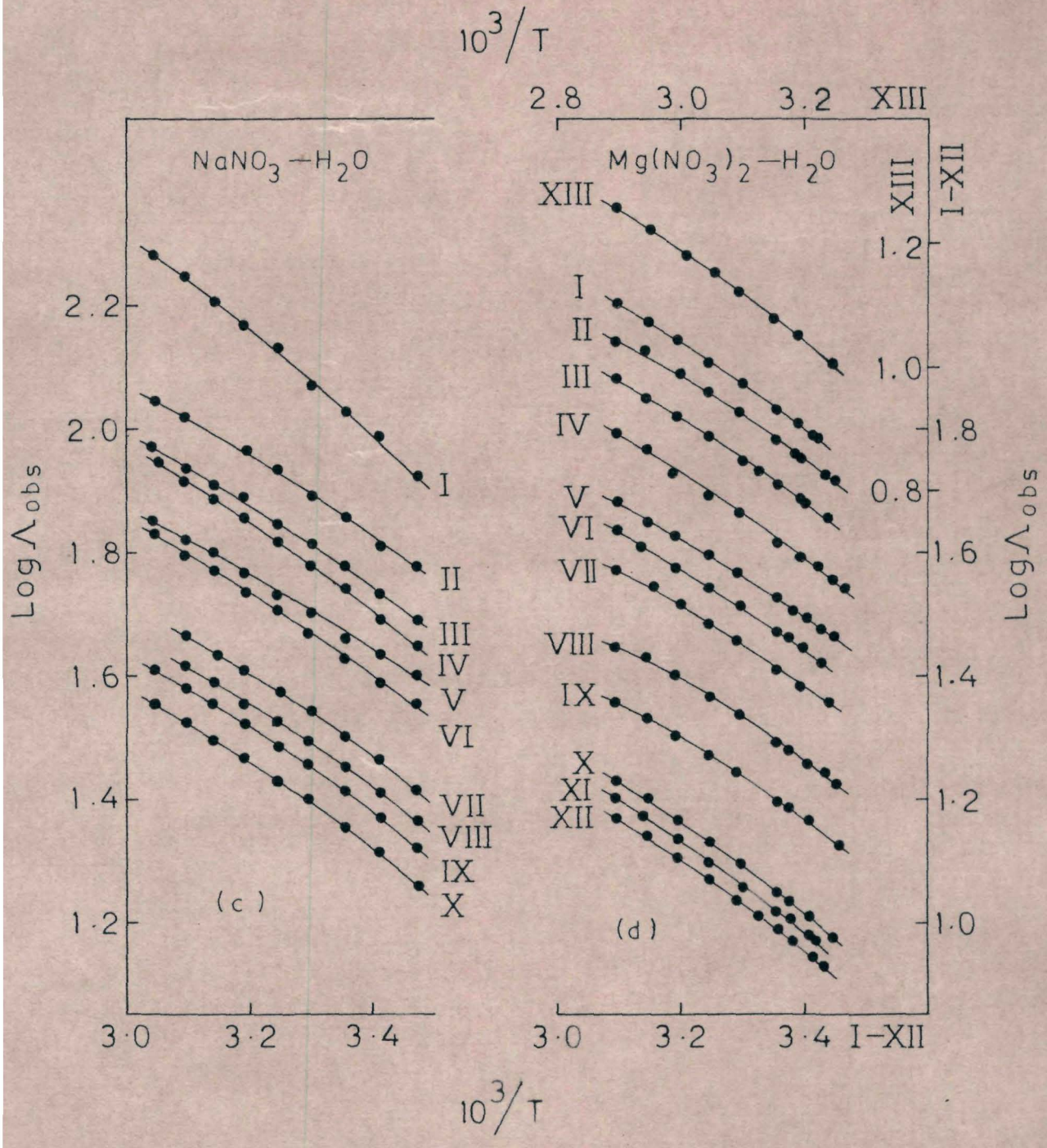

Fig 2-2b: Arrhenius plots for Λ of $NaNO_3$ - H_2O (the concentrations of the ten solutions, I - X, are in the same increasing order as given in Table 2-1f) and $Mg(NO_3)_2$-H_2O (the concentrations of the thirteen solutions, I - XIII, are in the same increasing order as given in Table 2-1b) systems.

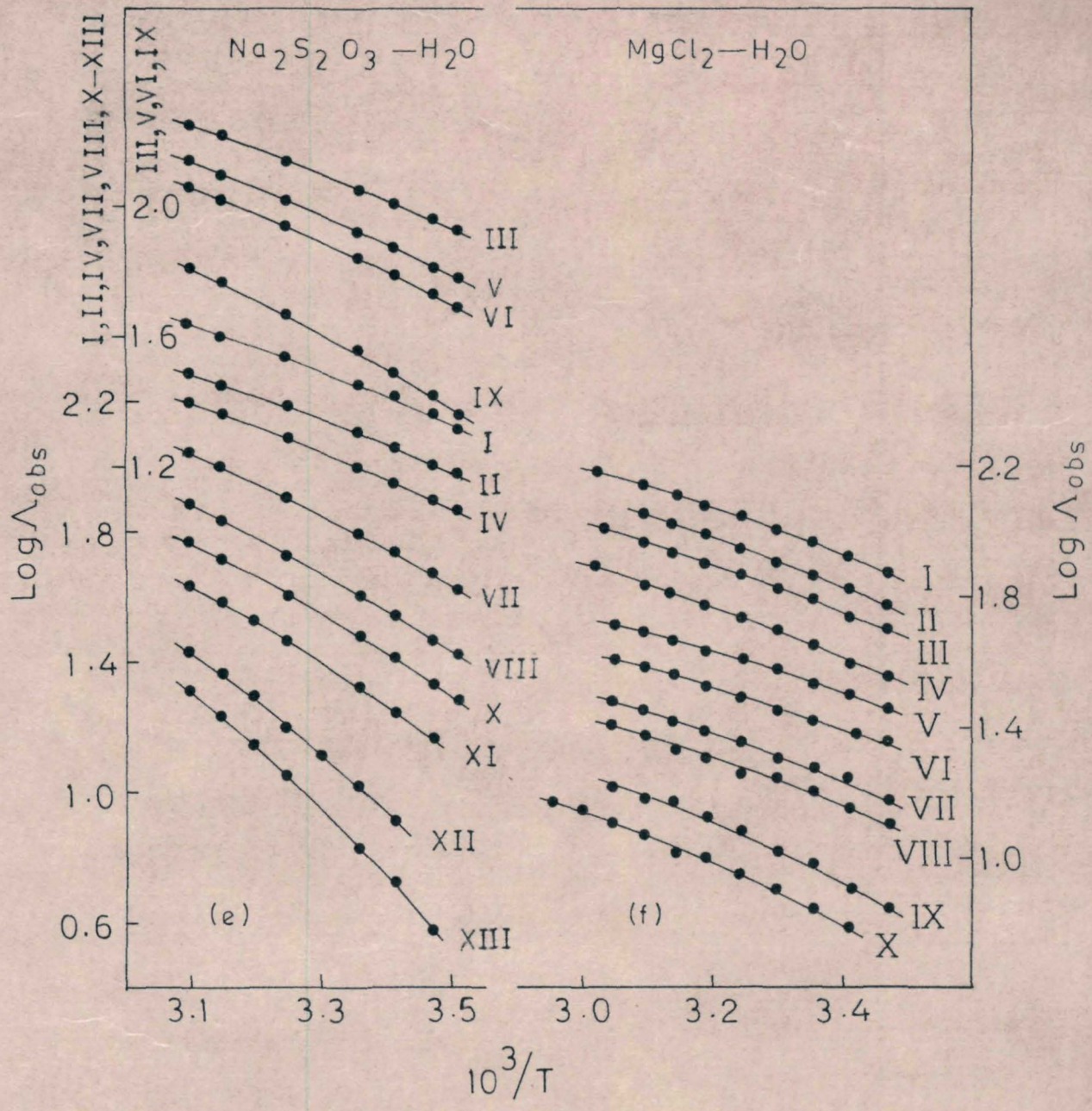

Fig 2-2c: Arrhenius plots for Λ of $Na_2S_2O_3$-H_2O (the concentrations of the thirteen solutions, I-XIII, are in the same increasing order as given in Table 2-1e) and $MgCl_2$-H_2O (the concentrations of the ten solutions, I- X, are in the same increasing order as given in Table 2-1c) systems.

Table 2-2a: Least-Squares Fitted Values of the Parameters of Eq(2-1) for Equivalent Conductance of $Ca(NO_3)_2$ - H_2O System.

m ($mol.kg^{-1}$)	$A_\Lambda \times 10^{-4}$	B_Λ	$T_o(K)$	Std. dev. in ln Λ
0.1305	3.9851	553.50	132.8	0.006
0.8116	2.4350	549.40	133.6	0.006
1.175	1.9698	538.48	135.6	0.010
1.752	1.3661	499.50	143.6	0.008
3.533	0.6572	475.42	148.4	0.045
3.953	0.6159	478.77	152.6	0.018
5.081	0.4978	485.07	159.0	0.014
6.450	0.3885	491.35	165.2	0.009
8.155	0.3168	503.14	178.2	0.002
8.864	0.2938	512.56	180.4	0.005
11.428	0.2370	522.40	193.6	0.007
12.790	0.2099	532.93	202.4	0.002

Table 2-2b: Least-Squares Fitted Values of the Parameters of Eq(2-1) for the Equivalent Conductance of $Mg(NO_3)_2$ - H_2O System.

m ($mol.kg^{-1}$)	$A_\Lambda \times 10^{-4}$	B_Λ	$T_o(K)$	Std. dev. in ln Λ
0.2297	3.1298	538.37	134.25	0.004
0.4243	2.6009	523.40	135.3	0.009
0.6753	2.1575	515.55	136.4	0.001
1.0524	1.7034	505.00	138.4	0.009
1.7055	1.1967	451.39	144.8	0.009
2.0428	0.9253	440.20	146.0	0.007
2.3300	0.7861	432.12	147.4	0.009
3.1050	0.5389	399.91	153.4	0.006
3.7251	0.4192	384.88	157.2	0.003
4.6299	0.3830	401.85	163.4	0.004
4.7091	0.3689	403.99	164.4	0.008
4.8578	0.3666	410.56	165.0	0.013
5.2393	0.3695	428.46	167.0	0.001

Table 2-2c: Least-Squares Fitted Values of the Parameters of Eq(2-1) for the Equivalent Conductance of $MgCl_2$ - H_2O System.

m ($mol.kg^{-1}$)	$A_\Lambda \times 10^{-4}$	B_Λ	T_o(K)	Std. dev. in ln Λ
0.1145	5.8935	601.56	132.4	0.014
0.3597	4.5935	589.64	134.0	0.005
0.7336	3.1943	552.21	136.2	0.012
1.5367	1.7092	480.04	142.2	0.032
2.1294	0.9940	428.13	146.0	0.009
2.8492	0.7718	425.52	147.6	0.013
3.7490	0.6356	431.16	153.0	0.022
4.2721	0.6040	444.88	155.4	0.021
5.3787	0.5642	486.05	161.4	0.030
5.9872	0.4731	494.57	164.0	0.022

Table 2-2d: Least-Squares Fitted Values of the Parameters of Eq(2-1) for the Equivalent Conductance of $NiCl_2$-H_2O System.

m ($mol.kg^{-1}$)	$A_\Lambda \times 10^{-4}$	B_Λ	$T_o(K)$	Std. dev. in ln Λ
0.1736	4.5356	558.47	132.8	0.003
0.7656	2.8299	523.89	135.6	0.027
1.1481	2.3258	509.24	137.6	0.028
2.1643	1.1435	473.40	140.8	0.008
2.7529	0.9076	468.33	143.2	0.003
3.2131	0.8992	481.16	147.0	0.010
3.7502	0.8624	496.16	149.2	0.018
4.1787	0.8496	513.38	151.4	0.019
4.7292	0.7698	519.99	154.0	0.017
4.9901	0.6800	527.20	154.6	0.015

Table 2-2e: Least-Squares Fitted Values of the Parameters of Eq(2-1) for Equivalent Conductance of $Na_2S_2O_3$ - H_2O System.

m ($mol.kg^{-1}$)	$A_\Lambda \times 10^{-4}$	B_Λ	$T_o(K)$	Std. dev. in ln Λ
0.0823	11.0747	581.85	134.2	0.007
0.5690	7.4369	578.76	134.6	0.006
0.8714	6.4861	566.13	137.0	0.010
1.2120	5.4437	540.96	141.8	0.013
1.7656	4.4272	527.86	144.6	0.031
2.3472	3.5391	510.23	147.8	0.041
2.8287	3.3097	506.55	150.0	0.076
4.0214	3.3140	531.55	160.2	0.053
4.6062	3.2814	531.92	164.6	0.005
5.1026	3.6185	547.54	169.0	0.002
6.2915	3.1458	549.38	174.8	0.005
8.6109	3.6633	579.46	189.0	0.008
9.8184	3.6823	594.40	194.1	0.003

Table 2-2f: Least-Squares Fitted Values of the Parameters of Eq(2-1) for the Equivalent Conductance of $NaNO_3$-H_2O System.

m ($mol.kg^{-1}$)	$A_\Lambda \times 10^{-4}$	B_Λ	$T_o(K)$	Std. dev. in ln Λ
0.1113	4.8894	530.28	134.0	0.062
1.0532	2.8756	509.22	136.0	0.011
1.8119	2.2788	498.98	137.0	0.003
2.5441	2.1326	496.76	138.1	0.002
3.3185	1.7214	489.24	138.8	0.022
4.3956	1.5338	478.25	140.4	0.012
6.2532	1.0941	462.11	143.6	0.006
7.3990	1.0293	465.93	145.2	0.004
8.3060	0.9541	467.28	145.6	0.004
9.8626	0.9042	473.36	147.6	0.009

system was observed in several anhydrous and hydrate melts[5-13] as well as in aqueous solutions[14] which has led to consider T_o to behave apparently like a thermodynamic parameter. However, at low fluidities T_o (Λ) and T_o (η) values have been found to differ from each other.[15,16] Obviously, the T_o (Λ) values of the electrolytic solutions under investigation vary linearly with m (Fig 2-3) according to the equation,

$$T_o = T_o(o) + Q_\Lambda\, m \qquad (2\text{-}2)$$

and this linear relationship may be understood in terms of the hydration phenomenon as discussed in the case of viscosity (cf. Chapter I). $T_o(o)$ is the T_o of pure solvent and Q_Λ is the slope. The values of Q_Λ are in agreement with the corresponding values of Q obtained on the basis of viscosity data.

For describing the concentration dependences of A_Λ and B_Λ parameters the same approach adopted in Chapter I may be used. Accordingly for A_Λ and B_Λ we can obtain expressions of the form

$$A_\Lambda = A'_\Lambda \exp(B^*_\Lambda / T_o) \qquad (2\text{-}3)$$

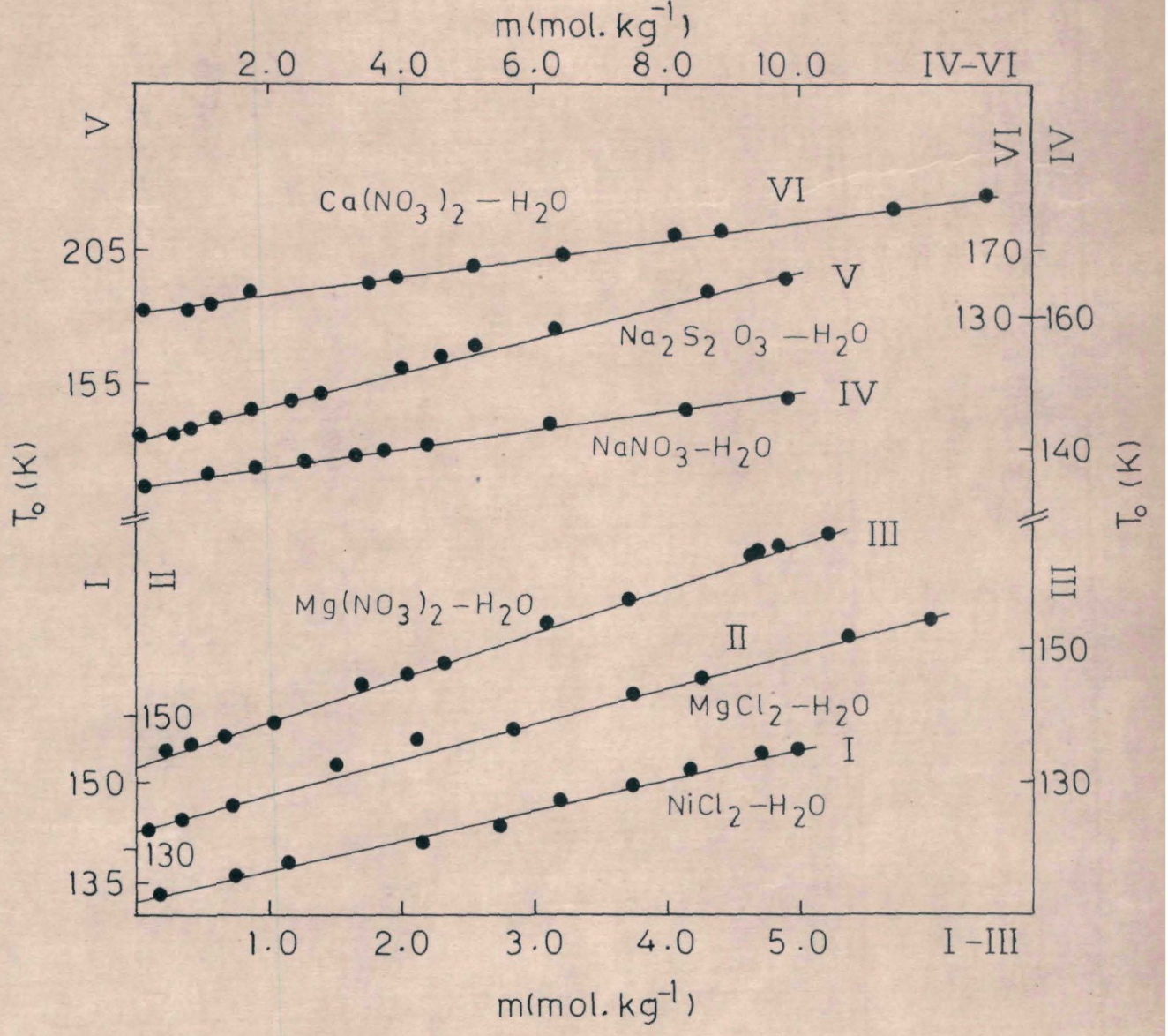

Fig 2-3: Plots of T_o vs. m for aqueous electrolytes.

and $B_\Lambda = B_{1\Lambda}\left[1-(\Delta C_1/\Delta C_2)\ T_o\right]$ (2-4)

A^*_Λ, B^*_Λ, and $B_{1\Lambda}$ are constants. ΔC_1 and ΔC_2 have the same meanings described in Chapter I. A linear variation of ln A_Λ with $1/T_o$ is apparent from Fig 2-4 and is in accordance with Eq(2-3). The trend in the variation of B_Λ with T_o (Fig 2-5) is similar to that of B_η and may be explained by the probable constancy of $\Delta C_1/\Delta C_2$ below the critical concentration, m_c, and by the linear increase of $\Delta C_1/\Delta C_2$ ratio with $1/T_o$ above m_c. It is worthwhile to note that the values of the critical concentrations obtained from the conductance and viscosity studies are closely comparable, whereas the values of B_Λ are found to be lower than the corresponding B_η values for a particular electrolytic system. The reason for such a difference in the values of B_η and B_Λ is discussed below in terms of activation energies.

By inserting the values of T_o, A_Λ, and B_Λ from Eqs(2-2), (2-3), and (2-4), respectively in Eq(2-1), an isothermal equation similar to Eq(1-12) may be obtained for Λ and it may be written as

$$\Lambda = a_{o\Lambda} \exp(b_{o\Lambda}m+c_{o\Lambda}m^2) \qquad (2-5)$$

where $a_{o\Lambda}$, $b_{o\Lambda}$, and $c_{o\Lambda}$ are constant parameters.

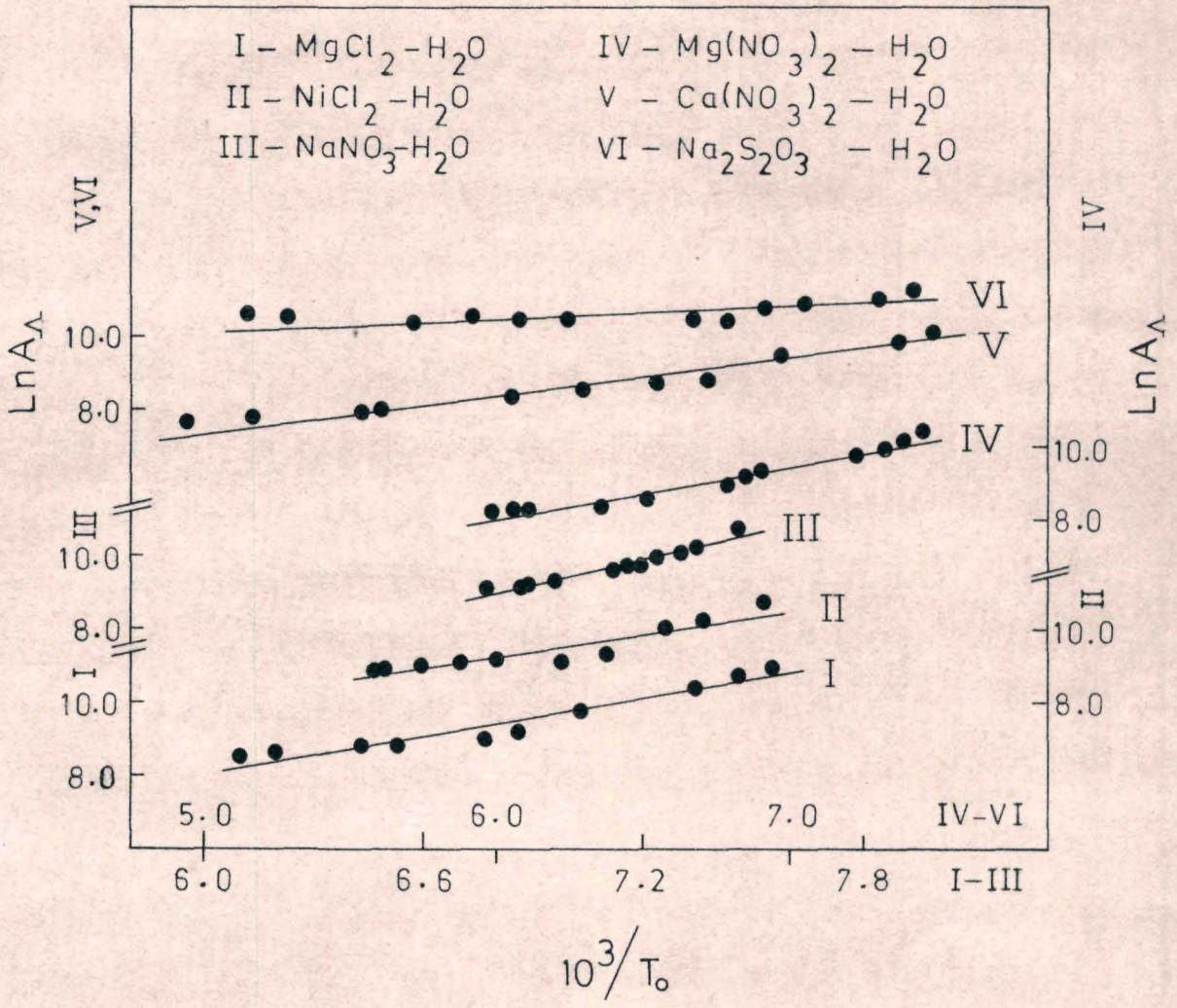

Fig 2-4: Plots of ln $\Lambda_\wedge$ vs. $1/T_o$ for aqueous electrolytes.

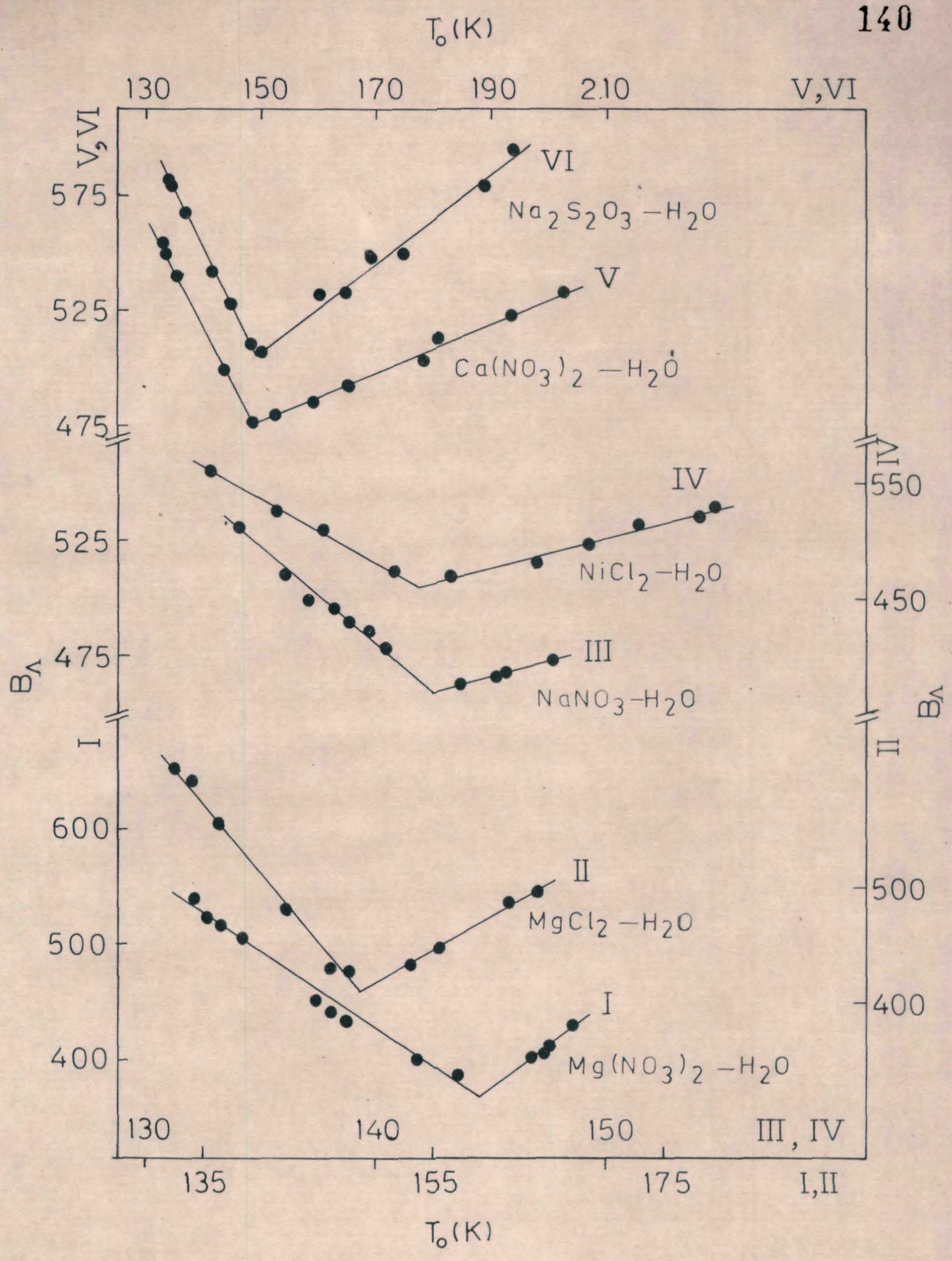

Fig 2-5: Plots of B_{Λ} vs. T_o for aqueous electrolytes.

The conductance data are least-squares fitted to Eq(2-5) in the three regions of concentrations separately, viz., below and above the critical concentration and the entire experimental concentration range. The computed values of $a_{o\Lambda}$, $b_{o\Lambda}$, and $c_{o\Lambda}$ obtained in this fashion are given in Tables 2-3. It is apparent from Tables 2-3 and also from the linearity of the plots of ln Λ versus $b_{o\Lambda}\, m + c_{o\Lambda}\, m^2$ (Fig 2-6) that Eq(2-5) describes satisfactorily the concentration dependence of Λ in the entire experimental range of concentration, in spite of a miniumum in the variation of B_Λ with m, as was the case with viscosity also.

The value of $a_{o\Lambda}$ may be interpreted as the equivalent conductance at infinite dilution and therefore its comparison is made with the reported[17] Λ_o values for the different electrolytic solutions under study. It may be noted that we have used for this purpose $a_{o\Lambda}$ values obtained from Eq(2-5) after least-squares fitting to this equation the limited Λ data lying below the critical concentration only. Comparison of this kind in the cases of all the six systems has revealed that the values of $a_{o\Lambda}$ are ~30-40% lower than the corresponding Λ_o values. Values of $a_{o\Lambda}$ obtained after the entire experimental concentration range to Eq(2-5) were found to be still lower (Table 2-3). However, such a

Table 2-3a: Least-Squares Fitted Values of the Parameters of Eq(2-5) for Equivalent Conductance of $Ca(NO_3)_2$ - H_2O System.

T(K)	Conc. range mol. kg^{-1}	$a_{c\Lambda}$	$b_{c\Lambda}$	$c_{c\Lambda} \times 10^2$	Std. dev. in ln Λ
298	0.1305 - 3.533	87.46	-0.7157	6.3696	0.019
	3.953 - 12.79	49.56	-0.3245	0.2799	0.049
	0.1305 - 12.79	71.64	-0.4289	0.3485	0.085
308	0.1305 - 3.533	104.16	-0.7115	6.6228	0.014
	3.953 - 12.79	61.24	-0.3370	-0.0105	0.045
	0.1305 - 12.79	86.24	-0.4330	0.5638	0.078
323	0.1305 - 3.533	130.19	-0.7059	6.9634	0.015
	3.953 - 12.79	78.82	-0.3482	0.2871	0.038
	0.1305 - 12.79	109.22	-0.4376	0.8152	0.071

Table 2-3b: Least-Squares Fitted Values of the Parameters of Eq(2-5) for Equivalent Conductance of $Mg(NO_3)_2$ - H_2O System.

T(K)	Conc. range mol. kg^{-1}	$a_{o\Lambda}$	$b_{o\Lambda}$	$c_{o\Lambda} \times 10^2$	Std. dev. in ln Λ
298	0.2297 - 4.6299	73.00	-0.4929	2.0158	0.032
	4.6299 - 4.8578	57.98	-22.669	230.5	0.021
	0.2297 - 4.8578	72.08	-0.4687	1.3265	0.035
308	0.2297 - 4.6299	17.10	0.6505	-16.325	0.011
	4.6299 - 5.2393	80.66	-4.0862	36.6249	0.009
	0.2297 - 5.2393	85.13	-0.4651	1.2520	0.036
323	0.2297 - 4.6299	108.62	-0.5219	2.6958	0.022
	4.6299 - 5.2393	98.19	-5.4776	51.3129	0.008
	0.2297 - 5.2393	106.70	-0.4894	1.8173	0.028

Table 2-3c: Least-Squares Fitted Values of the Parameters of Eq(2-5) for Equivalent Conductance of $MgCl_2$-H_2O System.

T(K)	Conc. range mol. kg^{-1}	$a_{o\Lambda}$	$b_{o\Lambda}$	$c_{o\Lambda} \times 10^2$	Std. dev. in ln Λ
288	0.1145 - 2.8492	75.69	-0.5816	5.5596	0.031
	3.7490 - 5.3787	7.84	0.6128	-11.7914	0.001
	0.1145 - 5.3787	70.95	-0.4105	-0.2256	0.051
308	0.1145 - 2.8492	110.63	-0.5497	3.6539	0.036
	3.7490 - 5.9872	46.09	-0.0672	-3.4615	0.018
	0.1145 - 5.9872	106.12	-0.4532	0.7654	0.041
323	0.1145 - 2.8492	141.82	-0.5626	3.6684	0.035
	3.7490 - 5.9872	74.45	-0.1670	2.4328	0.002
	0.1145 - 5.9872	135.73	-0.4664	1.0073	0.043

Table 2-3d: Least-Squares Fitted Values of the Parameters of Eq(2-5) for Equivalent Conductance of $NiCl_2$-H_2O System.

T(K)	Conc. range mol. kg^{-1}	$a_{o\Lambda}$	$b_{o\Lambda}$	$c_{o\Lambda} \times 10^2$	Std. dev. in ln Λ
293	0.1736 - 2.1643	113.96	-0.4735	-1.1544	0.006
	2.7529 - 4.9901	43.34	-0.1234	-3.8139	0.035
	0.1736 - 4.9901	88.84	-0.5115	1.1854	0.035
308	0.1736 - 2.1643	114.43	-0.4597	-1.9089	0.020
	2.7529 - 4.9901	52.07	-0.0926	-3.8185	0.024
	0.1736 - 4.9901	116.02	-0.5255	1.7627	0.035
323	0.1736 - 2.1643	144.79	-0.4976	-0.8107	0.043
	2.7529 - 4.9901	47.9136	0.0441	-5.0010	0.019
	0.1736 - 4.9901	146.07	-0.5562	2.7205	0.046

Table 2-3e: Least-Squares Fitted Values of the Parameters of Eq(2-5) for Equivalent Conductance of $Na_2S_2O_3$ - H_2O System.

T(K)	Conc. range mol. kg^{-1}	$a_{o\Lambda}$	$b_{o\Lambda}$	$c_{o\Lambda} \times 10^2$	Std. dev. in $\ln\Lambda$
288	0.0823 - 2.3472	152.49	-0.7037	11.0404	0.032
	2.8287 - 9.8184	108.01	-0.2932	-0.4686	0.035
	0.0823 - 9.8184	128.64	-0.3642	0.1059	0.070
308	0.0823 - 2.3472	228.58	-0.6968	12.1388	0.038
	2.8287 - 9.8184	187.34	-0.3233	0.3975	0.018
	0.0823 - 9.8184	192.96	-0.3459	0.6212	0.065
323	0.0823 - 2.3472	288.27	-0.6715	12.0658	0.039
	2.8287 - 9.8184	263.14	-0.3418	0.8525	0.024
	0.0823 - 9.8184	245.30	-0.3308	0.8272	0.066

Table 2-3f: Least-Squares Fitted Values of the Parameters of Eq(2-5) for Equivalent Conductance of $NaNO_3$-H_2O System.

T(K)	Conc. range mol. kg^{-1}	$a_{o\Lambda}$	$b_{o\Lambda}$	$c_{o\Lambda}$ x10^2	Std. dev. in ln Λ
288	0.1113 - 4.3956	84.69	-0.3360	2.9439	0.029
	6.2532 - 9.8626	59.34	-0.1522	0.3313	0.006
	0.1113 - 9.8626	79.37	-0.2437	0.9926	0.041
308	0.1113 - 4.3956	137.50	-0.4462	5.0314	0.045
	6.2532 - 9.8626	93.18	-0.1767	0.5187	0.032
	0.1113 - 9.8626	122.14	-0.2721	1.2545	0.071
323	0.1113 - 4.3956	178.46	-0.4872	5.7604	0.061
	6.2532 - 9.8626	100.66	-0.1461	0.3496	0.001
	0.1113 - 9.8626	155.73	-0.2858	1.3729	0.086

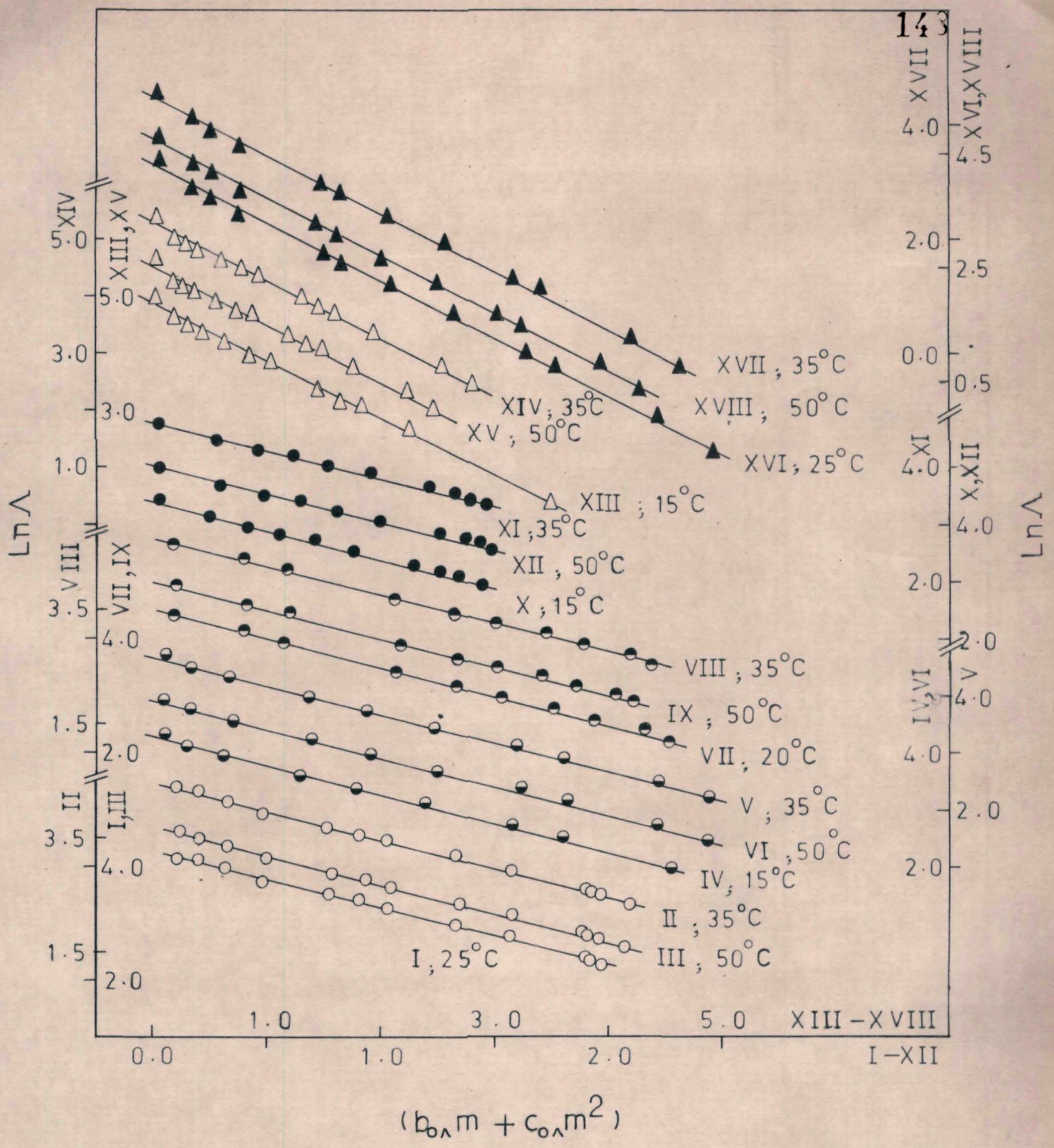

Fig 2-6: Plots of $\ln\Lambda$ vs. $b_{o\Lambda}m+c_{o\Lambda}m^2$ for aqueous electrolytes (O-$Mg(NO_3)_2$, ⊖-$MgCl_2$, ⊜-$NiCl_2$, ●-$NaNO_3$, Δ-$Na_2S_2O_3$, and ▲-$Ca(NO_3)_2$ solutions).

vast difference between $a_{O\Lambda}$ and Λ_O values is not surprising and may be attributed to two factors. Firstly, Eq(2-5) takes into account only the ion-solvent interactions (cf. Chapter I), but at low concentrations it is necessary to incorporate the contribution due to ion-ion interactions also which is normally represented by a (concentration)$^{1/2}$ term. Secondly, $a_{O\Lambda}$ values are obtained based on high concentration conductance data. On the other hand, Λ_O values are computed from the conductances measured at very low concentrations where Debye-Huckel square root law or its extended form is applicable. It is important to recognize here that Eq(2-5) as such cannot be employed to represent the conductance data of an electrolytic solution at very low concentrations which is also apparent from the fact that at such low concentrations T_o becomes almost invarient with concentration.[14] Therefore, in order to bring better agreement between $a_{O\Lambda}$ and Λ_O values it is essential to account for the ion-ion interactions also and an attempt to do this has been made in the subsequent chapter.

In addition to studying the concentration dependence of Λ, it is also important to study the trend in the

variation of specific conductance with concentration. We have, therefore, plotted specific conductance versus m isotherms at 35°C (Fig 2-7) for all the electrolytic solutions under investigation. From Fig 2-7 it is apparent that specific conductance maxima occur at 2.0, 2.2, 2.25, 2.25, and 2.85 $mol.kg^{-1}$ for $Ca(NO_3)_2 - H_2O$, $NiCl_2 - H_2O$, $MgCl_2 - H_2O$, $Mg(NO_3)_2 - H_2O$, and $Na_2S_2O_3 - H_2O$ systems, respectively, whereas in the case of $NaNO_3 - H_2O$ system specific conductance becomes rather constant beyond 4m instead of showing a decrease. The value of specific conductance maximum for a particular electrolyte has been found to be almost independent of temperature as observed in the case of several other systems also.[18] The value 2.0m (at 35°C) obtained by us for $Ca(NO_3)_2 - H_2O$ system is in good agreement with the value 2.01 m (at 0°C) reported by Angell and Bressel.[14] The specific conductance maximum is seen to be a general feature of electrolytic solutions[19-24] and results due to the fact that conductivity is equal to the product of concentration of charge carriers, mobility, and the absolute charge. Since charge concentration and mobility factors change in opposite directions when concentration is varied, a maximum value of the conductivity is reached when the charge concentration increase is exactly counterbalanced by the corresponding decrease of the ionic mobilities.

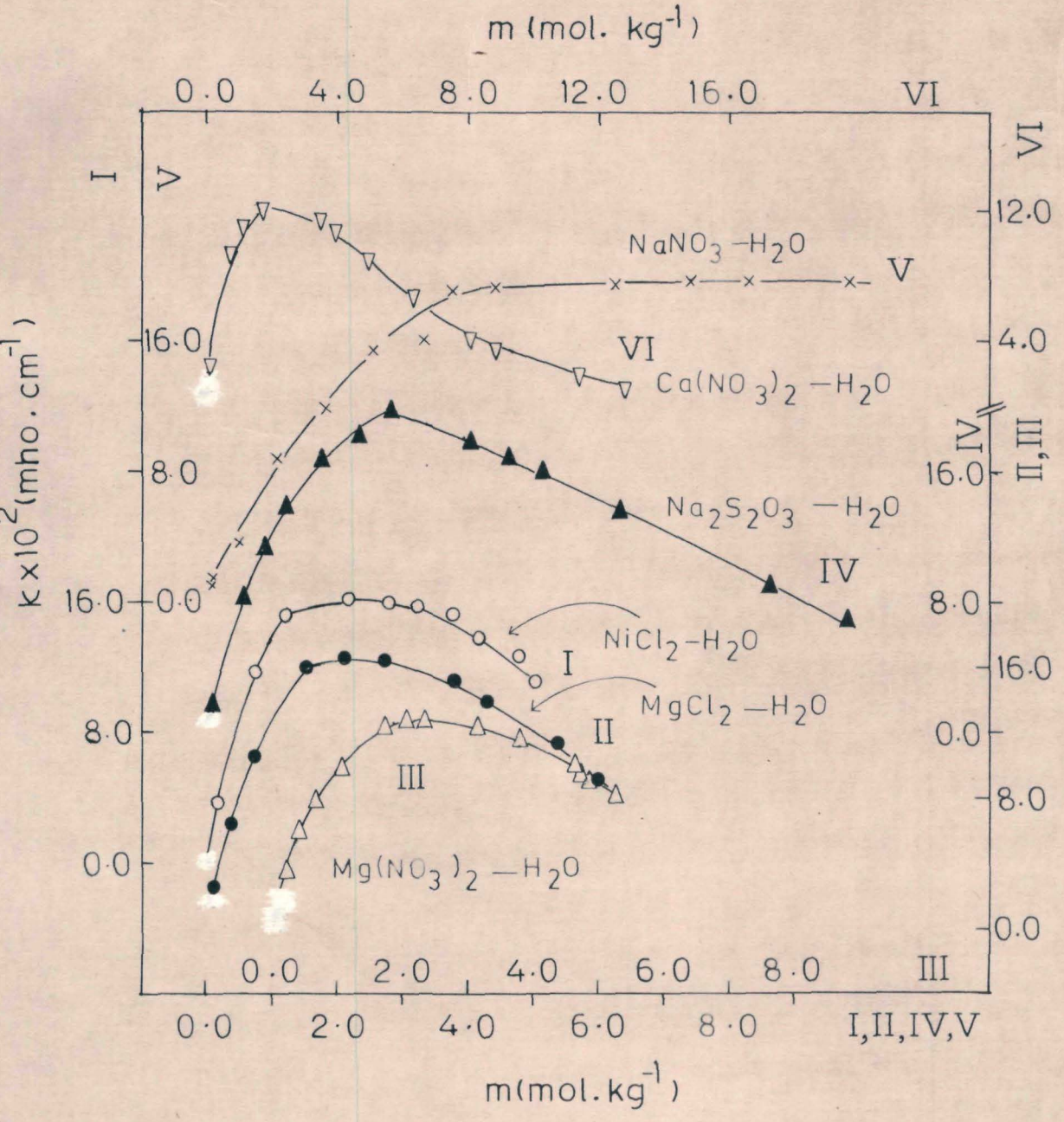

Fig 2-7: Plots of conductivity vs. m for aqueous electrolytes.

Therefore, the ascending portion of the conductivity versus concentration isotherm which falls in the dilute region may be governed by the charge concentration factor and the descending portion of this isotherm, on the other hand, may be considered to be controlled by the mobility factor. In the case of $NaNO_3$ - H_2O system it appears, however, that the mobility factor does not supersede the charge concentration factor, instead beyond the ascending portion of the conductivity versus concentration isotherm the decrease in ionic mobility seems to be almost nullified by an equal amount of increase in charge concentration thereby causing a plateau in the isotherm. The decrease in mobility with increasing solute concentration is normally attributed to the increase in viscosity of the solution.

Claes and Glibert[18] correlated the concentration corresponding to conductivity maximum, m_{max}, to hydration numbers of the ions. In the present study m_{max} for $Ca(NO_3)_2$ - H_2O and $Mg(NO_3)_2$ - H_2O systems are found to be 2.0 and 2.25 $mol.kg^{-1}$, respectively unlike the observation of Claes and Glibert who found that for the same anion m_{max} remains the same in the case of all the alkaline earth salts. A higher value of m_{max} obtained by us for $Mg(NO_3)_2$-H_2O system than for $Ca(NO_3)_2$ solution may be attributed

to the fact that Mg^{2+} is capable of holding more number of water molecules in the primary hydration sphere due to its higher charge to radius ratio than Ca^{2+}. This is in accordance with the higher value reported[25] for the radius of hydrated Mg^{2+} ion (4.28 Å) than for the hydrated Ca^{2+} ion (4.12 Å). On the other hand, same value of m_{max} is obtained for $Mg(NO_3)_2 - H_2O$ and $MgCl_2 - H_2O$ systems. Therefore, it appears that the m_{max} value of an electrolytic solution is determined by the nature of its cation, i.e., by the cationic charge to radius ratio, rather than by the nature of its anion. On the contrary, Claes and Glibert[18] obtained a lower value of m_{max} for chlorides than for nitrates of a given alkaline earth cation. It may further be noted that in the case of $NiCl_2 - H_2O$ system m_{max} is slightly lower than that of $MgCl_2 - H_2O$ system. This may again be attributed to the fact that Ni^{2+} ion has a smaller charge to radius ratio than Mg^{2+}. At this moment it is difficult to comment on the value of $m_{max} = 2.85$ obtained for $Na_2S_2O_3 - H_2O$ system as it requires similar study on more number of systems of this type. It may be noted that $NaNO_3 - H_2O$ system seems to have a high value for m_{max} which is consistent with the high value of m_{max} reported for $LiNO_3 - H_2O$ system.[18]

The specific conductance maximum may also be predicted from Eq(2-5) after substituting for Λ in terms of specific conductance, κ, and then by equating the first derivative of κ with respect to m to zero (Appendix - VI). The values of m_{max} so obtained using the least-squares fitted values of $a_{o\Lambda}$, $b_{o\Lambda}$, and $c_{o\Lambda}$ (considering the entire experimental range of concentration) are 2.23, 2.11, 2.30, 2.10, 3.20, and 4.10 $mol.kg^{-1}$ for $Ca(NO_3)_2 - H_2O$, $NiCl_2 - H_2O$, $MgCl_2 - H_2O$, $Mg(NO_3)_2 - H_2O$, $Na_2S_2O_3 - H_2O$, and $NaNO_3 - H_2O$ systems, respectively. The reasonably good agreement found between the experimental (Fig 2-7) and computed values of m_{max} is worth noting.

It is worthwhile to make a comparative study of conductance and viscous flows in terms of the corresponding activation energies. These activation energies are calculated using the expressions

$$E_{\Lambda} = B_{\Lambda} R \left[T/(T-T_o)\right]^2 \qquad (2\text{-}6)$$

and

$$E_{\eta} = B_{\eta} R \left[T/(T-T_o)\right]^2 \qquad (2\text{-}7)$$

where R is the gas constant. The values of E_{Λ} (Fig 2-8) and E_{η} (Fig 2-9) at 298K are plotted versus m for all the electrolytic solutions under study. In every electrolytic

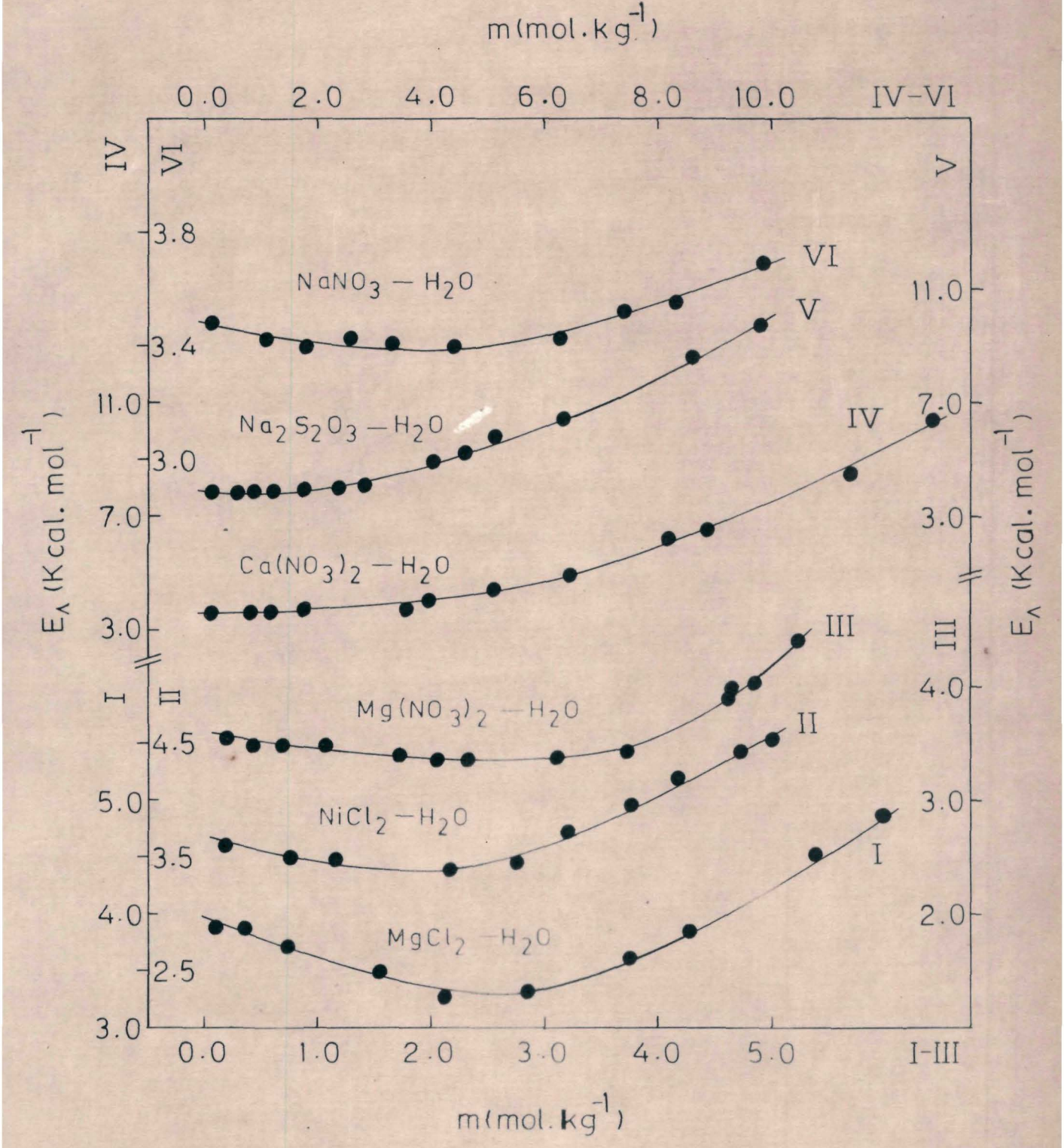

Fig 2-8: Plots of E_Λ vs. m for aqueous electrolytes.

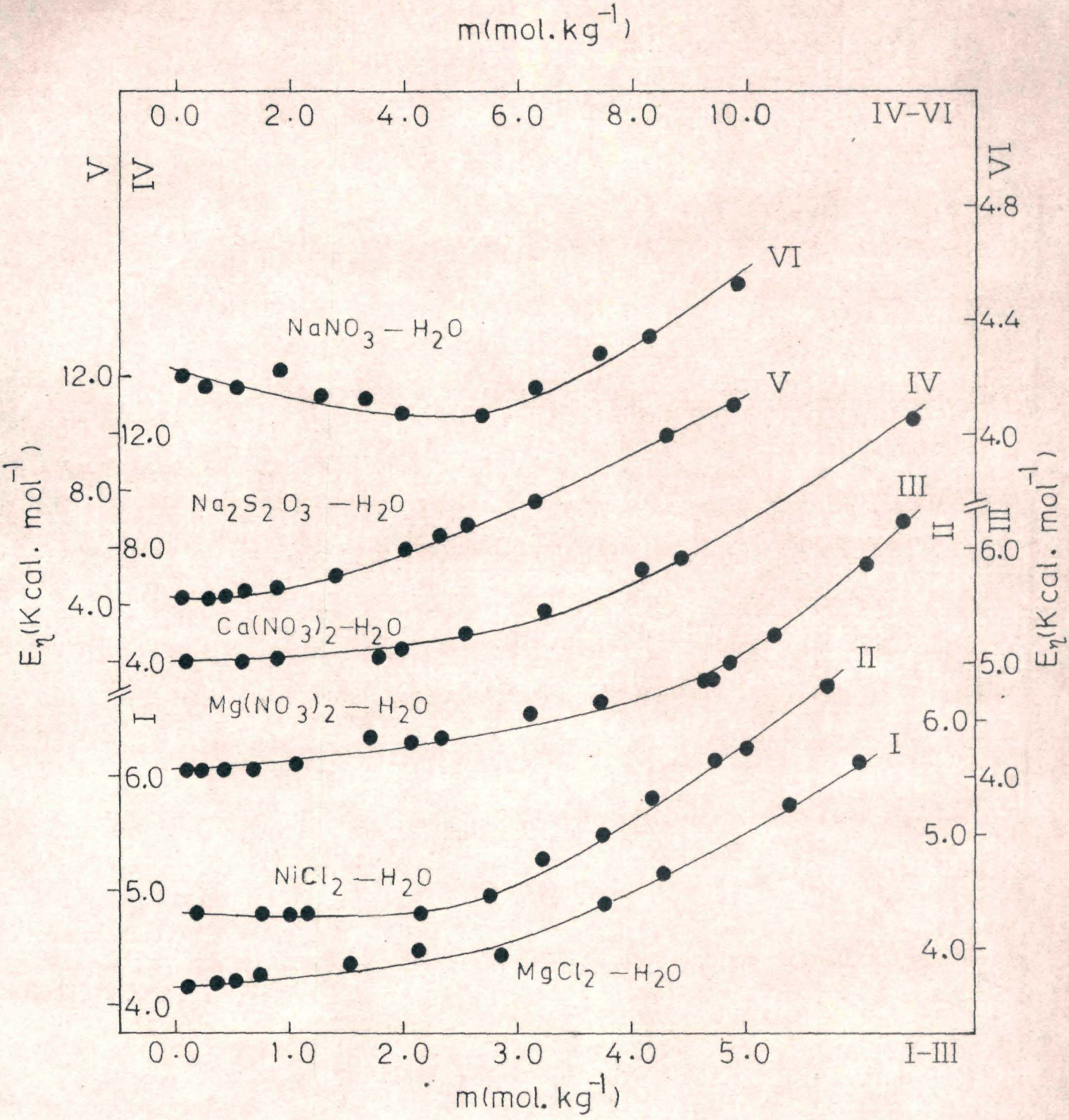

Fig 2-9: Plots of E_η vs. m for aqueous electrolytes.

solution studied here both E_Λ and E_η appear to decrease slightly or to remain almost invarient with m upto a particular concentration, m_a, and then they increase with m. Similar behaviour was also reported in several other aqueous systems.[18] The value of m_a for a particular solution at which its E_Λ and E_η isotherms (Figs 2-8 and 2-9) start ascending has been found to be comparable with its critical concentration. Such a trend in the concentration dependence of E_Λ and E_η is explainable in the light of Eqs(2-6) and (2-7). From Eq(2-6) it is apparent that the value of E_Λ is governed by the two VTF parameters, B_Λ and T_o. As we have already seen B_Λ decreases upto the critical concentration and then increases with m, whereas the term inside the square-bracket in Eq(2-6) increases with m throughout the experimental concentration range. Consequently, the concentration dependence of E_Λ up to the critical concentration is determined by the resultant of two oppositely varying factors thereby accounting for the observed trend. Beyond the critical concentration both B_Λ and $[T/(T-T_o)]^2$ terms increase with concentration and this causes an increase in E_Λ also. The nature of the concentration dependence of E_η may be explained similarly in the light of Eq(2-7).

It is interesting to note that in all the electrolytic

solutions considered here the value of E_η / E_Λ ratio is almost constant and lies in the range $\sim 1.1 - 1.3$ at any temperature and concentration. Such a value for E_η / E_Λ has also been reported in several other aqueous and molten salt systems.[6,8,10,18] The higher activation energy required for viscous flow compared to that for conductance flow actually manifests a higher value for B_η than B_Λ. The exact reason for the higher value of E_η than E_Λ is not known and this warrants a thorough understanding of the mechanism of transport process taking place in solutions and liquids. However, a qualitative description to this observation is usually given according to which viscous flow involves movement of molecular species (or ion-pairs) and the slow moving ion determines the viscosity of the solution, whereas in the case of conductance flow the fast moving ion determines the conductance of the solution.[8]

Furthermore, we have made an attempt to describe the dependence of Λ on viscosity by analyzing the concentration dependence of their product (Walden product). A plot of $\Lambda\eta$ product against molality is made and such isotherms at 35°C for all the electrolytes under investigation are illustrated in Fig 2-10. From these isotherms it

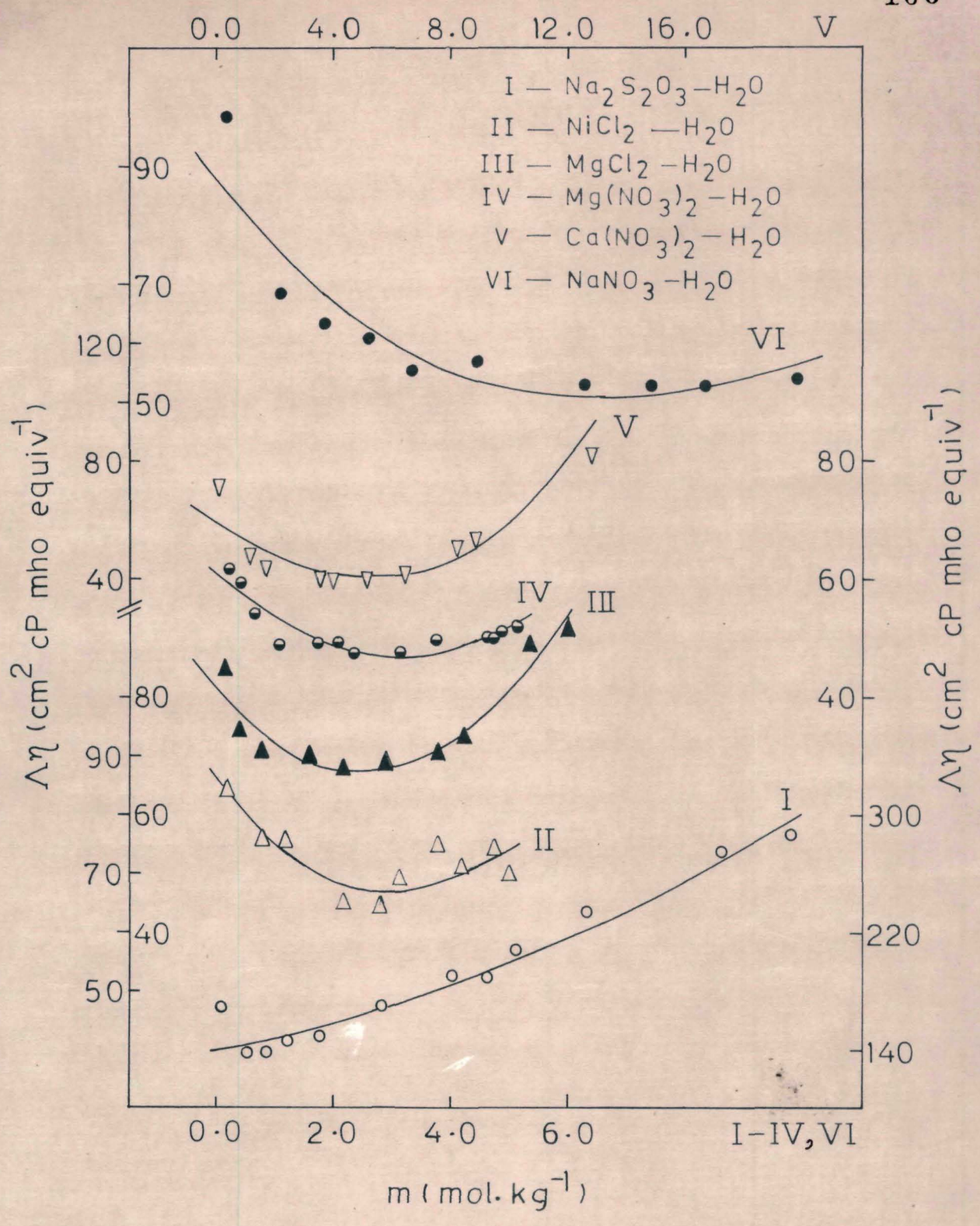

Fig 2-10: Plots of Walden product vs. m for aqueous electrolytes. Different notations denote the observed values and the solid lines represent the calculated values.

is apparent that in the case of each electrolyte $\Lambda\eta$ decreases initially and then increases after passing through a minimum. The concentration, m_ω, at which the $\Lambda\eta$ minimum occurs is a characteristic of the electrolyte considered as was the case with m_c, m_{max}, and m_a also. However, the value of m_ω seems to be independent of temperature as indicated by Seward.[26] The observed values of m_ω at 35°C are around 5.0, 3.0, 2.5, 3.0, 6.7, and 1.0 mol.kg^{-1} for $Ca(NO_3)_2 - H_2O$, $Mg(NO_3)_2 - H_2O$, $MgCl_2 - H_2O$, $NiCl_2 - H_2O$, $NaNO_3 - H_2O$, and $Na_2S_2O_3 - H_2O$ systems, respectively. It may be noted that the Walden product of aqueous solutions generally shows this kind of behaviour.[26-28] Such a behaviour of $\Lambda\eta$ is usually explained only in qualitative terms by saying essentially that the falling portion of the $\Lambda\eta$ versus m isotherm is governed by the conductance of the solution whereas its raising portion is due to the dominance of viscosity term in the Walden product. No expression is available in the literature which can predict such a $\Lambda\eta$ minimum. Yao and Bennion[29] made an attempt to employ the semiempirical Wishaw-Stokes equation[30] for this purpose, but this equation also failed to predict the falling and raising portions of the $\Lambda\eta$ product. Therefore, it is worth examining the feasibility of our isothermal equation in explaining the behaviour of $\Lambda\eta$ versus concentration isotherm. Using Eqs(2-5) and (1-12) $\Lambda\eta$ may be written as

$$\Lambda\eta = a_{\Lambda\eta} \exp(b_{\Lambda\eta} m + c_{\Lambda\eta} m^2) \qquad (2\text{-}8)$$

where $a_{\Lambda\eta} = a_{o\Lambda} a_{o\eta}$, $b_{\Lambda\eta} = b_{o\Lambda} + b_{o\eta}$, and $c_{\Lambda\eta} = c_{o\Lambda} + c_{o\eta}$. It may be noted that in all the systems studied here except for $Na_2S_2O_3$ solution $b_{o\Lambda}$ has a larger value than $b_{o\eta}$ with a negative sign. Accordingly $b_{\Lambda\eta}$ becomes a negative quantity and Eq(2-8) predicts a decrease in $\Lambda\eta$ with m at low concentrations. As the concentration increases the value of the positive $c_{\Lambda\eta} m^2$ term keeps on increasing and at some concentration it dominates over the negative $b_{\Lambda\eta}$ m term. Beyond this particular concentration (m_ω) therefore $\Lambda\eta$ will increase with concentration. Substituting the least-squares fitted values of $a_{o\Lambda}$, $a_{o\eta}$, $b_{o\Lambda}$, $b_{o\eta}$, $c_{o\Lambda}$, and $c_{o\eta}$ (cf. Chapter I for viscosity parameters) in Eq(2-8) we calculated $\Lambda\eta$ for the different solutions and the values thus obtained are also plotted in Fig (2-10). It is interesting to note that there is a reasonably good agreement between the observed and calculated values of $\Lambda\eta$. In the dilute concentration region, however, the fitting is not as satisfactory as in the concentrated region. This is anticipated due to unaccounting for the ion-ion interaction in our isothermal equations which becomes dominating at dilute region. This may also be the reason for not obtaining a $\Lambda\eta$ minimum from Eq(2-8) in the case of $Na_2S_2O_3$ solution. It is further interesting to note

that the values of m_ω obtained from Fig (2-10) after equating $d(\Lambda\eta)/dm$ to zero (5.17, 3.13, 2.52, 2.94, and 6.8 mol. kg^{-1} for $Ca(NO_3)_2 - H_2O$, $Mg(NO_3)_2 - H_2O$, $MgCl_2 - H_2O$, $NiCl_2 - H_2O$, and $NaNO_3 - H_2O$ systems, respectively) are closely comparable with their observed values.

Finally, in the light of the above discussions on B_Λ parameter, specific conductance, activation energy, and $\Lambda\eta$ product it may again be recognized (cf. Chapter I) that some sort of structural transition takes place in an electrolytic solution when the concentration is varied from dilute to very high value. From the values of m_c, m_{max}, m_a, and m_ω it is apparent that this transition does not occur at a definite concentration, but takes place over a concentration range. In $Ca(NO_3)_2 - H_2O$ system such a concentration range for the structural transition to occur was also proposed by Angell and Bressel.[14] Claes and Glibert[18] visualized this region as a 'no man's land' lying between two other regions, one of lower concentration and the other of higher concentration, with characteristic transport behaviours. In the region of lower concentration hydrated ions migrate in a dielectric medium formed by water molecules (primitive model). On the other hand, in the region of higher concentration water does not act as a dielectric

medium and the solution behaves like an ionic liquid with completely or partially hydrated ions (quasi-crystalline model). The fact that transition from primitive model to quasi-crystalline model takes place over a concentration range (through the 'no man's land') implies that the reorganization of solute ions and solvent molecules does not take place all of a sudden, rather it seems to be a gradual process. This further envisages that in the transition region both the primitive (water as continuous dielectric medium) and quasi-crystalline behaviours may coexist. This is in accordance with the view of Angell and coworkers[14,31] who also suggested that this kind of coexistance of two behaviours, viz., presence of some amount of quasi-crystallinity within the dielectric medium, must cause a liquid-liquid phase separation when the temperature of the solution is sufficiently lowered. The low-temperature light scattering studies made by Hsich, et al.[32] provide an experimental evidence to the occurrence of such a liquid-liquid phase separation.

References:

1. G. Adam and J.H. Gibbs, J. Chem. Phys., 43, 139 (1965).

2. S. Phang, Aust. J. Chem., 32, 1149 (1979).

3. C.A. Angell, J. Phys. Chem., 70, 3988 (1966).

4. R.C. Weast, ed., 'Handbook of Chemistry and Physics,' 58th Ed., CRC Press, Ohio, 1977.

5. H. Tweer, J.H. Simmons, and P.B. Macedo, J. Chem. Phys., 54, 1952 (1971).

6. N. Islam, M.R. Islam, S. Ahmad, and B. Waris, J. Amer. Chem. Soc., 97, 3026 (1975).

7. N. Islam, M.R. Islam, B. Waris, and K. Ismail, J. Phys. Chem., 80, 291 (1976).

8. C.T. Moynihan, J. Phys. Chem., 70, 3399 (1966).

9. C.T. Moynihan, C.R. Smalley, C.A. Angell, and E.J. Sare, J. Phys. Chem., 73, 2287 (1969).

10. N. Islam and K. Ismail, J. Phys. Chem., 79, 2180 (1975); ibid., 80, 1929 (1976); Indian J. Chem., 15A, 857 (1977); J. Polymer Sci., 17, 4021 (1979).

11. N. Islam, K.P. Singh, and S. Kumar, J. Chem. Soc. Faraday Trans. I, 75, 1312 (1979); Bull. Chem. Soc. Japan, 52, 579 (1979).

12. N. Islam, S. Kumar, and K.P. Singh, Can. J. Chem., 56, 1231 (1978).

13. S.K. Jain and R. Tamamushi, Can. J. Chem., 58, 1967 (1980).

14. C.A. Angell and R.D. Bressel, J. Phys. Chem., 76, 3244 (1972).

15. J.H. Ambrus, C.T. Moynihan and P.B. Macedo, J. Electrochem. Soc., 119, 192 (1972).

16. C.A. Angell and D.L. Smith, J. Phys. Chem., 86, 3845 (1982).

17. B.P. Levitt, ed., 'Findlay's Practical Physical Chemistry,' 9th Ed., Longman, 1973.

18. P. Claes and J. Glibert, 'Ionic Liquids', D. Inman and D.G. Lovering, eds., Plenum, New York, 1981.

19. A.N. Campbell and E.M. Kartzmark, Can. J. Chem., 30, 128 (1952).

20. A.N. Campbell, E.M. Kartzmark, M.E. Bednas, and J.T. Herron, Can. J. Chem., 32, 1051 (1954).

21. A.N. Campbell, G.H. Debus, and E.M. Kartzmark, Can. J. Chem., 33, 1508 (1955).

22. A.N. Campbell, J.B. Fishman, G. Rutherford, T.P. Schaefer, and L. Ross, Can. J. Chem., 34, 151 (1956).

23. A.N. Campbell and W.G. Patterson, Can. J. Chem., 36, 1004 (1958).

24. D.A. Lown and H.R. Thirsk, Trans. Faraday Soc., 67, 132 (1971).

25. E. Nightingale Jr., J. Phys. Chem., 63, 1381 (1959).

26. R.P. Seward, J. Amer. Chem. Soc., 77, 905 (1955).

27. R.P. Seward, J. Amer. Chem. Soc., 73, 515 (1951).

28. J.F. Chambers, J.M. Stokes, and R.H. Stokes, J. Phys. Chem., 60, 985 (1956).

29. N.P. Yao and D.N. Bennion, J. Phys. Chem., 75, 3586 (1971).

30. B.F. Wishaw and R.H. Stokes, J. Amer. Chem. Soc., 76, 2065 (1954).

31. C.A. Angell and E.J. Sare, J. Chem. Phys., 52, 1058 (1970).

32. S.Y. Hsich, R.W. Gammon, P.B. Macedo, and C.J. Montrose, J. Chem. Phys., 56, 1663 (1972).

CHAPTER III

VISCOSITY AND CONDUCTANCE OF AQUEOUS ELECTROLYTES - AN EXTENSION TO VERY LOW CONCENTRATION

Introduction

In the last two chapters a three-parameter isothermal equation was deduced to describe the concentration dependence of viscosities (Chapter I) and conductances (Chapter II) of electrolytic solutions. This equation may be written as

$$Y(\eta \text{ or } \Lambda) = a_{oy} \exp (b_{oy}m + c_{oy}m^2) \qquad (3\text{-}1)$$

where Y is the transport property, viscosity (η) or equivalent conductance (Λ). a_{oy}, b_{oy}, and c_{oy} are constant parameters for a particular electrolyte having different values in the cases of viscosity and conductance. m is the concentration of the solution in molality. It was shown that this equation takes into account only the ion-solvent interactions. Since at very low concentrations the ion-ion interactions predominate, Eq(3-1) must be modified to take into account this kind of interactions also so that the applicability of this equation may be extended to the dilute region. The significance of the ion-ion interactions at low concentrations has become more evident from the observations made in Chapter II which are (a) the value of $a_{o\Lambda}$ parameter for a particular electrolytic solution is considerably lower than its Λ_o value

and (b) the fitting of the $\Lambda\eta$ data to an equation based on Eq(3-1) at low concentrations is not as good as the fitting obtained at high concentrations.

In this chapter we have therefore made an attempt to improve Eq(3-1) by incorporating in it ion-ion interaction terms separately for viscosity and conductance. We have also extended the measurement of density, viscosity, and conductance of the six electrolytic solutions cited in the previous chapters to still lower concentrations with a view to examining the applicability of the modified isothermal equations to be obtained for viscosity and conductance.

Experimental Section

The method used for the measurement of density, viscosity, and conductance is the same as described under the Experimental Technique.

Results and Discussion

The measured density, viscosity, and equivalent conductance data for $Ca(NO_3)_2$-H_2O, $Mg(NO_3)_2$-H_2O, $MgCl_2$-H_2O, $NiCl_2$-H_2O, $Na_2S_2O_3$-H_2O, and $NaNO_3$-H_2O systems are summarized in Tables 3-1, 3-2, and 3-3, respectively.

Table 3-1: Least-Squares Fitted Values of the Parameters for the Density Equation, $\rho = a - bt$ (°C) of Electrolytic Solutions at Low Concentrations.

System	m ($mol.kg^{-1}$)	a ($g.\ cm^{-3}$)	b x 10^4 ($g.\ cm^{-3}.°C^{-1}$)	Std. dev. in ρ σ x 10^5
$Ca(NO_3)_2$-H_2O	7.376×10^{-4}	1.0092	4.1806	9.46
	2.170×10^{-3}	1.0106	4.3512	9.70
	8.677×10^{-3}	1.0119	4.4801	5.15
	2.598×10^{-2}	1.0134	4.3474	5.70
	7.812×10^{-2}	1.0204	4.7216	7.57
$Mg(NO_3)_2$-H_2O	2.266×10^{-3}	1.0183	5.7094	9.02
	4.533×10^{-3}	1.0177	5.5774	6.42
	9.072×10^{-3}	1.0124	4.5779	6.06
	2.336×10^{-2}	1.0156	4.8684	5.48
	6.851×10^{-2}	1.0214	5.0237	6.12
$MgCl_2$-H_2O	1.064×10^{-3}	1.0094	4.0237	6.46
	4.261×10^{-3}	1.0103	4.1924	9.52
	1.245×10^{-2}	1.0112	4.2240	4.00
	5.566×10^{-2}	1.0152	4.4514	6.49
	9.983×10^{-2}	1.0180	4.3608	7.87

Continued.

Table 3-1: (Continued)

System	m ($mol.kg^{-1}$)	a ($g.\ cm^{-3}$)	b x 10^4 ($g.cm^{-3}.°C^{-1}$)	Std. dev. in ρ σ x10^5
$NiCl_2$-H_2O	1.471x10^{-3}	1.0126	4.5873	8.70
	8.825x10^{-3}	1.0131	4.5270	6.42
	2.354x10^{-2}	1.0136	4.3182	5.32
	8.416x10^{-2}	1.0214	4.5820	6.22
$Na_2S_2O_3$-H_2O	1.652x10^{-3}	1.0124	4.7574	5.89
	4.136x10^{-3}	1.0106	4.3711	5.74
	8.503x10^{-3}	1.0112	4.3619	5.41
	1.887x10^{-2}	1.0129	4.5282	6.29
	8.230x10^{-2}	1.0201	4.3042	7.04
$NaNO_3$-H_2O	1.257x10^{-3}	1.0106	4.2391	9.03
	6.746x10^{-3}	1.0111	4.2848	6.45
	1.602x10^{-2}	1.0131	4.5856	9.02
	7.076x10^{-2}	1.0156	4.5716	7.21

Table 3-2: Viscosities (η) of Electrolytic Solutions as Functions of Concentration and Temperature.

System	m (mol. kg^{-1})	η(cP) 293K	298K	308K	323K	343K
$Ca(NO_3)_2 - H_2O$	7.376×10^{-4}	-	0.8927	0.7232	-	0.4213
	2.170×10^{-3}	-	0.8948	0.7242	-	0.4226
	2.598×10^{-2}	-	0.8972	0.7267	-	0.4273
	7.812×10^{-2}	-	0.9122	0.7361	-	0.4329
$Mg(NO_3)_2 - H_2O$	2.266×10^{-3}	-	0.8785	0.7131	0.5494	-
	9.072×10^{-3}	-	0.8913	0.7209	0.5529	-
	6.851×10^{-2}	-	0.9026	0.7320	0.5652	-
$MgCl_2 - H_2O$	1.064×10^{-3}	1.0190	-	0.7351	0.5599	-
	4.261×10^{-3}	1.0267	-	0.7438	0.5605	-
	1.245×10^{-2}	1.0303	-	0.7448	0.5678	-
	5.566×10^{-2}	1.0330	-	0.7451	0.5748	-
	9.983×10^{-2}	1.0673	-	0.7638	0.5912	-

Continued.

Table 3-2: (Continued)

System	m (mol. kg^{-1})	η(cP) 288K	293K	308K	318K	323K
$NiCl_2 - H_2O$	1.471×10^{-3}	1.1230	-	0.7208	-	0.5597
	8.825×10^{-3}	1.1387	-	0.7232	-	0.5608
	2.354×10^{-2}	1.1689	-	0.7430	-	0.5738
	8.416×10^{-2}	1.2303	-	0.7719	-	0.5821
$Na_2S_2O_3 - H_2O$	1.652×10^{-3}	1.1423	-	0.7198	0.6037	-
	8.503×10^{-3}	1.1496	-	0.7300	0.6083	-
	1.887×10^{-2}	1.1565	-	0.7335	0.6106	-
$NaNO_3 - H_2O$	1.257×10^{-3}	1.0088	-	0.7239	-	0.5571
	6.746×10^{-3}	1.0099	-	0.7244	-	0.5583
	1.602×10^{-2}	1.0103	-	0.7246	-	0.5588
	7.076×10^{-2}	1.0112	-	0.7260	-	0.5592

Table 3-3: Equivalent Conductances (Λ) of Electrolytic Solutions as Functions of Concentration and Temperature.

System	m (mol. kg^{-1})	Λ (mho cm^2 $equiv^{-1}$)			
		293K	298K	308K	323K
$Ca(NO_3)_2 - H_2O$	2.170×10^{-3}	-	123.95	151.09	191.04
	8.677×10^{-3}	-	112.27	136.04	173.32
	2.598×10^{-2}	-	100.43	121.60	154.09
	7.812×10^{-2}	-	86.729	103.82	120.23
$Mg(NO_3)_2 - H_2O$	2.266×10^{-3}	-	120.05	144.88	181.28
	4.533×10^{-3}	-	113.21	135.84	172.21
	9.072×10^{-3}	-	108.36	130.16	162.96
	2.336×10^{-2}	-	92.551	111.78	141.09
	6.851×10^{-2}	-	84.945	100.50	124.97
$MgCl_2 - H_2O$	5.566×10^{-2}	111.06	-	146.65	184.45

Continued.

Table 3-3: (Continued)

System	m (mol. kg^{-1})	Λ (mho cm^2 $equiv^{-1}$)			
		293K	308K	318K	323K
$NiCl_2 - H_2O$	8.825×10^{-3}	124.90	165.03	-	205.25
	2.354×10^{-2}	117.74	159.71	-	-
$Na_2S_2O_3 - H_2O$	1.652×10^{-3}	247.91	336.18	400.94	-
	4.136×10^{-3}	237.43	321.98	380.86	-
	1.887×10^{-2}	185.88	254.09	300.91	-
	8.230×10^{-2}	166.16	223.46	259.30	-
$NaNO_3 - H_2O$	6.746×10^{-3}	111.35	150.95	-	196.18
	1.602×10^{-2}	102.08	135.97	-	-
	7.076×10^{-2}	100.21	-	-	-

In order to take into account the effect of ion-ion interactions on viscosity we added a $m^{1/2}$ term to the right hand side of Eq(3-1) for viscosity. This has been done in the light of the fact that in the Jones-Dole[1] empirical equation valid at low concentrations the $c^{1/2}$ term has been interpreted as the contribution from interionic forces that tend to interfere with the flow of one layer of solution past another. The modified Eq(3-1) for viscosity may therefore be written as

$$\eta = Am^{1/2} + a_{o\eta} \exp (b_{o\eta} m + c_{o\eta} m^2) \qquad (3-2)$$

where A is the coefficient whose value actually determines the amount of contribution made to viscosity from the ion-ion interactions. It may be cited that Spedding and Pikal[2] also employed a similar hybrid equation by combining the Vand's equation[3] (corresponds to the ion-solvent interactions) with the Pitts equation[4] (corresponds to the ion-ion interactions) to explain the concentration dependence of viscosities of aqueous solutions of rare-earth chlorides.

A least-squares fitting of the complete viscosity data (the present low concentration data and the data obtained in Chapter I) for the different electrolytic solutions to Eq(3-2) was made and the values of the computed

parameters are given in Table 3-4. Such a fitting although represented the viscosity data reasonably well, it provided in some cases negative A coefficients as apparent from Table 3-4. A similar situation was faced by others[5,6] also while fitting the low-concentration viscosity data to the Jones-Dole equation. Such a result, however, appears to be without physical significance.[7] Therefore we calculated the values of A from its theoretical expression[8] and substituted these theoretical values into Eq(3-2) before least-squares fitting the viscosity data to this equation. In the case of $Na_2S_2O_3$ solution, the value of its equivalent conductance at infinite dilution required for estimating the mobility of $S_2O_3^{2-}$ ion which, in turn, is needed in the calculation of A value was obtained by extrapolating the plot of our low-concentration equivalent conductance data for $Na_2S_2O_3$ solution against $c^{1/2}$ (c is the concentration in equivalents per liter) to zero concentration (literature value of ionic conductance at infinite dilution for $S_2O_3^{2-}$ ion was not readily available). This method of assigning to A its theoretical value during the analysis of viscosity data rather than computing it from the least-squares fitting procedure was earlier adopted by other workers[2,5] also. The viscosity data were fitted to Eq(3-2)

Table 3-4: Values of Best-Fit Parameters for Eq(3-2) for the Viscosity (cP) of Electrolytic Solutions

System	T(K)	$a_{o\eta}$	$b_{o\eta}$	$c_{o\eta}$ x10^3	Ax10^2	Std. dev. in η σ x10^2
$Ca(NO_3)_2 - H_2O$	298.0	0.9627	0.2885	10.2934	-26.43	0.28
(7.376×10^{-4}m- 12.79m)	308.0	0.7645	0.3029	6.5379	-20.22	0.19
	343.0	0.4399	0.3168	-0.1803	-9.08	0.10
$Mg(NO_3)_2 - H_2O$	298.0	0.8550	0.2768	19.7056	10.1537	4.74
(2.266×10^{-3}m-6.3682m)	308.0	0.6820	0.2427	24.7741	14.1136	4.80
	323.0	0.5528	0.3784	-3.2256	-2.8990	5.55
$MgCl_2 - H_2O$	293.0	0.9839	0.2633	34.6246	19.7026	3.52
(1.064×10^{-3}m-5.9872m)	308.0	0.7229	0.2829	26.4398	9.8027	2.74
	323.0	0.5493	0.2803	23.5730	8.9862	2.25

Continued

Table 3-4: (Continued)

System	T(K)	$a_{o\eta}$	$b_{o\eta}$	$c_{o\eta} \times 10^3$	A x 10^2	Std. dev. in η
$NiCl_2$ - H_2O	288.0	1.1941	0.4138	5.9183	-20.75	0.069
(1.471 x 10^{-3}m-5.6853m)	308.0	0.7026	0.3161	18.9773	14.12	0.071
	323.0	0.5373	0.3113	15.2234	12.33	0.050
$Na_2S_2O_3$ - H_2O	288.0	1.1242	0.3156	30.4080	15.357	0.044
(1.652 x 10^{-3}m-9.8184m)	308.0	0.7388	0.4252	-6.5598	-9.8436	0.068
	318.0	0.6018	0.3868	-4.8588	2.6039	0.030
$NaNO_3$ - H_2O	293.0	1.0188	0.1229	-1.2191	-6.4740	0.024
(1.257 x 10^{-3}m-9.8626m)	308.0	0.7292	0.1281	-2.0402	-3.9544	0.013
	323.0	0.5579	0.1110	-0.6194	-0.8766	0.008

Concentration ranges are given within the parentheses.

using the above approach at different temperatures with an assumption that A varies negligibly with temperature.[5] The values of the parameter of Eq(3-2) obtained thus are listed in Table 3-5. The theoretical values calculated for A are also included in Table 3-5. The success of Eq(3-2) in describing the concentration dependence of viscosity of the different electrolytic solutions under study in the entire experimental range of concentration (from low to saturation point) is also apparent from the linearity of the plot of $\ln(\eta - Am^{1/2})$ versus $b_{o\eta}\, m + c_{o\eta}\, m^2$ (Fig 3-1).

Similarly we incorporated a term containing $m^{1/2}$ in the right hand side of Eq(3-1) for equivalent conductance keeping in view that such a term would account for the contribution to conductance due to ion-ion interactions at low-concentrations. The extended form of Eq(3-1) for equivalent conductance may therefore be written as

$$\Lambda = a_{o\Lambda} \exp(b_{o\Lambda}\, m + c_{o\Lambda}\, m^2) - S_o m^{1/2} \qquad (3\text{-}3)$$

where S_o is a constant parameter whose value depends upon the nature of the solvent and solute and on the temperature of the solution. The conductance data in the complete

Table 3-5: Least-Squares Fitted Values of the Parameters of Eq(3-2) for the Viscosity (cP) of Electrolytic Solutions after Substituting the Theoretical Values of A

System	T(K)	$a_{o\eta}$	$b_{o\eta}$	$c_{o\eta}$ x10^2	A	Std. dev. in ln η
$Ca(NO_3)_2 - H_2O$	298.0	0.8741	0.2730	1.2175	0.0164	0.034
(7.376×10^{-4}m-12.79m)	308.0	0.7077	0.2820	0.8815		0.034
	343.0	0.4128	0.2955	0.1936		0.038
$Mg(NO_3)_2 - H_2O$	298.0	0.8772	0.3142	1.2153	0.0078	0.014
(2.266×10^{-3}m-6.3682m)	308.0	0.7116	0.3079	1.2332		0.021
	323.0	0.5413	0.3548	0.0720		0.032
$MgCl_2 - H_2O$	293.0	1.0268	0.3284	2.1509	0.0170	0.015
(1.064×10^{-3}m-5.9872m)	308.0	0.7412	0.3202	1.9578		0.015
	323.0	0.5660	0.3230	1.1582		0.022

Continued.

Table 3-5: (Continued)

System	T(K)	$a_{o\eta}$	$b_{o\eta}$	$c_{o\eta}$ x10^2	A	Std. dev. in ln η
$NiCl_2$ - H_2O	288.0	1.1504	0.3508	1.8838	0.0171	0.021
(1.471 x 10^{-3}m-5.6853m)	308.0	0.7298	0.3579	1.1243		0.018
	323.0	0.5576	0.3631	0.6041		0.016
$Na_2S_2O_3$ - H_2O	288.0	0.1195	0.4534	-0.2138	0.0077	0.044
(1.652 x 10^{-3}m-9.8184m)	308.0	0.7251	0.4064	-0.4448		0.017
	318.0	0.6280	0.3852	-0.5230		0.027
$NaNO_3$ - H_2O	293.0	1.0044	0.0960	0.0981	0.0062	0.014
(1.257 x 10^{-3}m-9.8626m)	308.0	0.7187	0.1056	-0.0245		0.021
	323.0	0.5549	0.1011	0.0151		0.009

Concentration ranges are given within the parentheses.

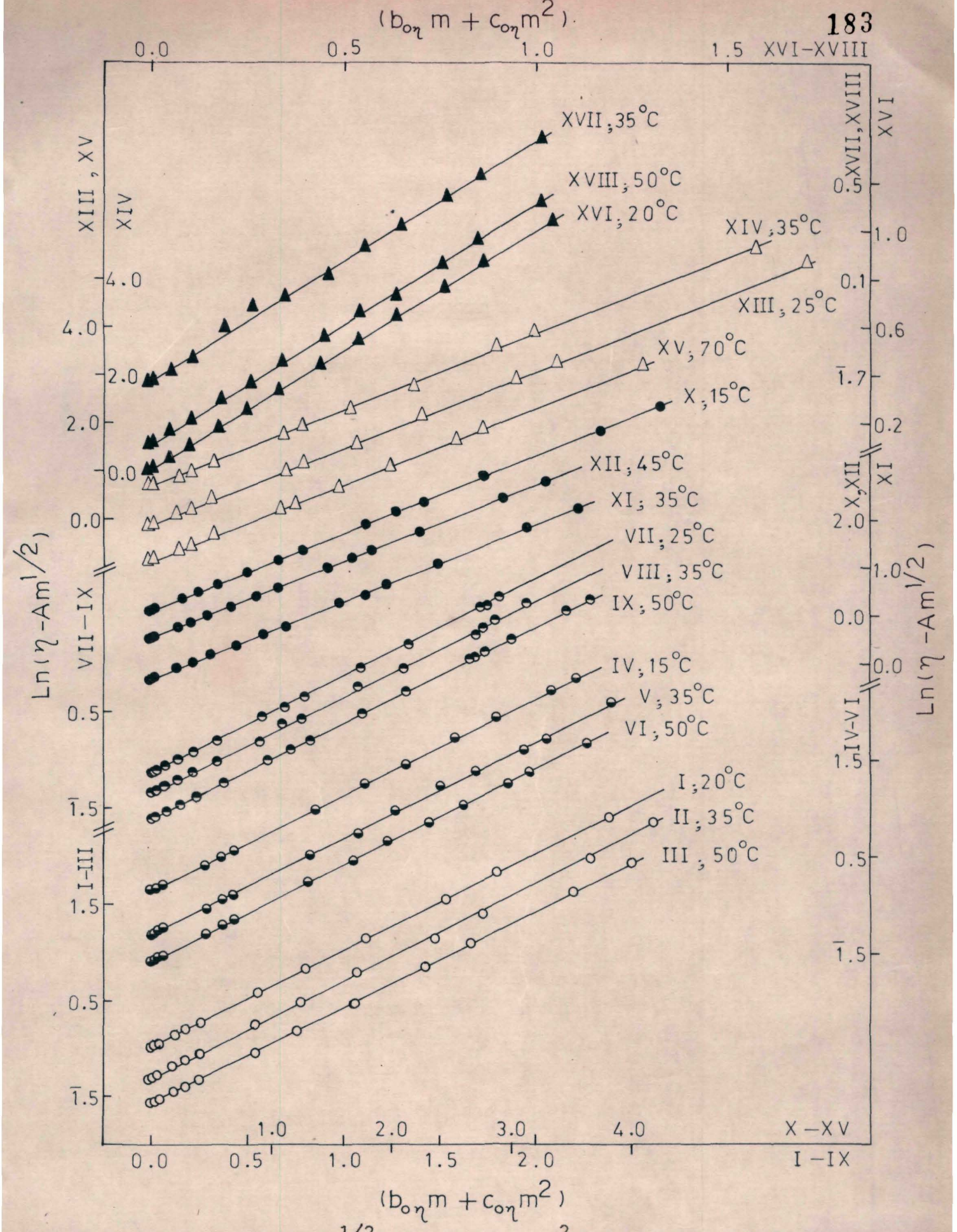

Fig 3-1: Plots of $\ln(\eta - Am^{1/2})$ vs. $b_{o\eta}m + c_{o\eta}m^2$ for aqueous electrolytes (O-$MgCl_2$, ⊖-$NiCl_2$, ⊖-$Mg(NO_3)_2$, ●-$Na_2S_2O_3$, Δ-$Ca(NO_3)_2$, and ▲-$NaNO_3$ solutions).

experimental range of concentration (present data and the data from Chapter II) were least-squares fitted to Eq(3-3) and the computed values of the parameters are listed in Table 3-6 at three different temperatures for each electrolyte under consideration. In all the systems the value of S_o has been found to be positive and hence it may be correlated with the S parameter (limiting slope) of the theoretical expression[9] for conductance in the low-concentration region. As apparent from Table 3-6 the value of S_o increases with increasing temperature which is consistent with a similar dependence shown by S parameter also.[10,11]

It is worthwhile to note that the values of the $a_{o\Lambda}$ term which was equated to the Λ_o term in the preceding chapter have increased considerably after the inclusion of $S_o m^{1/2}$ term in the expression for Λ . Therefore, the lower values obtained in Chapter II for $a_{o\Lambda}$ than the corresponding Λ_o values are undoubtedly due to the omission of the ion-ion interaction term in Eq(2-5). The striking agreement obtained between the $a_{o\Lambda}$ and Λ_o values of $NaNO_3$ and $MgCl_2$ solutions is interesting to note. For instance, at 298K, for $NaNO_3$ solution $a_{o\Lambda}$ (obs.) = 121.51 mho cm^2 $equiv^{-1}$ and Λ_o(Calc.[12]) = 121.5 mho cm^2 $equiv^{-1}$ and for $MgCl_2$

Table 3-6: Least-Squares Fitted Values of the Parameters for Eq(3-3) for the Equivalent Conductance (mho cm^2 $equiv^{-1}$) of Electrolytic Solutions.

System	T(K)	$a_{o\Lambda}$	$b_{o\Lambda}$	$c_{o\Lambda}$	S_o	Std. dev. in ln Λ
$Ca(NO_3)_2 - H_2O$	298.0	151.64	0.2986	-0.0145	202.96	0.129
(2.170×10^{3}m-12.79m)	308.0	185.64	0.3053	-0.0149	254.04	0.134
	323.0	234.26	0.3046	-0.0149	319.53	0.133
$Mg(NO_3)_2 - H_2O$	298.0	143.97	0.6536	-0.0801	246.51	0.094
(2.266×10^{-3}m-5.2393m)	308.0	175.17	0.6421	-0.0754	303.70	0.098
	323.0	218.52	0.6358	-0.0743	376.16	0.095
$MgCl_2 - H_2O$	293.0	116.08	0.1389	-0.0067	83.09	0.043
(5.566×10^{-2}m-5.9872m)	308.0	152.57	0.1283	-0.0054	106.86	0.044
	323.0	208.06	0.2096	-0.0143	176.08	0.036

Continued.

Table 3-6: (Continued)

System	T(K)	$a_{o\Lambda}$	$b_{o\Lambda}$	$c_{o\Lambda}$	S_o	Std. dev. in ln Λ
$NiCl_2 - H_2O$	293.0	138.39	0.2953	-0.0272	136.50	0.031
(8.825×10^{-3}m-4.9901m)	308.0	185.37	0.3072	-0.0284	188.02	0.031
	323.0	225.64	0.2802	-0.0246	218.03	0.027
$Na_2S_2O_3 - H_2O$	293.0	276.43	0.3151	-0.0192	331.28	0.098
(1.652×10^{-3}m-9.8184m)	308.0	376.60	0.3241	-0.0200	456.77	0.100
	318.0	453.15	0.3386	-0.0212	569.41	0.100
$NaNO_3 - H_2O$	293.0	110.79	0.0462	-0.0003	47.02	0.019
(6.746×10^{-3}m-9.8626m)	308.0	148.78	0.0305	-0.0009	60.48	0.028
	323.0	193.97	0.0164	-0.0022	77.30	0.038

Concentration ranges are given within the parentheses.

solution $a_{o\Lambda}$ (obs.) = 126.47 mho cm^2 $equiv^{-1}$ and Λ_o(Calc.[12]) = 128.6 mho cm^2 $equiv^{-1}$. It may be noted that wherever least-squares fitted values of $a_{o\Lambda}$ at 298K required for the above kind of comparison were not available in Table 3-6, they were estimated in those cases from the values of $a_{o\Lambda}$ at other temperatures by plotting ln $a_{o\Lambda}$ versus 1/T as this plot in such a narrow range of temperature was found to be linear.[13] In the case of $Na_2S_2O_3$ solution the $a_{o\Lambda}$ value was found to be ~10% higher than the Λ_o value. The value of Λ_o for $Na_2S_2O_3$ solution was estimated from our low-concentration conductance data for this solution as mentioned above. In $Ca(NO_3)_2$, $Mg(NO_3)_2$, and $NiCl_2$ solutions, the $a_{o\Lambda}$ values are found to be about 15% higher than the corresponding Λ_o values.[12,14] Although the above agreement between the $a_{o\Lambda}$ and Λ_o values of $Ca(NO_3)_2$, $Mg(NO_3)_2$, $NiCl_2$, and $Na_2S_2O_3$ solutions is within 15%, it still appears to be a reasonable agreement in the light of the fact that the $a_{o\Lambda}$ value is obtained by fitting the conductance data in a wide range of concentration (very low to saturation point) whereas Λ_o value is computed using conductance data limited to very dilute region. Such a close resemblance between the $a_{o\Lambda}$ and Λ_o values of $NaNO_3$ and $MgCl_2$ solutions and an agreement within a reasonable range between the values of these two parameters for the rest of the solutions under study appear to support without doubt the

feasibility of Eq(3-3) for representing the conductance data of electrolytic solutions in a wide range of concentration. Moreover, the linearity of the plot (Fig 3-2) of $\ln (\Lambda + S_o m^{1/2})$ versus $b_{o\Lambda} m + c_{o\Lambda} m^2$ emphasizes further the applicability of Eq(3-3) in describing the concentration dependence of conductance in the entire experimental range of concentration.

Furthermore, it is worth estimating the values of the $\Lambda\eta$ product from the expression

$$\Lambda\eta = \left[a_{o\Lambda} \exp(b_{o\Lambda} m + c_{o\Lambda} m^2) - S_o m^{1/2}\right] \left[Am^{1/2} + a_{o\eta} \exp(b_{o\eta} m + c_{o\eta} m^2)\right] \qquad (3\text{-}4)$$

so that any improvement in the closeness of the observed and calculated values of $\Lambda\eta$ caused by the insertion of ion-ion interaction parameters, viz., $Am^{1/2}$ and $S_o m^{1/2}$, may be examined (cf. Chapter II). In Fig 3-3 we have plotted both the observed and calculated values of $\Lambda\eta$ at 35°C versus concentration. From this plot it is evident that Eq(3-4) satisfactorily fits the $\Lambda\eta$ data in the whole experimental range of concentration unlike the case with Eq(2-8) which could not reproduce satisfactorily the $\Lambda\eta$ data at low-concentrations. The remarkable success of Eq(3-4) in representing the $\Lambda\eta$ data at high as well as low concentrations is, of course, attributable to the presence of ion-ion interaction terms in this equation.

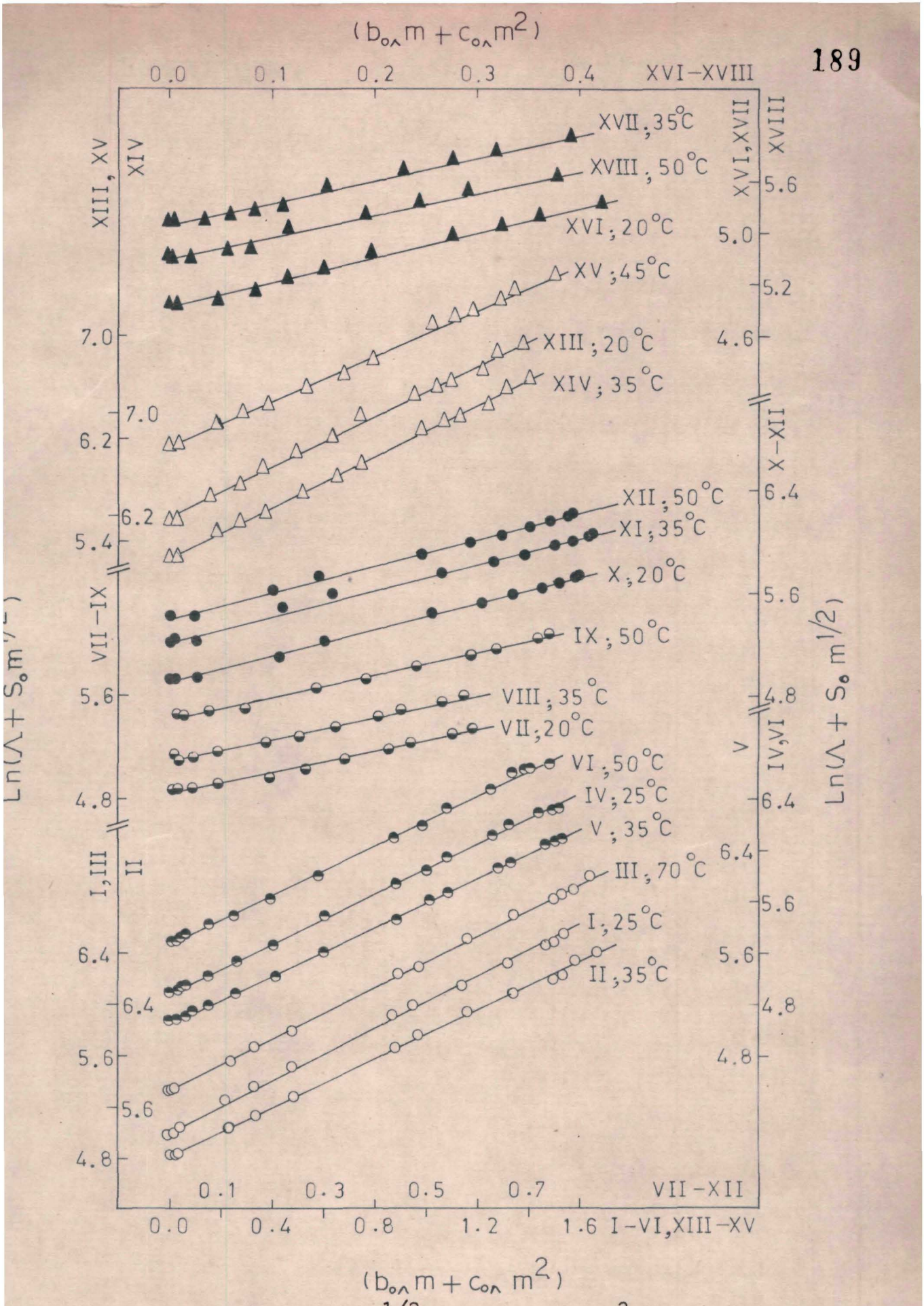

Fig 3-2: Plots of $\ln(\Lambda + S_o m^{1/2})$ vs. $b_{o\Lambda}m + c_{o\Lambda}m^2$ for aqueous electrolytes (o-$Ca(NO_3)_2$, ⊖-$Mg(NO_3)_2$, ⊖-$MgCl_2$, ●-$NiCl_2$, Δ-$Na_2S_2O_3$, and ▲-$NaNO_3$ solutions).

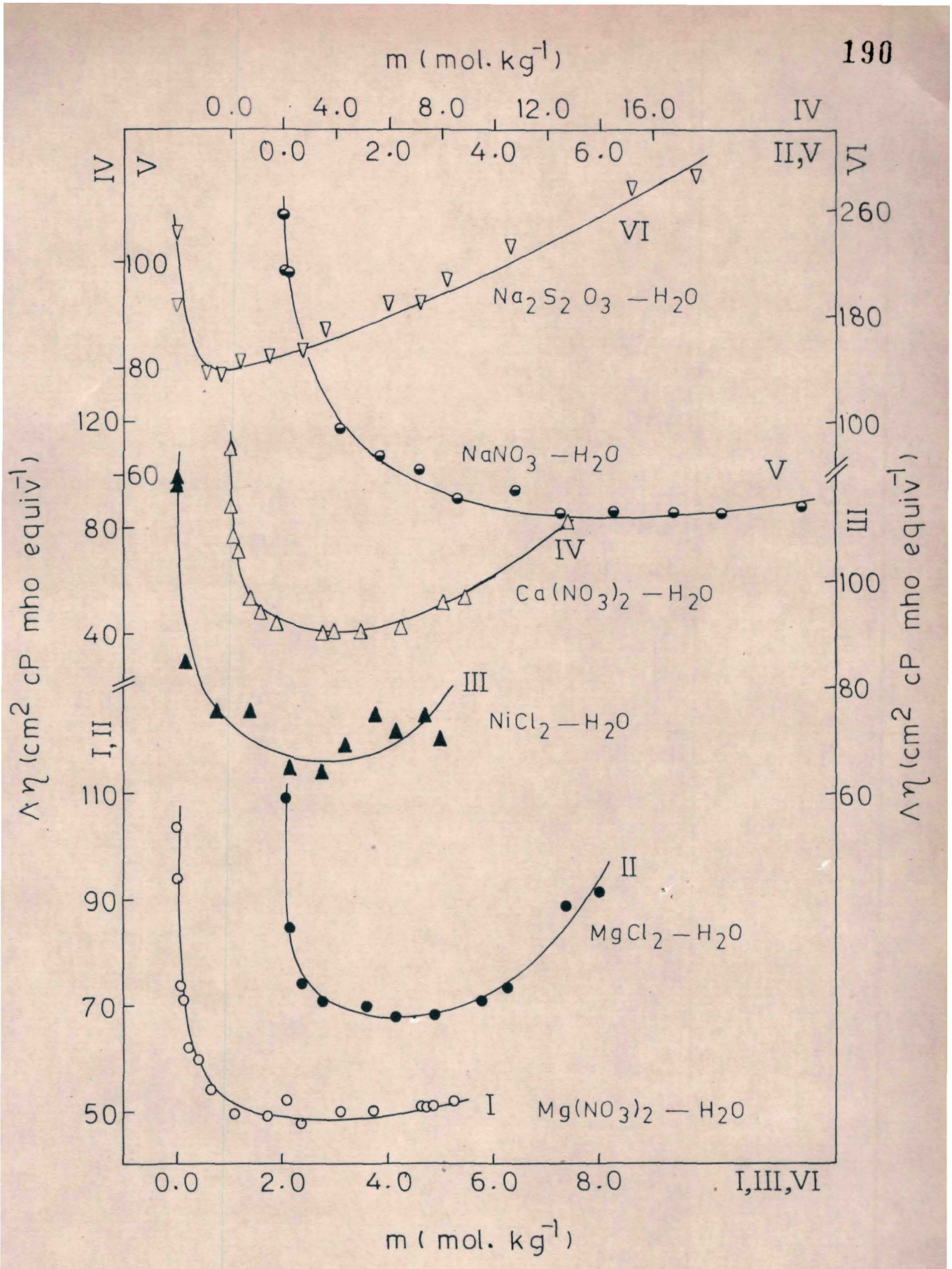

Fig 3-3: Plots of Walden product vs. m for aqueous electrolytes. Different notations denote the observed values whereas the solid lines represent the calculated values.

It is also worth noting that the minimum which was not present in the calculated values of $\Lambda\eta$ of $Na_2S_2O_3$ solution using Eq(2-8) has now been observed in the $\Lambda\eta$ values estimated from Eq(3-4) and the concentration at which this minimum occurs coincides with the observed value, of concentration. Such an achievement of Eq(3-4) provides additional support to the applicability of Eqs(3-2) and (3-3) in explaining the concentration dependence of viscosity and conductance, respectively, of electrolytic solutions in the concentration range varying from very low value upto the saturation point.

Finally, an attempt has been made to correlate the isothermal Eq(3-4) with the semi-empirical equation of Wishaw and Stokes[15] which has also shown some success in describing the conductance data upto a high concentration. In order to achieve this we approximated (Appendix VII) the Wishaw-Stokes equation at low concentration to

$$\Lambda\eta = Q_1 - Q_2 c^{1/2} + Q_3 c - Q_4 c^{3/2} + Q_5 c^2 \qquad (3\text{-}5)$$

where Q_1, Q_2, Q_3, Q_4, and Q_5 are constants for a given electrolytic solution at a particular temperature. Similarly, at low concentrations Eq(3-4) may also be approximated (Appendix VII)

to an expression of the form

$$\Lambda\eta = Q_1^* + Q_2^* m^{1/2} + Q_3^* m + Q_4^* m^{3/2} + Q_5^* m^2 \qquad (3\text{-}6)$$

where Q_1^*, Q_2^*, Q_3^*, Q_4^*, and Q_5^* are again constant parameters for an electrolytic solution at isothermal condition. At low concentrations $m \approx c$ and Eq(3-6) may be considered to become identical with Eq(3-5) and the coefficients of the different powers of concentration in the two equations may be equated to each other. The advantage of this kind of correlation is that it enables us to estimate the value of the ion-size parameter, a° for the different electrolytes because of the fact that Q_3 is related to a° (Appendix VII). The values of a° estimated in this manner at 35°C are found to be 6.92, 11.63, 5.38, 8.02, 9.05, and 4.12 Å for $Ca(NO_3)_2 - H_2O$, $Mg(NO_3)_2 - H_2O$, $MgCl_2 - H_2O$, $NiCl_2 - H_2O$, $Na_2S_2O_3 - H_2O$, and $NaNO_3 - H_2O$ systems, respectively. The value 4.12 Å obtained for the a° value of $NaNO_3$ solution at 35°C appears to be comparable with the value 3.3 Å reported[16] for this system at 25°C (a° has been found to increase with temperature[10,11]). Strictly speaking, the above approach may be effectively used for evaluating the a° parameter only if the low-concentration data are used in the least-squares fitting to Eq(3-4). In view of this fact the above value of a° (4.12 Å) for $NaNO_3$

solution which is computed using the parameters obtained by least-squares fitting the $\Lambda\eta$ data in the entire experimental concentration range to Eq(3-4) seems to be quite reasonable in comparison with the reported[16] value. We could not make at the moment an estimation of the correctness of the a° values calculated for the rest of the systems as the literature values were not readily available for the comparison sake. It may, however, be noted that the calculated a° values of $Ca(NO_3)_2$ - H_2O, $MgCl_2$ - H_2O, and $NiCl_2$ - H_2O systems are comparable with the values of the sum of their respective hydrated ionic radii.[17] Accordingly the different solutes considered here appear to exist in the associated form in aqueous solutions as suggested by Janz et al.[16] in the case of $NaNO_3$. The above meaningful values of a° derived from the parameters of Eqs(3-2) and (3-3) appear to justify again the validity of these equations.

Therefore, it may be concluded by emphasizing that equation of the type (3-2) or (3-3) may be successfully employed to describe the concentration dependence of viscosity or conductance of electrolytic solutions in a wide range of concentration.

References:

1. G. Jones and M.Dole, J. Amer. Chem. Soc., 51, 2950 (1929).
2. F.H. Spedding and M.J. Pikal, J. Phys. Chem., 70, 2430 (1966).
3. V. Vand, J. Phys. Colloid Chem., 52, 277; 300; 314 (1948).
4. E. Pitts, Proc. Roy. Soc. London, A217, 43 (1953).
5. N.P. Yao and D.N. Bennion, J. Phys. Chem., 75, 1727 (1971).
6. R.L. Kay, J. Vituccio, C. Zawoyski, and D.F. Evans, J. Phys. Chem., 70, 2336 (1966).
7. H.S. Harned and B.B. Owen, 'The Physical Chemistry of Electrolytic Solutions', 3rd Ed., Reinhold, New York, 1958.
8. J.R. Partington, 'An Advanced Treatise on Physical Chemistry', Longman, Green and Co., London, 1951.
9. H. Falkenhagen, W. Ebeling, and W.D. Kraeft, 'Ionic Interactions', Vol. I, Ch. 2, S. Petrucci, ed., Academic Press, New York, 1971.
10. R.L. Kay, J. Amer. Chem. Soc., 82, 2099 (1960).
11. M. Goffredi and T. Shedlovsky, J. Phys. Chem., 71, 2176 (1967).

12. T. Shedlovsky and L. Shedlovsky, 'Physical Methods of Chemistry', Vol. I, Part IIA, Ch. III, A. Weissberger, ed., Wiley-Interscience, New York, 1971.

13. S. Glasstone, 'An Introduction to Electrochemistry', p. 61, East-West Press, New Delhi, 1975.

14. K. Murata, Bull. Chem. Soc. Japan, 3, 47 (1928).

15. B.F. Wishaw and R.H. Stokes, J. Amer. Chem. Soc., 76, 2065 (1954).

16. G.J. Janz, B.G. Oliver, G.R. Lakshminarayanan, and G.E. Mayer, J. Phys. Chem., 74, 1285 (1970).

17. E.R. Nightingale, J. Phys. Chem., 63, 1381 (1959).

PART II

MOLTEN ELECTROLYTES

CHAPTER IV

CONCENTRATION DEPENDENCE OF FLUIDITY AND CONDUCTANCE OF BINARY MELTS*

---

* Publication at present based on this study:

1. S. Mahiuddin and K. Ismail, Bull. Chem. Soc. Japan, 54, 2525 (1981).

Introduction

In Part I an isothermal equation has been obtained to describe the variation in viscosity and conductance of electrolytic solutions with concentration. This isothermal equation was derived from the Adam-Gibbs equation[1] by introducing the empirical nature of the temperature dependence of heat capacity.

A large amount of literature[2-9] on the transport properties of binary molten systems containing at least one component as the hydrated salt has been accumulated. The temperature dependence of the transport properties of all such molten salt systems has been described in terms of the VTF equation,

$$Y(\phi, \Lambda) = A_y T^{-1/2} \exp\left[-B_y/(T-T_{o_y})\right] \qquad (4\text{-}1)$$

where Y is the transport property, either fluidity (ϕ) or equivalent conductance (Λ). T is the absolute temperature. A_y, B_y, and T_{o_y} are the three constant parameters. Empirically all these three parameters have been found to have dissimilar types of concentration dependence. B_y

remains almost independent of concentration in binary systems containing either anhydrous or hydrated salts (or both) unlike the case with electrolytic solutions. The ideal glass transition temperature, T_{o_y} has been found to vary linearly with concentration in almost all the binary melts studied. Such a linear dependence of T_{o_y} on concentration has been explained on the basis of cohesive energy or cationic potential[10] of the system. On the other hand, the dependence of A_y parameter on concentration is comparatively less understood and the nature of this dependence is found to be inconsistent in the systems studied. For instance, studies made by Islam and cowrkers[5-8] have revealed a linear dependence of A_y on concentration. Instead, Moynihan et al.[4] observed a linear variation of $\ln A_y$ with concentration in the molten mixture of calcium nitrate tetrahydrate and cadmium nitrate tetrahydrate. They also observed that this kind of trend in the variation of A_y was contrary to the behaviour expected from the free volume model.[11]

The objective of this chapter is therefore to obtain an analytical expression to describe the observed trend in the variation of A_y with concentration and then to derive an isothermal equation for representing the concentration

dependence of fluidity and conductance of binary mixtures containing hydrate melt or melts. The approach used for this purpose is the same as that adopted for electrolytic solutions (cf. Chapter I), namely, to insert the empirically observed temperature dependence of heat capacity in the Adam-Gibbs equation.

Derivation of the new isothermal equation

It is interesting to note from the reported heat capacity data for hydrate melts[12] and molecular liquids[13,14] that their heat capacity also exhibits a linear dependence on temperature in the glassy as well as liquid regions. Accordingly the configurational heat capacity, ΔC_p may be written as

$$\Delta C_p = \Delta C_o + \Delta C_1(T-T_o) \qquad (4-2)$$

where ΔC_o and ΔC_1 have the same meanings defined in Chapter I. It may be noted that ΔC_1 becomes a negative, zero, or positive term depending upon the relative rates of change (linear) of heat capacity of liquid and glass with temperature. For example, in $Ca(NO_3)_2 \cdot 4H_2O$,[12] $Cd(NO_3)_2 \cdot 4H_2O$,[12] $Mg(OAc)_2 \cdot 4H_2O$,[12] o-terphenyl,[13,14] α-phenyl-o-cresol,[14] and

phenyl salicylate[14] ΔC_l is found to be a negative quantity and Eq(4-2) resembles with the function used by Laughlin and Uhlmann[14] for ΔC_p as well as with one of the probable functions suggested by Privalko.[15]

On substituting Eq(4-2) in the Adam-Gibbs equation and then by making proper approximations, the VTF equation may be derived in a similar manner described in Chapter I. Consequently, we get an expression for A_y as

$$A_y = A_{oy} \exp(B_{oy}/T_{oy}) \qquad (4-3)$$

where A_{oy} and B_{oy} are constant parameters for a given binary molten mixture. Furthermore, by taking into account in Eq(4-1) the constancy of B_y and the linear variation of T_{oy} with mole fraction of the solute, x, the expression for Y becomes

$$Y = A_{oy} \exp\left[B_{oy}/(T_o(o) \pm Qx)\right] \exp\left[-B_y/(T-T_o(o)\mp Qx)\right] \qquad (4-4)$$

where Q is the slope of the linear variation of T_{oy} with x and $T_o(o)$ is the T_o of pure melt forming the solvent. Eq(4-4) may be approximated[16] by neglecting the higher powers of x to

$$Y = A_y^* \exp (\mp Q_y^* x) \qquad (4\text{-}5)$$

where $A_y^* = A_{oy} \exp \left[B_{oy}/T_o(o) - B_y/(T-T_o(o))\right]$ and

$Q_y^* = B_{oy} Q/T_o(o) + B_y Q/(T-T_o(o))^2$. The negative sign of the exponent in Eq(4-5) is valid when T_o increases with x and the positive sign corresponds to the case of T_o decreasing with x.

On the application of Eqs(4-3) and (4-5)

A. Before examining the application of Eq(4-5) to melts containing hydrated salts, it is preferable to justify first the suitability of Eq(4-3) for describing the variation of A_y parameter with concentration. Therefore, exemplary plots of $\ln A_y$ versus $1/T_{oy}$ using their reported values are drawn in Fig 4-1 for some of the molten mixtures, viz., $Zn(NO_3)_2 \cdot 6.33\ H_2O + Ca(NO_3)_2 \cdot 4.1\ H_2O$,[7a] $Ca(NO_3)_2 \cdot 4.09\ H_2O + Cd(NO_3)_2 \cdot 4.07\ H_2O$,[4] $Ca(NO_3)_2 \cdot 3.91\ H_2O + CoCl_2$,[5b] $Cd(NO_3)_2 \cdot 4.1\ H_2O + NiCl_2$,[6] $Cd(NO_3)_2 \cdot 4.1\ H_2O + CoCl_2$,[6] and $Zn(NO_3)_2 \cdot 6.27\ H_2O + CoCl_2$.[7b] The linearity of these plots justifies the validity of Eq(4-3). Furthermore, on substituting the linear concentration dependence of T_o(decrease or increase) in Eq(4-3) it approximates[16] to

$$\ln A_y = A'_{oy} \mp B'_{oy} x \qquad (4\text{-}6)$$

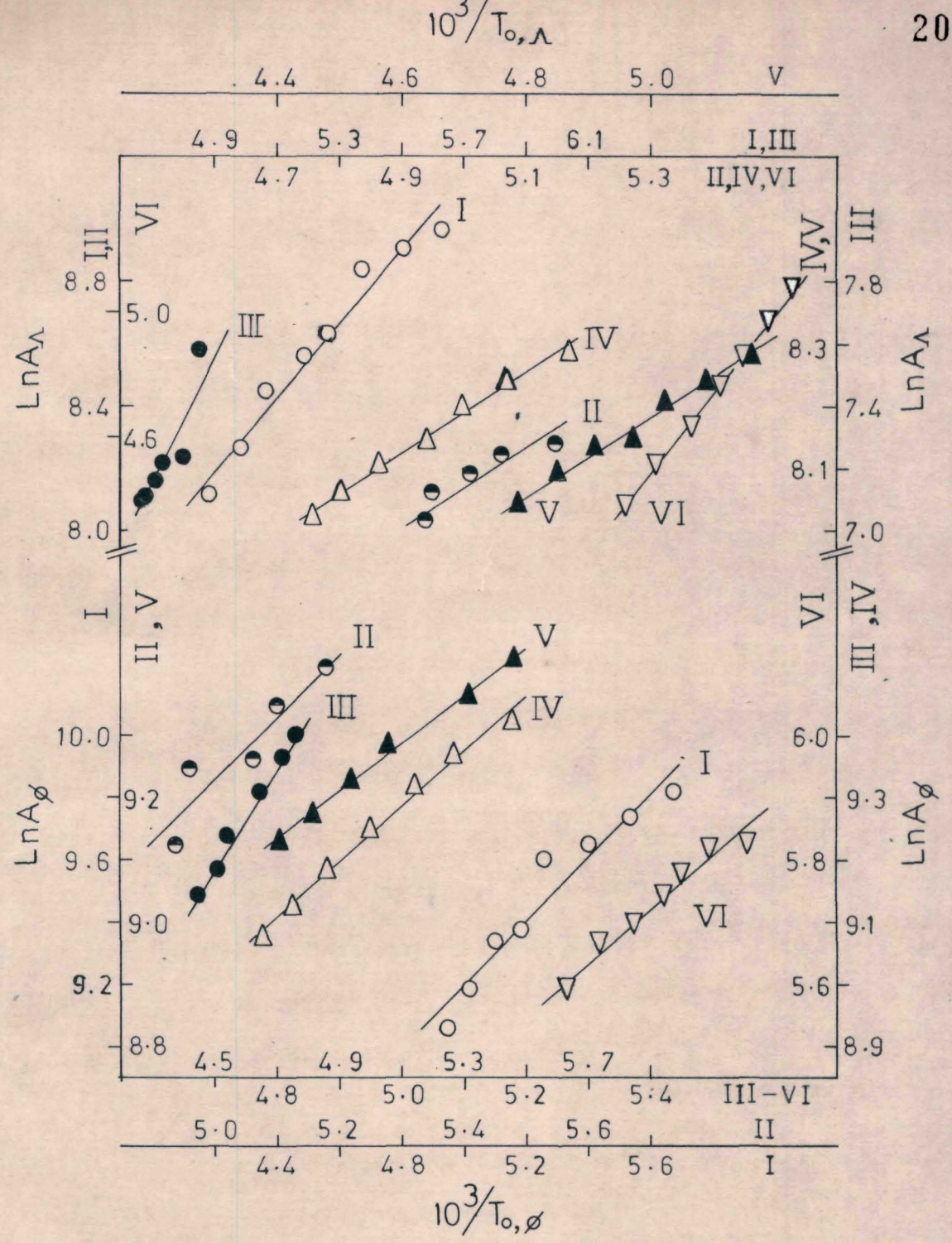

Fig 4-1: Plots of ln A_y vs. $1/T_{o,y}$ for binary melts. The system numbers I to VI correspond to the six systems given in Table 4-1 and are in the same order.

where $A'_{oy} = \ln A_{oy} + B_{oy}/T_o(o)$ and $B'_{oy} = B_{oy}Q/T_o(o)^2$.
It is interesting to find that Eq(4-6) explains the empirical behaviour of A_y with concentration in molten $Ca(NO_3)_2 \cdot 4.09 H_2O + Cd(NO_3)_2 \cdot 4.07 H_2O$ mixture which could not be explained[4] on the basis of the free volume model.[11]

To verify the applicability of Eq(4-5), the reported fluidity and equivalent conductance data at 313°K for the various molten mixtures cited above are least-squares fitted to Eq(4-5). The values of A_y^* and Q_y^* so obtained are listed in Table 4-1. Plots of ln Y (at 313°K) versus x are also drawn which are illustrated in Fig 4-2. It is apparent from Table 4-1 and from the linearity of the plots of ln Y versus x (Fig 4-2) that Eq(4-5) describes satisfactorily the concentration dependences of transport properties of binary molten mixtures containing hydrate melts. It is worthwhile to note that the isothermal Eq(4-5) has only two adjustable parameters unlike the cases with the expressions reported earlier[5b,17, 18] which contain either three or more than three adjustable parameters. The applicability of Eqs(4-3) and (4-5) also reinforces the view that the concentration dependence of transport properties of such binary melts is completely governed by the behaviour of the ideal glass transition temperature with concentration.

Table 4-1 Best fit Parameters for Eq(4-5) for the Fluidity and Equivalent Conductance of Glass-Forming Melts

Melts	A_y^*	Q_y^*	Std.dev in ln Y
$Zn(NO_3)_2 \cdot 6.33H_2O$-$Ca(NO_3)_2 \cdot 4.1H_2O$	1.9401	-1.8714	0.029
	(1.4351)	(-1.6966)	(0.046)
$Ca(NO_3)_2 \cdot 4.09H_2O$-$Cd(NO_3)_2 \cdot 4.07H_2O$	-0.0498	0.7681	0.017
	(-0.2163)	(0.6215)	(0.012)
$Ca(NO_3)_2 \cdot 3.91H_2O$-$CoCl_2$	-0.1054	-9.8721	0.020
	(-0.3662)	(-10.6646)	(0.106)
$Cd(NO_3)_2 \cdot 4.1H_2O$-$NiCl_2$	0.7641	-10.0624	0.020
	(0.4589)	(-9.6243)	(0.016)
$Cd(NO_3)_2 \cdot 4.1H_2O$-$CoCl_2$	0.7797	-9.0010	0.036
	(0.4891)	(-8.4575)	(0.042)
$Zn(NO_3)_2 \cdot 6.27H_2O$-$CoCl_2$	1.9078	-2.1327	0.038
	(1.3715)	(-3.0096)	(0.033)

Parameters for equivalent conductance are within the parentheses.

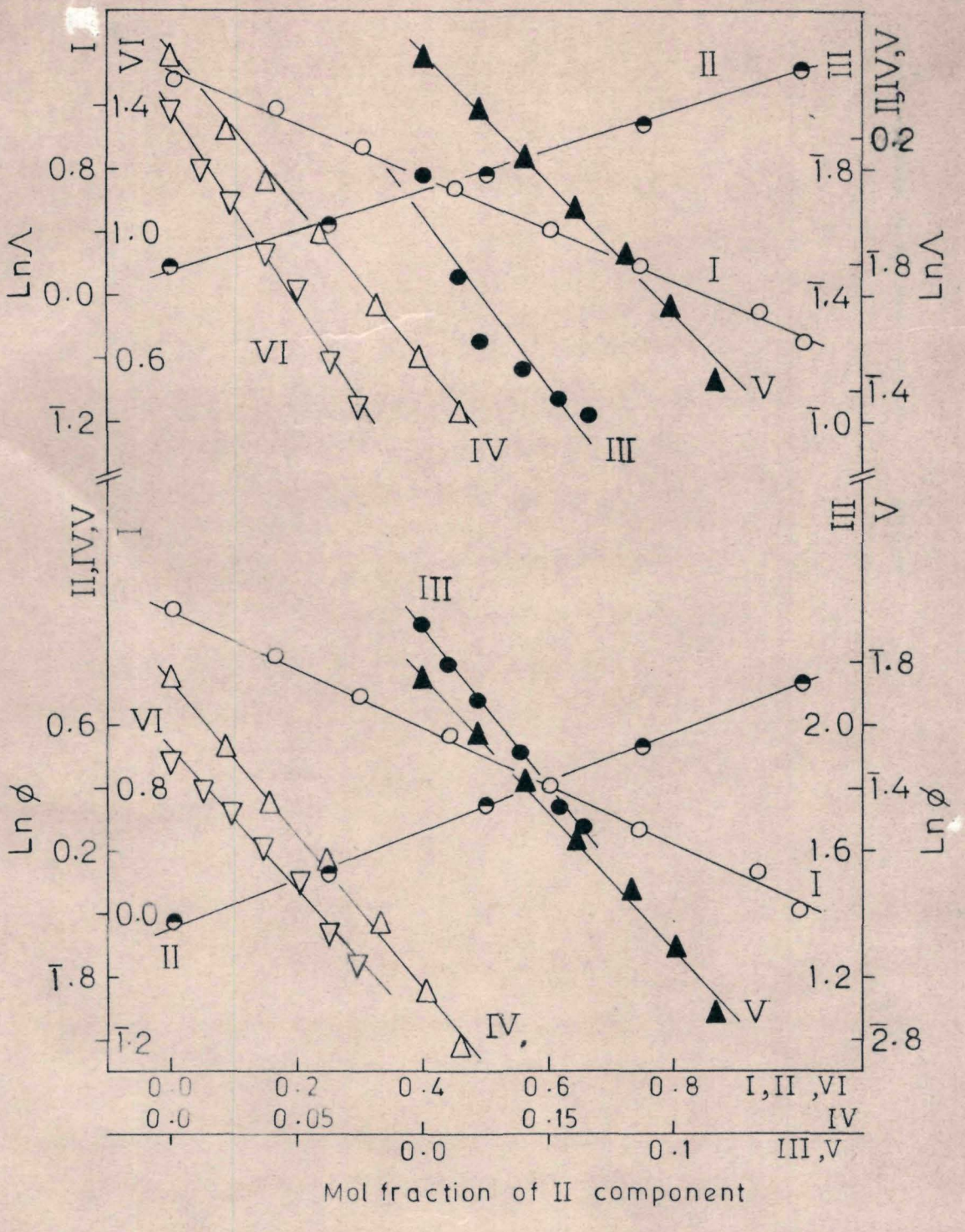

Fig 4-2: Plots of ln γ vs. mole fraction of the second component for binary melts. The system numbers I-VI correspond to the six systems given in Table 4-1 and are in the same order.

B. Calcium nitrate tetrahydrate-Potassium thiocyanate System

Surprisingly, when a similar attempt as above was made to apply Eq(4-3) to describe the concentration dependence of the reported[5a] A_y parameter for molten $Ca(NO_3)_2 \cdot 3.99\ H_2O$ - KSCN system, a trend contrary to what was anticipated from Eq(4-3) was observed. This inspired us to reinvestigate the behaviour of this molten system. An interesting feature of this system reported by Islam and Ismail[5a] is that it behaves ideally with respect to molar volume. We measured the densities of this binary system again as functions of temperature and composition with a view to seek for a plausible explanation for the failure of Eq(4-3) to account for the type of dependence observed for the A_y parameter of this melt on composition.

Experimental Section

Reagent grade (E.Merck) calcium nitrate tetrahydrate, m.p. 43.5°C, was used in the molten state. The exact number of moles of water per mole of calcium nitrate was determined by the EDTA titration method and was found to be 3.18. Potassium thiocyanate was recrystallized twice from double distilled water and dried over P_2O_5 in a vacuum desiccator.

Mixtures of $Ca(NO_3)_2 \cdot 3.18\ H_2O$ and KSCN were prepared by the method described by Islam and Ismail.[5a] Density measurements were made as described under Experimental Techniques.

Results and Discussion

The measured densities (ρ) of $Ca(NO_3)_2 \cdot 3.18\ H_2O$-KSCN melts are given in Table 4-2 in the form of a linear function,

$$\rho = a - bT \qquad (4\text{-}7)$$

where a and b are constants. From these density data the corresponding molar valumes (V) are calculated using the expression

$$V = (x_1M_1 + x_2M_2)/\rho \qquad (4\text{-}8)$$

where x refers to mole fraction and M to molecular weight. Suffixes 1 and 2 correspond to $Ca(NO_3)_2 \cdot 3.18\ H_2O$ and KSCN, respectively. The molar volumes obtained in this manner have also been least-squares fitted to a linear equation,

$$V = V_o' + b' T \qquad (4\text{-}9)$$

Table 4-2: Parameters for Eq(4-7) for the Density of $Ca(NO_3)_2 \cdot 3.18\ H_2O$ - KSCN Melts.

Mole fraction of KSCN (x_2)	a ($g.\ cm^{-3}$)	$bx10^4$ ($g.\ cm^{-3}K^{-1}$)	Std. dev. in ρ
0.0 (325 - 349K)	2.0201	9.2676	0.0002
0.0265 (306 - 323K)	1.9946	8.7379	0.0002
0.1599 (320 - 340K)	1.9960	8.8876	0.0003
0.3533 (318 - 339K)	1.9888	8.8419	0.0003
0.4499 (320 - 341K)	1.9873	8.8400	0.0003
0.5414 (327 - 348K)	1.9829	8.7780	0.0003

The temperature ranges of density measurement are given within the parentheses.

where V_o' and b' are constants at a particular concentration and their values are listed in Table 4-3. As the system under study has an inherent tendency to supercool the temperature dependence of molar volume may also be represented as

$$V = V_o + b' (T-T_o) \qquad (4-10)$$

where V_o is the molar volume at T_o and is known as the intrinsic volume. Comparison of Eqs(4-9) and (4-10) gives that

$$V_o' = V_o - b' T_o \qquad (4-11)$$

From Fig 4-3a it may be noticed that both V_o' and b' vary linearly with the mole fraction of KSCN, x_2. Presuming that V_o and T_o vary linearly with concentration,[5a] Eq(4-11) becomes on introducing the linear concentration dependences of all the terms

$$m_1 = m_2 - m_3 T_{o1} + b'_1 m_4 - m_3 m_4 x_2 \qquad (4-12)$$

where m_1, m_2, m_3, and m_4 are the respective slopes of linear variations of V_o', V_o, b', and T_o with x_2. T_{o1} and b'_1 are the values of T_o and b', respectively for pure $Ca(NO_3)_2 \cdot 3.18\ H_2O$ melt. From Eq(4-12) it may be understood that the

Table 4-3: Parameters for Eq(4-9) for the Molar Volume of $Ca(NO_3)_2 \cdot 3.18\ H_2O$-KSCN Melts.

x_2	V_o' ($cm^3 \cdot mol^{-1}$)	b' ($cm^3 \cdot mol^{-1} \cdot K^{-1}$)	Std. dev. in V	V_o ($cm^3 \cdot mol^{-1}$)
0.0	106.90	0.0675	0.027	120.81
0.0265	106.00	0.0662	0.018	119.64
0.1599	97.97	0.0618	0.022	110.70
0.3533	86.65	0.0544	0.017	97.86
0.4499	80.81	0.0509	0.020	91.30
0.5414	75.34	0.0476	0.015	85.15

Values of the intrinsic volume are calculated from the expression, $V_o = V_o' + 206\ b'$

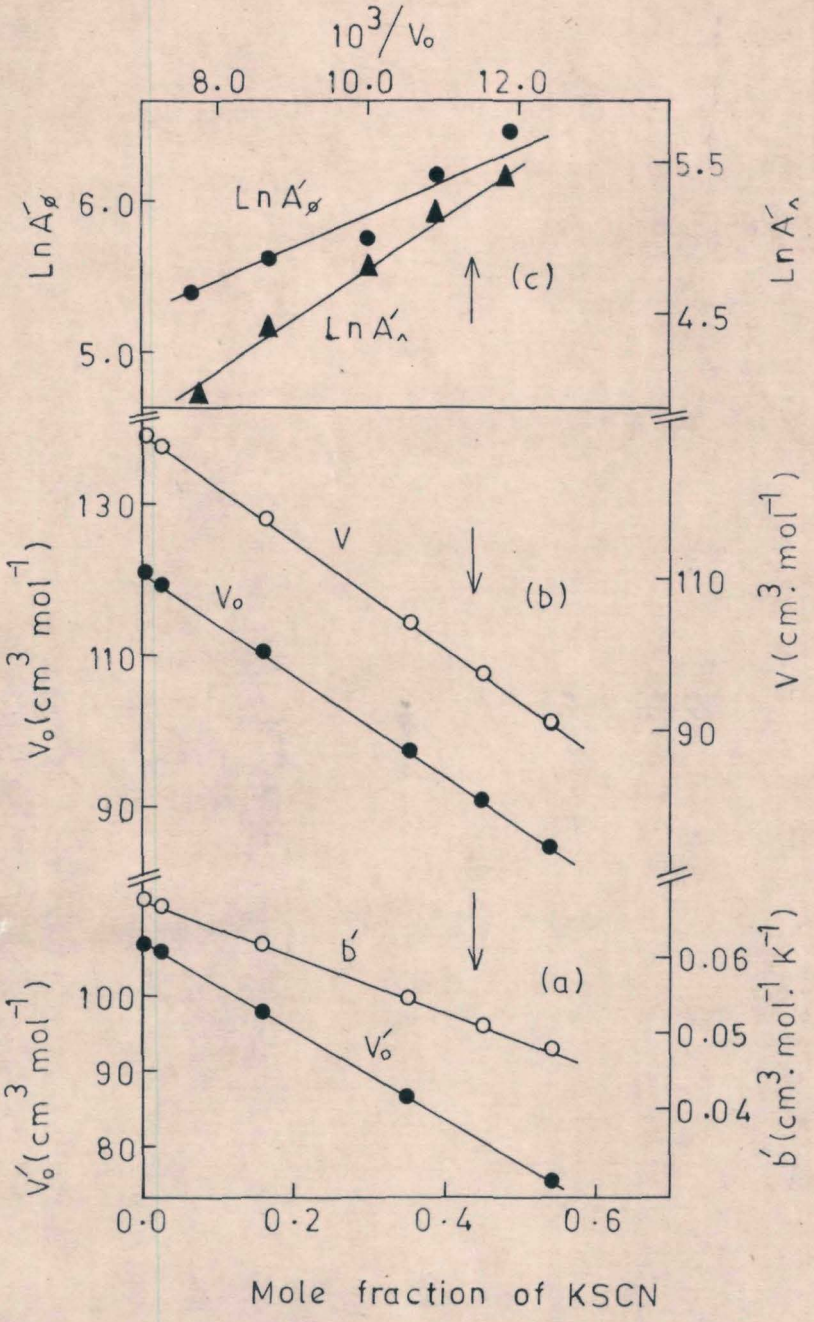

Fig 4-3: Plots of (a) V_o' and b' vs. mole fraction of K^+, (b) V_o and V vs. mole fraction of K^+, and (c) ln A_y' vs. $1/V_o$ for molten calcium nitrate tetrahydrate-potassium thiocyanate system.

observed constancy of m_1 appears to be explainable only when T_o becomes almost independent of solute concentration. In such a case $m_4 \approx o$ and Eq(4-12) reduces to

$$m_1 = m_2 - m_3 T_{o_1} \qquad (4\text{-}13)$$

With the knowledge of the reported[4,5a,17,19] values of T_o for calcium nitrate tetrahydrate, the T_o value for $Ca(NO_3)_2 \cdot 3.18\ H_2O$ may be considered as nearly equal to 206°K. Substituting this value for T_{o_1} and also the values of $m_1 = 59.1\ cm^3\ mol^{-1}$ and $m_3 = 0.037\ cm^3\ mol^{-1}K^{-1}$ obtained from Fig 4-3a in Eq(4-13), the value of m_2 may be determined which is found to be $66.7\ cm^3\ mol^{-1}$. This value of m_2 is also in agreement with the observed value of the slope of the plot of V_o versus concentration (Fig 4-3b), the value of V_o (Table 4-3) being obtained from Eq(4-11) after keeping T_o as 206°K. It is worthy to note that the present extrapolated value of $V_o = 54.0\ cm^3\ mol^{-1}$ for pure KSCN coincides with the value obtained in a similar manner using computed values of V_o from the transport property data of $Ca(NO_3)_2 \cdot 3.99\ H_2O$-KSCN melts.[5a] Such an agreement in the V_o value of pure KSCN estimated independently from the molar volume and transport property data appears to envisage that the assumption made regarding the concentration independent nature of T_o

is justifiable. Accordingly, the T_o value of pure KSCN may be considered as nearly the same as that of $Ca(NO_3)_2 \cdot 3.18\ H_2O$ which we have taken as 206°K. This value is closely comparable with the value 203°K for the T_o of KSCN computed from its electrical conductance data.[20] Moreover, it has been found that the concentration dependence of V_o predominantly governs the variation of V with x_2 for the $Ca(NO_3)_2 \cdot 3.18\ H_2O$-KSCN melts. As reported earlier[5a] V is found to be additive within ± 2% error. The molar volumes of pure KSCN at low temperatures required for testing the additivity of V are estimated from the same linear function for its density above the melting point.[21]

The above discussion envisages that in calcium nitrate tetrahydrate-potassium thiocyanate melt the concentration dependence of transport properties is most probably governed by the V_o parameter rather than by the T_o term. This view therefore accounts for the failure of Eq(4-3) in the binary melt under study. In order to confirm this view we considered an equivalent form of the VTF equation, viz.,

$$Y\ (\phi, \Lambda) = A'_y \exp\left[-B'_y/(V-V_{oy})\right] \qquad (4\text{-}14)$$

where A'_y and B'_y are constant parameters similar to the A_y

and B_y parameters of Eq(4-1). Using the reported[5a] values of A'_y and V_o for the $Ca(NO_3)_2 \cdot 3.99\ H_2O$-KSCN melt we plotted ln A'_ϕ and ln A'_Λ versus $1/V_o$ (Fig 4-3c) and it is interesting to note that these plots are fairly linear with positive slopes. This reinforces the above inference that in molten calcium nitrate tetrahydrate-potassium thiocyanate system the intrinisic volume controls the nature of the concentration dependence of transport properties. Consequently, for this kind of binary molten mixture (in which solute and solvent have nearly the same T_o value) Eq(4-3) may be modified to

$$A'_y = A'_{oy} \exp (B'_{oy}/V_o) \qquad (4\text{-}15)$$

where A'_{oy} and B'_{oy} are concentration independent parameters.

References:

1. G. Adam and J.H. Gibbs, J. Chem. Phys., 43, 139 (1965).
2. C.A. Angell, J. Electrochem. Soc., 112, 1224 (1965).
3. J. Braunstein, J. Chem. Educ., 44, 223 (1967).
4. C.T. Moynihan, C.R. Smalley, C.A. Angell, and E.J. Sare, J. Phys. Chem., 73, 2287 (1969).
5. (a) N. Islam and K. Ismail, J. Phys. Chem., 78, 2180 (1975); (b) ibid., 80, 1929 (1976); (c) Indian J. Chem., 15A, 857 (1977).
6. N. Islam, S. Kumar, and K.P. Singh, Can. J. Chem., 56, 1231 (1978).
7. (a) N. Islam, K.P. Singh, and S. Kumar, J. Chem. Soc. Faraday Trans. I, 75, 1312 (1979); (b) Bull. Chem. Soc. Japan, 52, 579 (1979).
8. N. Islam and A. Ali, Can. J. Chem., 57, 2028 (1979).
9. S.K. Jain, J. Phys. Chem., 82, 1272 (1978).
10. C.A. Angell, J. Phys. Chem., 68, 1917 (1964).
11. M.H. Cohen and D. Turnbull, J. Chem. Phys., 31, 1164 (1959).
12. C.A. Angell and J.C. Tucker, J. Phys. Chem., 78, 278 (1974).
13. R.J. Greet and D. Turnbull, J. Chem. Phys., 47, 2185 (1967).

14. W.T. Laughlin and D.R. Uhlmann, J. Phys. Chem., 76, 2317 (1972).

15. V.P. Privalko, J. Phys. Chem., 84, 3307 (1980).

16. Approximation made is $1/(T_o(o) \pm \theta x) \approx [1/T_o(o)] \; [1 \mp \theta x/T_o(o)]$

17. C.A. Angell, J. Phys. Chem., 70, 3988 (1966).

18. C.A. Angell, J. Chem. Phys., 46, 4673 (1967).

19. C.T. Moynihan, J. Phys. Chem., 70, 3399 (1966).

20. P. Dulieu and P. Claes, Bull. Chem. Soc. Chim. Belg., 82, 639 (1973).

21. D.H. Kerridge, 'Advances in Molten Salt Chemistry', Vol III, Ch. 5, J. Braunstein, G. Mamantov, and G.P. Smith, eds., Plenum Press, New York, 1975.

CHAPTER V

TEMPERATURE AND CONCENTRATION DEPENDENCE OF FLUIDITY AND CONDUCTIVITY OF TERNARY MELTS- MIXED ALKALI EFFECT IN $0.3\,[xKSCN-(1-x)NaSCN]$ $-0.7\,Ca(NO_3)_2 \cdot 4.06\,H_2O$

Introduction

In this chapter we have extended our study on transport properties to a ternary molten system containing two alkali ions in a hydrate melt. The purpose of this study is two-fold, (a) to investigate an interesting property, termed as mixed-alkali effect, exhibited by this kind of systems and (b) to examine the applicability of a three-parameter isothermal equation of the type derived in Chapters I and II in describing the transport properties of such ternary systems.

The mixed alkali effect (MAE)[1,2] refers to deviations (mostly minima or maxima are observed) from additivity in isotherms of various physical properties as function of composition, when one alkali metal cation is progressively replaced by another in a glass or melt. In general, it is found that there is no MAE for equilibrium properties like molar volume, elastic modulus, heat capacity, etc. In mixed alkali systems these properties show either linear variations with composition or small deviations from additivity which are not larger than those encountered in nonmixed alkali systems. On the other hand, a very pronounced MAE is observed for properties related to ionic transport. The MAE has been found to occur for shear viscosity and glass transition

temperature also. This effect has been observed in a variety of oxide glasses[1-6] as well as in other molten salts.[7,8]

It may be pointed out that studying the MAE has got two important implications. Firstly, in glasses a knowledge of the change in properties with chemical composition is important to the glass technologist because of its relevance to controlling of properties, selection and substitution of raw materials, and development of glass compositions with specific properties. Secondly, the MAE observed for the ionic conductivity is of immense theoretical importance. This is because of the fact that in glasses of constant alkali content, e.g., $xK_2O - (1-x)Na_2O-4SiO_2$[9] where all the current is carried by Na^+ and/or K^+ ions, the conductivity of mixed glasses can be reduced by a factor of 10^4 or 10^5 compared with that of single-alkali glasses measured at the same temperature. Such large departures from additivity clearly constitute a major breakdown of the principle of independent migration of ions, which works well for dilute aqueous electrolytes. This appears to imply that the theory of ionic conduction in mixed-alkali glasses is different from that in dilute aqueous electrolytes.

It has recently been suggested[10] that in order to have an improved understanding of the MAE it would be worthwhile to examine the behaviour of highly concentrated

solutions(hydrate melts) containing mixed alkali ions. To date only a few studies of this kind have been made. Moynihan[11] studied the electrical conductivity of x $NaNO_3$ -(0.2-x) KNO_3 - 0.8 $Ca(NO_3)_2$.4.09 H_2O melt and failed to observe the MAE in the temperature range from -5 to 70°C. Ingram et al.[10] measured the viscosities and conductivities of x K_2SiO_3-(1-x) Na_2SiO_3-7H_2O systems in the temperature range -70 to $\sim$ 20°C and observed deviations from additivity in both the properties. However, no minimum or maximum was found to occur in the viscosity or conductivity isotherm even at very low temperatures. On the other hand, Ingram et al.[10] observed a shallow minimum in the conductivity isotherm at isofluidity condition, that too in the low fluidity region, and they considered this as an evidence for the onset of the MAE. Easteal and Emson[12] noticed the MAE for glass transition temperature in 0.45 $[xLiNO_3-(1-x)KNO_3]$ -0.55 $Ca(NO_3)_2$.4.09H_2O melt and they made a suggestion that the MAE becomes significant when the total alkali ion concentration is high as revealed by the study on anhydrous mixed-alkali melts[13] also. Besides, Easteal[14] observed in 0.45 $[xLiNO_3-(1-x)KNO_3]$ -0.55 $Ca(NO_3)_2$.4.09H_2O and 0.45 $[xLiNO_3-(1-x)KNO_3]$ -0.55 $Ca(NO_3)_2$.6.545 H_2O melts deviations of viscosity and conductivity from additivity.

In the present work we have measured density, viscosity,

and conductivity of molten 0.3 [xKSCN-(1-x)NaSCN] -0.7 $Ca(NO_3)_2$ 4.06H_2O system as functions of temperature and x.

Experimental Section

Both KSCN and NaSCN (SD Reagent grade) were recrystallized twice from distilled water and dried over P_2O_5 in a vacuum desiccator. Calcium nitrate tetrahydrate (E. Merck Reagent grade) was used as solvent in the molten state without further purification. The actual H_2O/Ca^{2+} mole ratio in calcium nitrate tetrahydrate was determined to be 4.06 from the EDTA titration.

Although KSCN is soluble upto ~65 mole % in calcium nitrate tetrahydrate,[15] it was found that NaSCN dissolves only upto ~ 30 mole % at about 50°C. Therefore, the total alkali concentration was kept as 0.3 mole fraction. Keeping the concentration of calcium nitrate tetrahydrate constant at 0.7 mole fraction, six samples were made by varying the amounts of KSCN and NaSCN such that the total alkali concentration was maintained at 0.3 mole fraction. Samples were prepared by a method similar to that described by Islam and Ismail.[15]

Density, viscosity, and conductivity measurements of these molten systems were made as described under Experimental Techniques. For measurements upto 85°C water was used as bath

liquid and above this temperature refined vegetable oil was used in place of water.

Results and Discussion

Densities (ρ) of 0.3 [xKSCN-(1-x)NaSCN] -0.7 $Ca(NO_3)_2 \cdot 4.06\ H_2O$ melts were found to be linear functions of temperature and are presented in Table 5-1 in the form of least-squares fits to the equation

$$\rho(g.cm^{-3}) = a - bt\ (°C) \qquad (5\text{-}1)$$

where a and b are empirical constants.

The measured values for the fluidity (ϕ) and conductivity (κ) of the above systems are given in Table 5-2. In Figs 5-1 and 5-2 the temperature dependence of ϕ and κ is illustrated in the form of Arrhenius plots. From these plots it is apparent that both ϕ and κ show non-Arrhenius temperature dependence. Such a temperature dependence of transport properties is typical of highly concentrated aqueous solutions. The conductivity and fluidity data were therefore least-squares fitted to the VTF equation of the form

$$Y(\phi,\kappa) = A_y \exp\left[-B_y/(T-T_{oy})\right] \qquad (5\text{-}2)$$

Table 5-1: Least-Squares Fitted Values of the Parameters of the Density Eq(5-1) for 0.3 [xKSCN-(1-x) NaSCN] -0.7 $Ca(NO_3)_2 \cdot 4.06\ H_2O$ Melts.

x	a (g. cm^{-3})	b x 10^4 (g. cm^{-3}. $°C^{-1}$)	Std. dev. in ρ σ x 10^4
0.0	1.7278	8.2338	1.83
0.2	1.7572	9.4244	2.32
0.4	1.7578	9.8096	2.05
0.6	1.7334	8.4142	2.91
0.8	1.7486	8.7229	2.45
1.0	1.7569	9.0695	3.31

Table 5-2: Conductivity (κ) and Fluidity (ϕ) of 0.3 [xKSCN-(1-x) NaSCN] -0.7 $Ca(NO_3)_2$. 4.06 H_2O Melts as Functions of Temperature and Composition.

T(K)	$\kappa \times 10^2$ (mho cm^{-1}) and $\phi \times 10^2$ (cP^{-1})					
	x = 0.0	x = 0.2	x = 0.4	x = 0.6	x = 0.8	x = 1.0
288.0	-	-	0.199	0.191	0.189	0.185
293.0	-	-	0.296	0.285	0.285	0.279
			(0.219)	(0.276)	(0.253)	(0.270)
298.0	-	-	0.426	0.409	0.405	0.406
			(0.338)	(0.402)	(0.384)	(0.408)
303.0	0.547*	0.602	0.597	0.568	0.568	0.573
	(0.168)*	(0.454)	(0.509)	(0.583)	(0.558)	(0.592)
308.0	0.757*	0.788	0.793	0.763	0.758	0.763
		(0.649)	(0.696)	(0.819)	(0.780)	(0.821)
313.0	1.008*	1.028	1.007	0.962	0.994	0.998
		(0.894)	(0.964)	(1.107)	(1.068)	(1.115)
318.0	1.300*	1.306	1.287	1.254	1.252	1.250
		(1.211)	(1.289)	(1.475)	(1.422)	(1.479)
323.0	1.667	1.617	1.599	1.576	1.574	1.560
		(1.581)	(1.680)	(1.913)	(1.847)	(1.915)
328.0	2.028	1.973	1.944	1.898	1.909	1.890
		(2.068)	(2.149)	(2.419)	(2.347)	(2.418)
333.0	2.435	2.342	2.303	2.282	2.273	2.270
	(1.315)	(2.532)	(2.672)	(2.998)	(2.908)	(2.992)

Continued.

Table 5-2 (Continued)

T(K)	$\kappa \times 10^2$ (mho cm^{-1}) and $\phi \times 10^2$ (cP^{-1})					
	x = 0.0	x = 0.2	x = 0.4	x = 0.6	x = 0.8	x = 1.0
338.0	2.825	2.754	2.744	2.704	2.692	2.690
	(1.678)	(3.104)	(3.279)	(3.654)	(3.539)	(3.626)
343.0	3.282	3.211	3.169	3.144	3.144	3.150
	(2.119)	(3.761)	(3.964)	(4.392)	(4.096)	(4.395)
348.0	3.755	3.714	3.674	3.630	3.641	3.640
	(2.572)	(4.469)	(4.739)	(5.214)	(5.077)	(5.223)
353.0	4.309	4.248	4.203	4.159	4.159	4.220
	(3.133)	(5.251)	(5.588)	(6.110)	(5.956)	(6.123)
358.0	4.929	4.772	4.772	4.688	4.697	4.790
		(6.133)	(6.480)	(7.121)	(6.963)	(7.112)
363.0	5.545	-	-	-	-	-
	4.363)					
368.0	6.143	-	-	-	-	-
373.0	6.673	-	-	-	-	-
	(5.887)					
378.0	7.259	-	-	-	-	-
383.0	7.985	-	-	-	-	-
388.0	8.556	-	-	-	-	-
393.0	9.214	-	-	-	-	-

Fluidity data are within the parentheses.

* Calculated from Eq(5-2) using best-fit parameters.

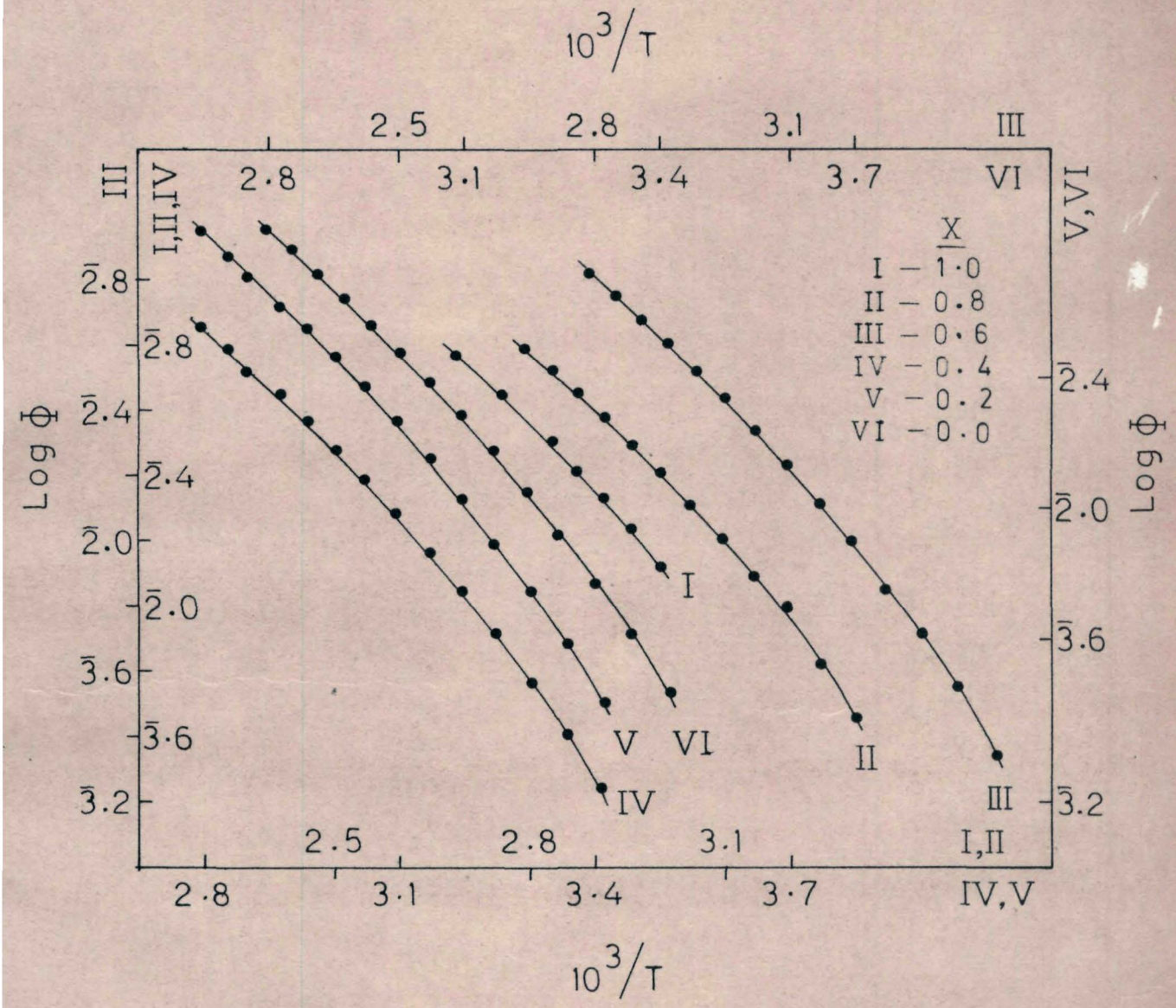

Fig 5-1: Arrhenius plots for fluidity of 0.3 [XKSCN-(1-X)NaSCN] -0.7$Ca(NO_3)_2$.4.06 H_2O melts.

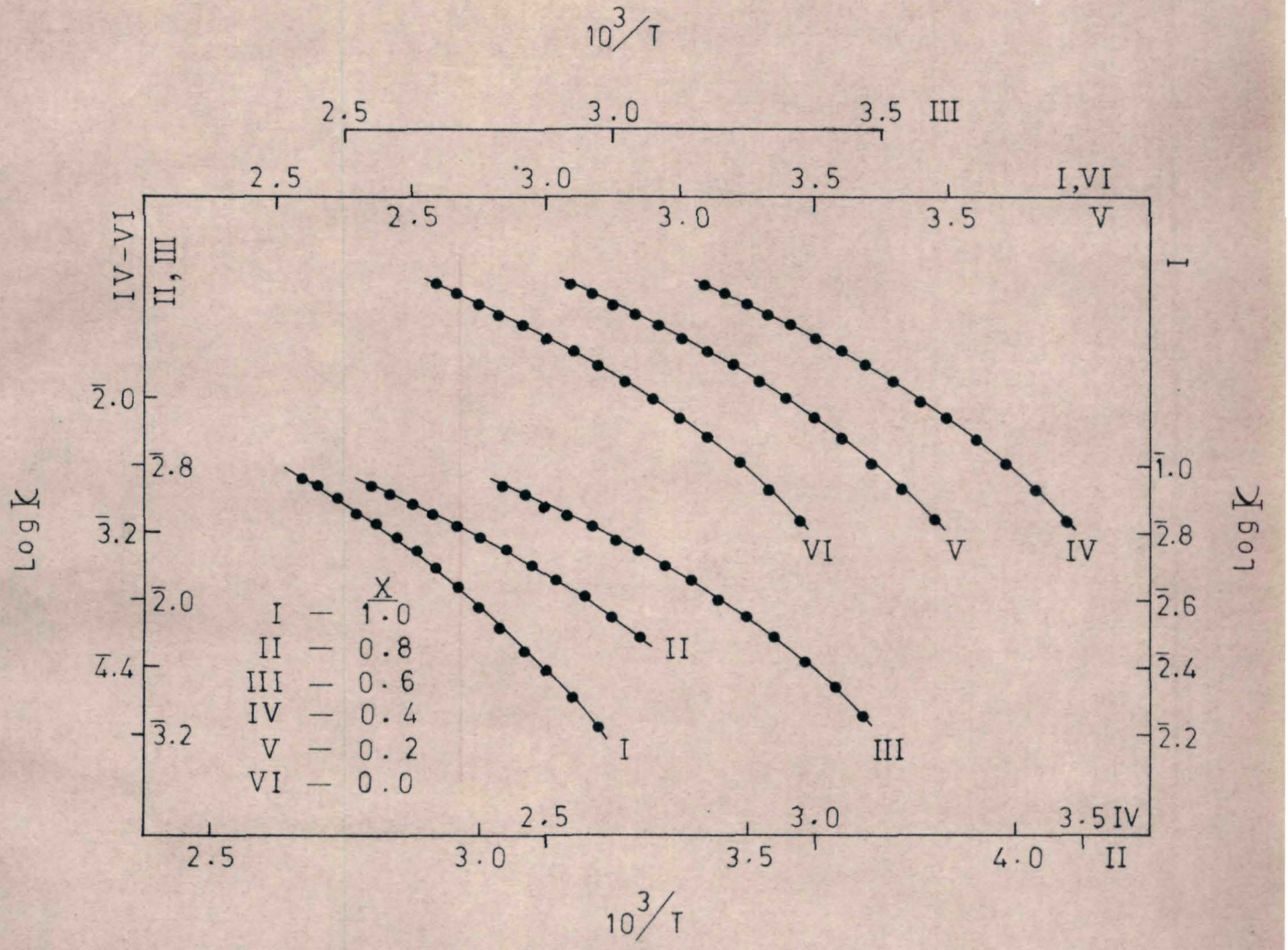

Fig 5-2: Arrhenius plots for conductivity of 0.3 [XKSCN- (1-X) NaSCN]-0.7$Ca(NO_3)_2$.4.06 H_2O melts.

where Y refers to either fluidity or conductivity. A_y, B_y, and T_{oy} have the same meanings as defined in earlier chapters. In Eq(5-2) we have neglected the preexponential temperature term owing to its insignificant contribution to the temperature dependence of Y. The best-fit values of the parameters A_y, B_y, and T_{oy} are presented in Table 5-3. From Table 5-3 it may be seen that there is no regular trend in the variation of T_o with composition. A relatively high T_o value has been obtained for 0.3 NaSCN-0.7 $Ca(NO_3)_2$. 4.06 H_2O system. Similarly a high value for T_o of Na_2SiO_3-$7H_2O$ system was observed by Ingram et al.[10] while investigating the MAE in supercooled xK_2SiO_3-$(1-x)Na_2SiO_3$-$7H_2O$ mixtures. Irregular trend in the variation of T_o with composition was also observed in binary melts containing hydrated salts.[15,16] In such cases an alternative method suggested by Moynihan et al.[16] is normally adopted for the data analysis. According to this method the data analysis is done by keeping in view the empirical facts that the B_y term is almost composition independent and T_{ok} is nearly equal to $T_{o\phi}$. The sets of values obtained for A_y, B_y, and T_{oy} using the above alternative method for data analysis are listed in Table 5-4. Approximately constant values for B_ϕ and B_k were chosen in the light of the B_y values reported earlier for $Ca(NO_3)_2$.3.99 H_2O - KSCN melts.[15] It may be noted from Tables5-3 and 5-4 that

Table 5-3: Values of the Best-fit Parameters of Eq(5-2) for the Conductivity (mho cm^{-1}) and Fluidity (cP^{-1}) of $0.3\,[x\,KSCN-(1-x)\,NaSCN]-0.7\,Ca(NO_3)_2\,4.06\,H_2O$ Melts.

x	A_y	B_y	T_{oy}	Std. dev. in κ or ϕ, $\sigma \times 10^4$
0.0	0.9544	383.93	228.63	4.41
	(4.0022)	(646.02)	(219.92)	(1.21)
0.2	1.5397	509.83	211.16	0.92
	(4.0333)	(600.20)	(214.67)	(0.62)
0.4	1.7988	547.54	207.23	0.96
	(5.2762)	(655.34)	(208.98)	(0.81)
0.6	1.4948	501.61	213.06	0.95
	(5.7198)	(665.67)	(206.28)	(0.73)
0.8	1.5539	510.92	211.95	0.62
	(8.3811)	(769.61)	(197.44)	(4.50)
1.0	2.3100	601.78	202.79	1.15
	(6.1088)	(683.02)	(204.61)	(0.79)

Parameters for fluidity are within the parentheses.

Table 5-4: Least-Squares Fitted Values of the Parameters of Eq(5-2) for the Conductivity (mho cm^{-1}) and Fluidity (cP^{-1}) of 0.3 [xKSCN-(1-x) NaSCN] -0.7 $Ca(NO_3)_2$ 4.06 H_2O Melts Selected such that B_κ and B_ϕ Values are almost constant and $T_{o\kappa} \approx T_{o\phi}$

x	A_y	B_y	T_{oy}	Std. dev. in κ or ϕ $\sigma \times 10^4$
0.0	1.4616	500.35	211.00	6.62
	(5.4412)	(728.15)	(212.00)	(1.72)
0.2	1.6944	533.04	208.60	1.06
	(5.0477)	(651.98)	(210.00)	(1.62)
0.4	1.7988	547.54	207.23	0.96
	(5.4442)	(664.55)	(208.00)	(0.91)
0.6	2.1352	581.84	205.00	2.68
	(5.7198)	(665.67)	(206.28)	(0.73)
0.8	2.2609	593.67	204.00	3.19
	(5.9787)	(680.60)	(205.40)	(4.72)
1.0	2.3100	601.78	202.79	1.15
	(6.1088)	(683.02)	(204.61)	(0.79)

Parameters for fluidity are within the parentheses.

for some of the compositions the modified values of A_y, B_y, and T_{oy} are the same as their best-fit values. The new T_{oy} values (Table 5-4) increase linearly with the increase in Na^+ ion fraction (Fig 5-3a) as was the case in x K_2SiO_3-(1-x) Na_2SiO_3-$7H_2O$[10] and 0.2 [x $NaNO_3$-(1-x) KNO_3] -0.8 $Ca(NO_3)_2$.4.09 H_2O[11] systems also.

In order to examine the presence of the MAE in the present system under investigation we plotted ln ϕ versus concentration, $x = K^+/(Na^+ + K^+)$, at different temperatures (Fig 5-3b). Deviation of ϕ from additivity is observed even at 80°C (Fig 5-3b) which therefore indicates the presence of the MAE for fluidity in 0.3 [x KSCN-(1-x)NaSCN] -0.7 $Ca(NO_3)_2$.4.06 H_2O system. Similar deviations of ϕ from additivity were reported in other ternary systems[10,14] also. On the other hand, electrical conductivity appears to be additive at higher temperatures (at 50°C and above) as evident from Fig 5-4a. Electrical conductivity becoming additive at a relatively lower temperature was noticed in the x K_2SiO_3-(1-x)Na_2SiO_3-$7H_2O$ system[10] also. From Fig 5-4a it may be seen that the MAE for electrical conductivity starts existing in the form of a maximum in the κ isotherm at temperatures below 50°C. This is contrary to what was observed in 0.2 [x $NaNO_3$-(1-x)KNO_3] -0.8 $Ca(NO_3)_2$.4.09 H_2O[11] and x K_2SiO_3-(1-x)Na_2SiO_3-$7H_2O$[10] melts wherein such a MAE was not detected even upto a very low temperature.

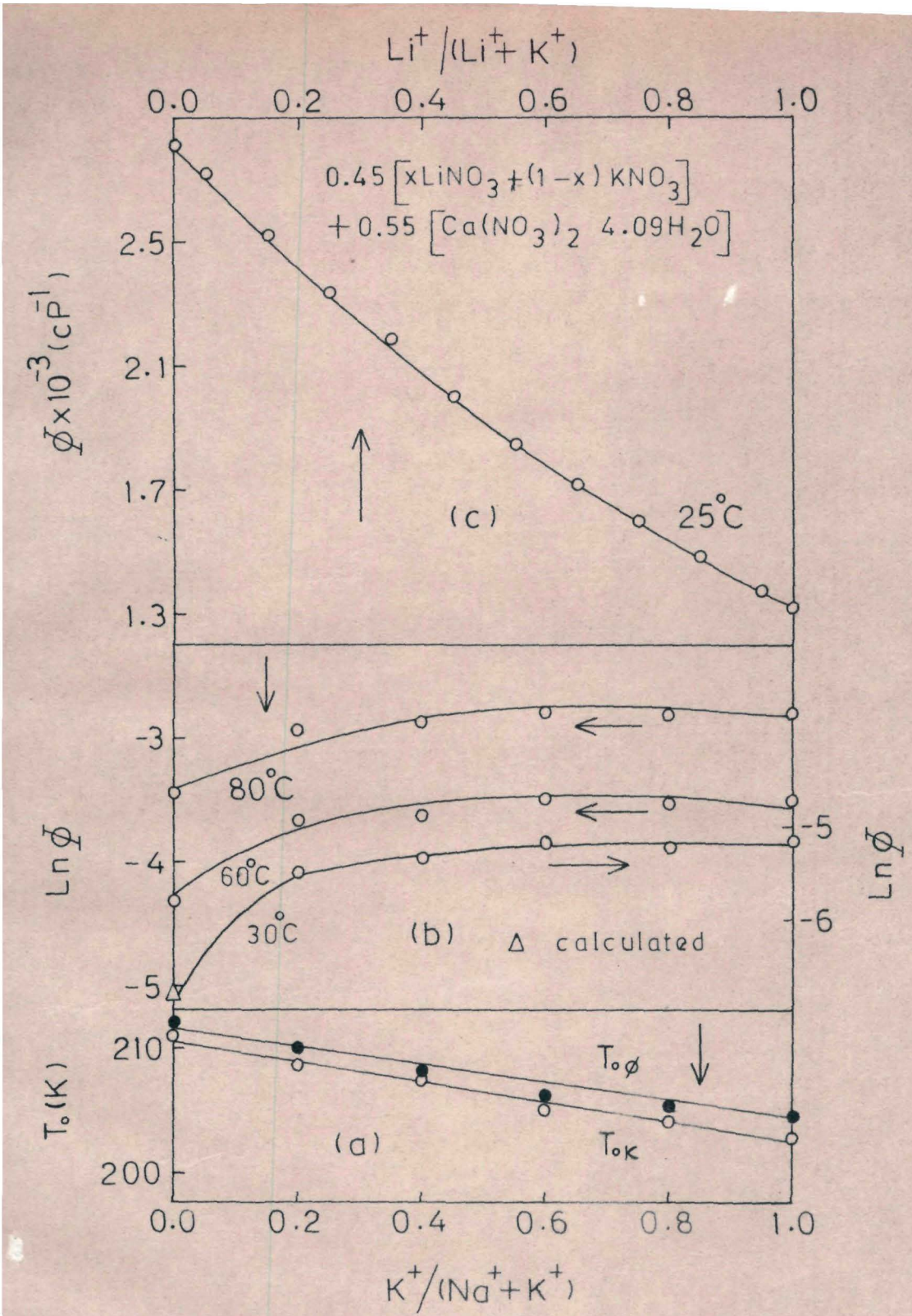

Fig 5-3: Plots of (a) T_o and (b) Lnϕ vs. X for $0.3\left[XKSCN\text{-}(1-X)NaSCN\right] - 0.7Ca(NO_3)_2.4.06H_2O$ melts and (c) of ϕ vs. X for $0.45\left[XLiNO_3\text{-}(1-X)KNO_3\right] - 0.55Ca(NO_3)_2.4.09\ H_2O$ melts (ref. 14). In Figs 5-3b and 5-3c, open circles and solid curves represent observed and calculated values, respectively.

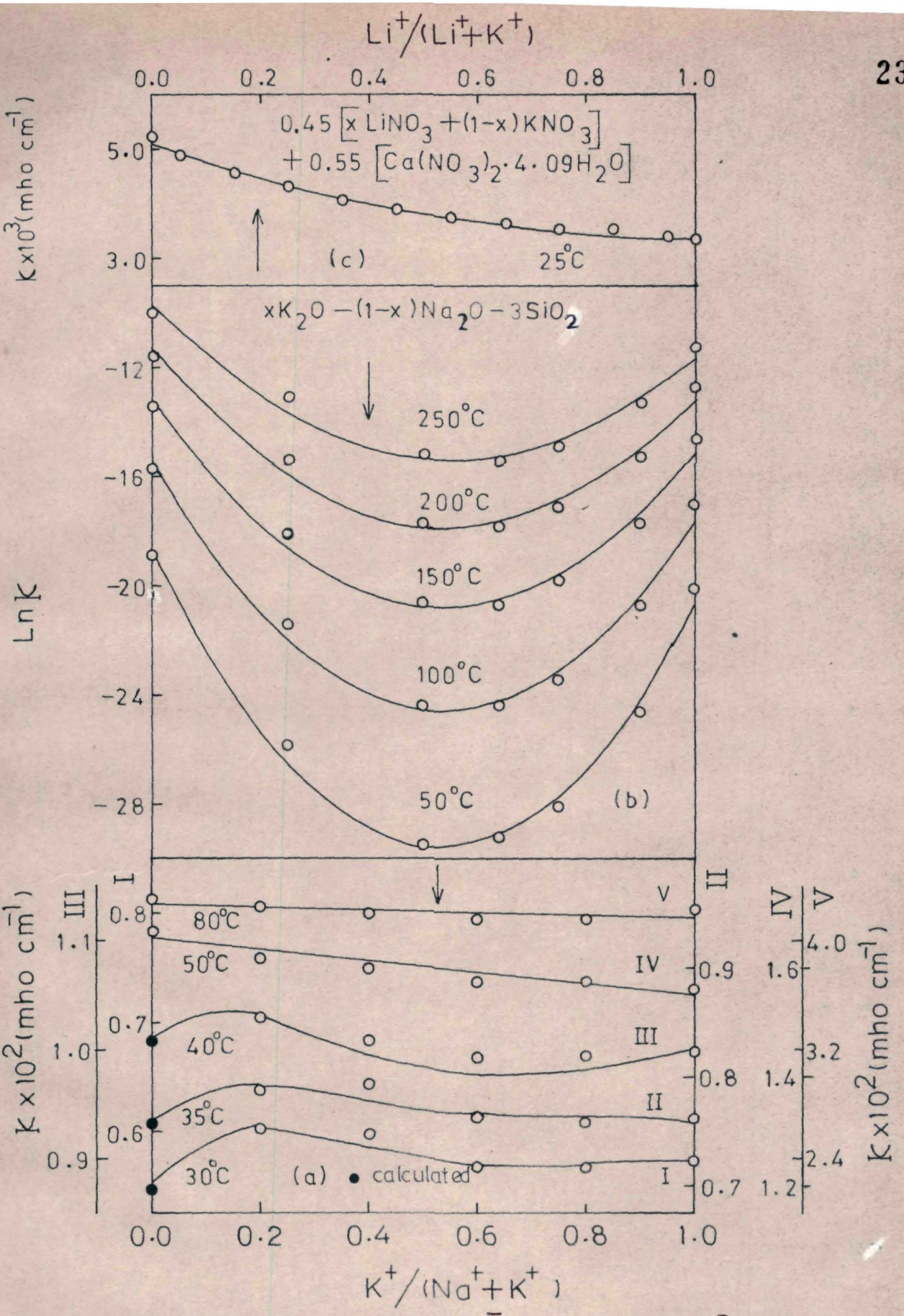

Fig 5-4: Plots of (a) K vs. X for $0.3[XKSCN-(1-X)NaSCN]-0.7Ca(NO_3)_2.4.06H_2O$ melts, (b) of Ln K vs. X for $XK_2O-(1-X)Na_2O-3SiO_2$ systems (ref. 11), and (c) of K vs. X for $0.45[XLiNO_3-(1-X)KNO_3]-0.55\ Ca(NO_3)_2\cdot 4.09H_2O$ melt (ref. 14). Open circles and solid curves represent observed and calculated values, respectively.

It, therefore, appears that the anion framework of the mixed-alkali system also plays a significant role in determining the MAE.

A common feature observed in all the ternary molten systems studied which contain water molecules is that initially the conductivity of the system at a particular temperature increases by the replacement of Na^+ by K^+ or, in general, by the replacement of a smaller alkali ion by another alkali ion of larger size. Although similar trend was observed in many of the anhydrous mixed-alkali systems,[3] there are some anhydrous systems[9,17] which also show an initial decrease in κ by the addition of an alkali ion of larger size.

We made an attempt to least-squares fit the ϕ and κ data for the system under study to an isothermal equation of the form

$$Y(\phi,\kappa) = a_{oy} \exp (b_{oy}x + c_{oy}x^2) \qquad (5\text{-}3)$$

where a_{oy}, b_{oy}, and c_{oy} are empirical constants. This equation was derived earlier for electrolytic solutions (Chapters I and II) as well as for binary hydrate melts

(Chapter IV) from the VTF equation by inserting the concentration dependences of the three VTF parameters, viz., A_y, B_y, and T_{oy}. Derivation of Eq(5-3) from the VTF equation was possible due to the empirically observed linear variation of T_{oy} with x (or molality, m). In the present case also T_o varies linearly with x (Fig 5-3a) and presuming that A_y and B_y are nearly concentration independent Eq(5-3) may still be derived from Eq(5-2). However, it may be pointed out that there are evidences for non-linear variation of glass transition temperature with composition.[12,14,18] In such cases Eq(5-3) may at the moment be considered simply as an expression of empirical origin.

The least-squares fitted values of the parameters a_{oy}, b_{oy}, and c_{oy} for fluidity and conductivity of molten $0.3\,[x\ KSCN-(1-x)NaSCN]\ -0.7\ Ca(NO_3)_2.4.06\ H_2O$ system are given in Table 5-5. A reasonably good fit has been obtained as apparent from Figs 5-3b and 5-4a also.

In order to establish further the success of Eq(5-3) in presenting the electrical conductivity data, we also made an attempt to least-squares fit the reported κ data for $x\ K_2O-(1-x)Na_2O_3-3\ SiO_2$[11,17] mixtures, an exemplary system which exhibits pronounced MAE. It is interesting to note from Table 5-5 as well as from Fig 5-4b that Eq(5-3)

Table 5-5: Least-Squares Fitted Values of the Parameters of Eq(5-3) for Conductivity (mho cm^{-1}) and Fluidity (cP^{-1}) of Different Mixed-Alkali Systems.

System	T(K)	a_{oy}	b_{oy}	c_{oy}	Std. dev. in ln Y
0.3 [xKSCN-(1-x)	303.0	-5.0608	-0.2547	0.1504	0.011
NaSCN] -0.7 $Ca(NO_3)_2$·		(-5.1444)	(0.1028)	(-0.5178)	(0.031)
4.06 H_2O	308.0	-4.8136	-0.1245	0.0580	0.010
	313.0	-4.5222	-0.3095	0.2278	0.012
	333.0	(-3.5724)	(0.8864)	(-1.5494)	(0.103)
	353.0	(-2.8443)	(0.7023)	(-1.2477)	(0.079)
x K_2O-(1-x)Na_2O	323.0	-18.5341	-42.0013	39.7617	0.482
-3 SiO_2	373.0	-15.4593	-34.3287	32.1873	0.435
	423.0	-13.1845	-28.2858	26.3478	0.392
	473.0	-11.3487	-24.0394	22.2172	0.346
	523.0	-9.7431	-20.4513	18.5366	0.337
0.45 [xLiNO_3-(1-x)	298.15	-5.2775	-0.7457	0.3412	0.013
KNO_3] -0.55		(-0.9644)	(0.7633)	(-0.0071)	(0.002)
$Ca(NO_3)_2$·4.09H_2O*					

Parameters for fluidity are within the parentheses.

*In this system fluidity is expressed in $(Pa\ s)^{-1}$.

satisfactorily fits the conductivity data for the above system in spite of the fact that its conductivity passes through a deep minimum. Eq(5-3) has been found to fit the reported fluidity and electrical conductivity data for $0.45\left[xLiNO_3-(1-x)KNO_3\right]-0.55\ Ca(NO_3)_2.4.09\ H_2O$[14] system also (Table 5-5 and Figs 5-3c and 5-4c). In the absence of a satisfactory theoretical approach to account for the MAE, the success shown by the empirical isothermal Eq(5-3) in representing the data on transport properties of mixed-alkali systems is worth registering. Presumably Eq(5-3) may be given a theoretical footing on the basis of Adam-Gibbs model.[19]

Although MAE is observed in the present system under study at constant temperatures, Moynihan's time-scale criterion[11] for detecting the MAE seems to be more rational. Moynihan[11] suggested that the MAE occurs in liquids or melts only when solid-like conduction mechanism is operating and that the mobile cations can hop from one recognizable site to another before the anion framework has time to rearrange. According to this criterion the structure of the medium must be fixed for examining the presence of the MAE or, more precisely, the time scale for rearrangement of the local

structure be long compared to that required for the local diffusion of alkali cations (monovalent cations in general) from site to site. Based on this concept Ingram et al.[10] estimated that the MAE might become detectable when $\kappa/\phi > 5$, κ in mho.cm^{-1} and ϕ in P^{-1}. Therefore, for detecting the MAE an isofluidity condition is more appropriate than an isothermal condition. Accordingly, we plotted κ versus x at constant fluidity values (Fig 5-5). Conductivity values of the system under interest at constant fluidity values, both within and outside the experimental fluidity range, required for the plotting were calculated from Eq(5-2) using the best-fit values of the A_y, B_y, and T_{oy} parameters given in Table 5-3. From Fig 5-5 it may be seen that the MAE exists even when the κ/ϕ ratio has a very low value much less than the value 5 suggested by Ingram et al.[10] The present study therefore appears to reveal that it is not possible to have a universal time-scale for detecting the MAE and the time-scale may vary from system to system.

It may further be noted from Fig 5-5 that at the isofluidity condition the conductivity of the system decreases initially by replacing Na^+ by K^+ ion which is contrary to the observation made at isothermal condition. Similar behaviour at isofluidity condition was also noticed in

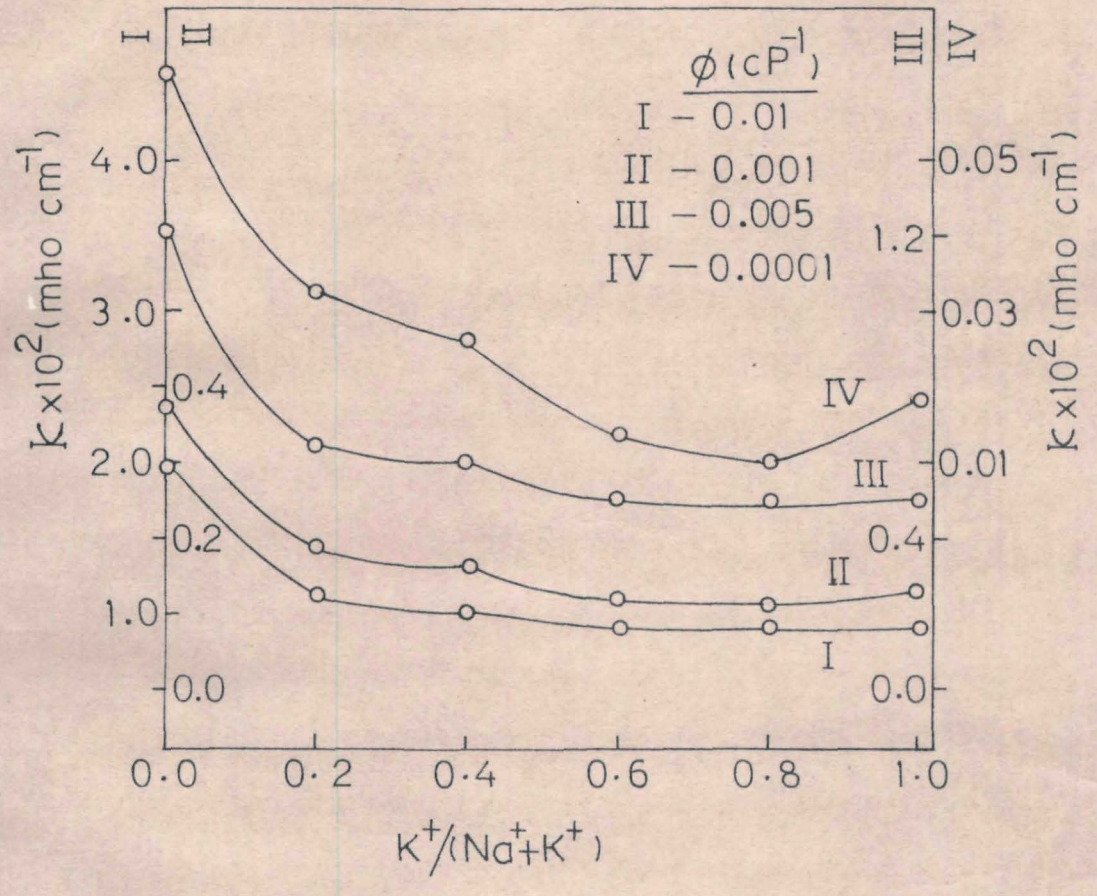

Fig 5-5: Plots of K vs. X at isofluidity conditions for $0.3\left[XKSCN-(1-X)NaSCN\right] - 0.7Ca(NO_3)_2 \cdot 4.06\ H_2O$ Melts.

x K_2SiO_3-(1-x)Na_2SiO_3-7 H_2O system.[10] Ingram et al.[10] gave a mechanistic interpretation to such a conductivity behaviour on the assumption that the paired cations form the mobile species in x K_2SiO_3-(1-x)Na_2SiO_3-7H_2O system. A similar structural interpretation may be advanced to the conductivity behaviour of the present system of interest. Under the isofluidity condition the anion matrix of the single-alkali system containing Na^+ ion may be presumed to provide some preferential sites to the $(Na_2)^{2+}$ pairs to jump. As KSCN is added, the size of the anion matrix increases causing an increase in the number of preferential sites which, in turn, might result into an increase in the conductivity of the system. This, however, does not happen and, on the other hand, the added K^+ ions interact with the Na^+ ion forming a sort of $(NaK)^{2+}$ unlike pairs which are likely to be less mobile than $(Na_2)^{2+}$ owing to their larger size. Consequently, the concentration of mobile species, $(Na_2)^{2+}$, decreases by the addition of KSCN which may perhaps be responsible for the initial decrease in conductivity. Beyond $\sim$ 0.8 K^+ ion fraction the conductivity of the system again increases as evident from Fig 5-5. In this region all the Na^+ ions appear to be paired with the K^+ ions, but the excess of K^+ ions may pair among themselves as $(K_2)^{2+}$ and form the mobile species. The fact that the

minimum in the conductivity does not occur at 0.5x appears to imply that in the mixed-alkali melt some amount of like pairs, $(Na_2)^{2+}$ or $(K_2)^{2+}$ or both, and unlike pairs, $(NaK)^{2+}$, are present at all concentrations. In the light of the above probable interpretation it may be visualized that the conductance process in mixed-alkali systems is governed by three factors, viz., concentration of the preferential sites, concentration of the mobile species, and the mobility. At isofluidity condition the last factor, i.e., the mobility of the mobile species, is however constant and the first two factors may be responsible for determining the conductivity of the system. In $0.3\left[x\ KSCN\text{-}(1\text{-}x)NaSCN\right]\text{-}0.7\ Ca(NO_3)_2 \cdot 4.06\ H_2O$ system the concentration of the mobile species appears to dominate over the first factor (concentration of the preferential sites). This may likely be due to the possibility that the number of preferential sites supplied by the anion matrix is quite large compared to the number of mobile species (which may be true even in the single-alkali system) and as a result the increase in the concentration of these sites by the addition of KSCN may not be affecting the conductivity.

References:

1. J.O. Isard, J. Non-Cryst. Solids, 1,235 (1969).
2. D.E. Day, J. Non-Cryst. Solids, 21, 343 (1976).
3. R.M. Hakim and D.R. Uhlmann, Phys. Chem. Glasses, 8, 174 (1967).
4. J.P. Poole, J. Amer. Ceram. Soc., 32, 230 (1949).
5. R.F. Bartholomew, J. Non-Cryst. Solids, 12, 321 (1973).
6. H.M. Van Ass and J.M. Stevels, J. Non-Cryst. Solids, 14, 131 (1974); 15, 215 (1974); 16, 46 (1974).
7. E.R. Van Artsdalem and I.S. Yoffe, J. Phys. Chem., 59, 118 (1955).
8. O.J. Kleppa and L.S. Hersh, J. Chem. Phys., 34, 351 (1961).
9. A.K. Varshneya, J. Amer. Ceram. Soc., 57, 37 (1974).
10. M.D. Ingram, K. King, D. Kranbuehl, and M. Adel-Hadadi, J. Phys. Chem., 85, 289 (1981).
11. C.T. Moynihan, J. Electrochem. Soc., 126, 2144 (1979).
12. A.J. Easteal and M.C. Emson, J. Phys. Chem., 84, 3330 (1980).
13. K.A. Konstanyan, 'The Structure of Glass', Vol II, Consultants Bureau, New York, 1960.
14. A.J. Easteal, Aust. J. Chem., 34, 1853 (1981).
15. N. Islam and K. Ismail, J. Phys. Chem., 79, 2180 (1975).

16. C.T. Moynihan, C.R. Smalley, C.A. Angell, and E.J. Sare, J. Phys. Chem., 73, 2287 (1969).

17. L.P. Boesch, Ph.D. Thesis, Catholic University of America, 1975.

18. A.J. Easteal and I.M. Hodge, J. Phys. Chem., 74, 730 (1970).

19. G. Adam and J.H. Gibbs, J. Chem. Phys., 43, 139 (1965).

APPENDIX I

Derivation of Eq(1-6)

According to Eq(1-5),

$$\eta = AT^{1/2} \exp\left\{ B/\left[T\Delta C_2 \ln (T/T_o)+T\Delta C_1(T-T_o)\right]\right\} \qquad (I-1)$$

The significances of the terms are already defined in Chapter I. At low temperatures,

$$\ln (T/T_o) \approx (T-T_o)/T_o \qquad (I-2)$$

Substituting this in Eq(I-1), we obtain

$$\eta = AT^{1/2} \exp\left\{BT_o/T(T-T_o)\Delta C_2\left[1+\Delta C_1 T_o/\Delta C_2\right]\right\} \qquad (I-3)$$

Since $\Delta C_1 T_o$ is empirically found to be very much less than ΔC_2, we may write

$$1/(1+\Delta C_1 T_o/\Delta C_2) \approx 1-\Delta C_1 T_o/\Delta C_2 \qquad (I-4)$$

In the light of this approximation Eq(I-3) now becomes

$$\eta = AT^{1/2} \exp\left[B'/T(T-T_o)\right] \qquad \text{Eq(1-6)}$$

where $B' = (BT_o/\Delta C_2)\ (1-\Delta C_1 T_o/\Delta C_2)$

APPENDIX II

Derivation of Eq(1-12)

According to Eq(1-11),

$$\eta = A^* \exp\left\{\left[-B^*/(T_o(o)+\Omega m)\right] + \left[B_1+\Omega_1(T_o(o)+\Omega m)\right]/\left[T-T_o(o)-\Omega m\right]\right\} \tag{II-1}$$

$$= A^* \exp\left\{-\left[B^*/T_o(o)\right]\left[1/(1+\Omega'm)\right] + \left[B_1/(T-T_o(o))\right]\right.$$
$$\left[1/(1-\Omega''m)\right] + \left[\Omega_1 T_o(o)/(T-T_o(o))\right]\left[1/(1-\Omega''m)\right] + \left[\Omega_1 \Omega m/(T-T_o(o))\right]$$
$$\left.\left[1/(1-\Omega''m)\right]\right\} \tag{II-2}$$

where $\Omega' = \Omega/T_o(o)$ and $\Omega'' = \Omega/(T-T_o(o))$.

Since the values of Ω' and Ω'' are normally in the range from ~ 0.04 to ~ 0.05 (or < 0.04), in electrolytes upto their saturation points $\Omega'm$ and $\Omega''m$ may be considered as quantities having values < 1. It may therefore be approximated that

$$1/(1+\Omega'm) \approx 1-\Omega m$$

and $$1/(1-\Omega''m) \approx 1+\Omega m$$

Applying these approximations in Eq(II-2) and then simplifying, we obtain

$$\eta = a_{o\eta} \exp\left(b_{o\eta} m + c_{o\eta} m^2\right) \qquad \text{Eq(1-12)}$$

where $a_{o\eta} = A^* \exp\{-[B^*/T_o(o)] + [B_1/(T-T_o(o)]$

$+ [\Omega_1 T_o(o)/(T-T_o(o))]\}$

$b_{o\eta} = [B^*\Omega'/T_o(o)] + [B_1\Omega''/(T-T_o(o))] + [\Omega_1 T_o(o)\Omega''/(T-T_o(o)]$

$+ [\Omega_1\Omega/(T-T_o(o))]$,

and $c_{o\eta} = \Omega_1\Omega\,\Omega''/(T-T_o(o))$

APPENDIX III

Derivation of Vand's Equation

From Eq(1-12), we get

$$\eta = a_{o\eta} \exp(b_{o\eta} m + c_{o\eta} m^2) \qquad \text{(III-1)}$$

At low concentrations, $c_{o\eta} m^2$ term may be neglected and Eq(III-1) reduces to

$$\eta = a_{o\eta} \exp(b_{o\eta} m) \qquad \text{(III-2)}$$

m is related to c(molar concentration) through the expression

$$m = 1000c/(1000\rho - cM) \qquad \text{(III-3)}$$

where M is the molecular weight of the solute and ρ the density of the solution. From our study we know that ρ varies linearly with c. Therefore, Eq(III-3) may be written as

$$m = c/(a' - b'c) \qquad \text{(III-4)}$$

where a' and b' are constant terms. Substituting this result in Eq(III-2), we obtain

$$\eta = a_{o\eta} \exp\left[b_{o\eta} c/(a' - b'c)\right] \qquad \text{(III-5)}$$

It may be seen that Eq(III-5) is similar to the Vand's equation.

APPENDIX IV

Relation between Eq(1-12) and the Angell-Bressel equation

The relation between m and the mole percent, x may be written as

$$m = 55.51x/(100-x) \qquad \text{(IV-1)}$$

Substituting this in the reduced form of Eq(1-12), i.e., Eq(1-12) without the $c_{o\eta} m^2$ term, we get

$$\eta = a_{o\eta} \exp\left[55.51\, b_{o\eta} x/(100-x)\right] \qquad \text{(IV-2)}$$

This equation may also be written as

$$\eta = a^* \exp\left[(b^* + b_1 x)/(100-x)\right] \qquad \text{(IV-3)}$$

where a^*, b^*, and b_1 are constant parameters. Angell and Bressels' equation is of the form

$$\eta = A' \exp\left[DT_o/(x_o-x)\right] \qquad \text{(IV-4)}$$

where A' and D are constant parameters. x_o is the concentration at which the reference temperature, T becomes the glass transition temperature of the system. Eq(IV-4) after substituting for the linear variation of T_o with x may be written as

$$\eta = A' \exp\left[(D_1+D_2x)/(x_o-x)\right] \qquad \text{(IV-5)}$$

where D_1 and D_2 are again constant terms. It may now be seen that Eq(IV-3) obtained from our isothermal equation, Eq(1-12), is similar to Eq(IV-5) derived from Angell and Bressels' equation at the reference temperature equal to the glass-transition temperature of the pure solute.

APPENDIX V

Derivation of Suryanarayana and Venkatesans' Equation from Eq(1-12)

Reduced form of Eq(1-12) may be written in terms of the mole fraction, x as

$$\eta = a_{o\eta} \exp \left[55.51\ b_{o\eta} x/(1-x) \right] \qquad (V-1)$$

At the saturation point if x_s is the concentration in mole fraction, we get

$$\eta_s = a_{o\eta} \exp \left[55.51\ b_{o\eta} x_s/(1-x_s) \right] \qquad (V-2)$$

The ratio η / η_s may now be written as

$$\eta/\eta_s = \exp \left\{ \left[55.51\ b_{o\eta} x/(1-x) \right] - \left[55.51\ b_{o\eta} x_s/(1-x_s) \right] \right\} \qquad (V-3)$$

For a particular electrolytic solution x_s is constant and therefore

$$\eta/\eta_s \equiv \eta_p = A' \exp \left[55.51\ b_{o\eta} x/(1-x) \right] \qquad (V-4)$$

where $A' = \exp \left[-55.51\ b_{o\eta} x_s/(1-x_s) \right]$

Approximating $1/(1-x)$ to $(1+x)$, Eq(V-4) may be written as

$$\eta_p = A' \exp \left[55.51\ b_{o\eta} x(1+x) \right] \qquad (V-5)$$

Neglecting the x^2 term in Eq(V-5), we obtain

$$\eta_p = A' \exp \left(B' x_p \right) \qquad (V-6)$$

where $B' = 55.51\ b_{o\eta} x_s$ and $x_p = x/x_s$

It may be recognized that Eq(V-6) is identical with the empirical equation of Suryanarayana and Venkatesan.

APPENDIX VI

Calculation of m_{max} from Eq(2-5)

The relation between the equivalent conductance, Λ and the specific conductance, κ is given by

$$\Lambda = 1000\ \kappa/c \qquad \text{(VI-1)}$$

where c is the molar concentration. Substitution of the relation between c and m (molal concentration) from Eq(III-4) into Eq(VI-1) gives for κ an expression of the form

$$\kappa = \Lambda a' m/1000(1+b'm) \qquad \text{(VI-2)}$$

where a' and b' are constant parameters (cf. Appendix III). Substituting the expression for Λ from Eq(2-5), we get

$$\kappa = a_{o\Lambda}\, a'm\, \exp\,(b_{o\Lambda}m+c_{o\Lambda}m^2)/1000(1+b'm) \qquad \text{(VI-3)}$$

By equating the first derivative of κ with respect to m to zero, we obtain

$$2c_{o\Lambda}\, b'm^3 + (b_{o\Lambda}b'+2c_{o\Lambda})m^2+b_{o\Lambda}m+1 = 0 \qquad \text{(VI-4)}$$

Eq(VI-4) may be easily solved to compute the m_{max} values for the different electrolytic solutions.

APPENDIX VII

Wishaw-Stokes Equation - An approximate form

The Wishaw-Stokes equation is written as

$$\Lambda = (\eta_o/\eta)\left[\Lambda_o - \beta c^{1/2}/(1+B' c^{1/2})\right]\left[1-\alpha c^{1/2}\ (\exp(B'' c^{1/2})-1)/\right.$$
$$\left.(B'' c^{1/2}(1+B' c^{1/2}))\right] \qquad \text{(VII-1)}$$

where $\alpha = 8.204 \times 10^5/(\epsilon_o T)^{3/2}$, $\beta = 82.5/\eta_o(\epsilon_o T)^{1/2}$,

$B' = 50.29\ a^o/(\epsilon_o T)^{1/2}$, and $B'' = 0.2929 \times 50.29\ a^o/(\epsilon_o T)^{1/2}$.

ϵ_o is the dielectric constant of the solvent, η_o the viscosity of the solvent, T the absolute temperature, c the molar concentration, and a^o the ion-size parameter.

Eq(VII-1) may be approximated, by putting $\exp(B'' c^{1/2}) \approx 1+B'' c^{1/2}$, to

$$\Lambda = (\eta_o/\eta)\left[\Lambda_o - \beta c^{1/2}/(1+B' c^{1/2})\right]\left[1-\alpha c^{1/2}/(1+B' c^{1/2})\right] \qquad \text{(VII-2)}$$

By approximating $1/(1+B' c^{1/2})$ to $1-B' c^{1/2}$, Eq(VII-2) takes the form

$$\Lambda = (\eta_o/\eta)\ (\Lambda_o - \beta c^{1/2} + \beta B' c)\ (1-\alpha c^{1/2} + \alpha B' c) \qquad \text{(VII-3)}$$

Eq(VII-3) may be rearranged as

$$\Lambda\eta = Q_1 - Q_2\ c^{1/2} + Q_3 c - Q_4 c^{3/2} + Q_5 c^2 \qquad \text{(VII-4)}$$

where $Q_1 = \Lambda_o \eta_o$, $Q_2 = \eta_o(\Lambda\alpha + \beta)$,

$Q_3 = \eta_o(\Lambda_o\alpha B' + \alpha\beta + \beta B')$, $Q_4 = 2\eta_o\alpha\beta B'$, and

$Q_5 = \eta_o\alpha\beta(B')^2$

It may be noticed that Q_3 is related to a^o.

Approximate form of Eq(3-4) for $\Lambda\eta$

By neglecting the $c_{o\Lambda}$ and $c_{o\eta}$ terms in Eq(3-4), we obtain

$$\Lambda\eta = \left[a_{o\eta}\exp(b_{o\eta}m) + Am^{1/2}\right]\left[a_{o\Lambda}\exp(b_{o\Lambda}m) - S_o m^{1/2}\right] \qquad \text{(VII-5)}$$

Eq(VII-5) may be approximated, by putting $\exp(b_{o\eta}m) \approx 1 + b_{o\eta}m$ and $\exp(b_{o\Lambda}m) \approx 1 + b_{o\Lambda}m$, to

$$\Lambda\eta = (a_{o\eta} + a_{o\eta}b_{o\eta}m + Am^{1/2})(a_{o\Lambda} + a_{o\Lambda}b_{o\Lambda}m - S_o m^{1/2}) \qquad \text{(VII-6)}$$

Eq(VII-6) rearranges to the form

$$\Lambda\eta = Q_1^* + Q_2^* m^{1/2} + Q_3^* m + Q_4^* m^{3/2} + Q_5^* m^2 \qquad \text{(VII-7)}$$

where $Q_1^* = a_{o\eta}a_{o\Lambda}$, $Q_2^* = Aa_{o\Lambda} - S_o a_{o\eta}$, $Q_3^* = a_{o\eta}a_{o\Lambda}(b_{o\eta} + b_{o\Lambda}) - AS_o$, $Q_4^* = A\,a_{o\Lambda}b_{o\Lambda} - S_o\,a_{o\eta}b_{o\eta}$, and

$Q_5^* = a_{o\eta}\,b_{o\eta}\,a_{o\Lambda}\,b_{o\Lambda}$

By equating the coefficient of c in Eq(VII-4) to the coefficient of m in Eq(VII-7), which is actually true at low concentrations, we obtain a relation

$$\eta_o(\Lambda_o \alpha B' + \alpha\beta + \beta B') = a_{o\eta} a_{o\Lambda}(b_{o\eta} + b_{o\Lambda}) - A S_o \qquad \text{(VII-8)}$$

Therefore, a^o may be computed from the expression

$$a^o = [(\epsilon_o T)^{1/2}/50.29]\left[(a_{o\eta}\, a_{o\Lambda}\, (b_{o\eta}+b_{o\Lambda}) - A S_o - \alpha\beta\eta_o)/ (\Lambda_o\eta_o\alpha + \eta_o\beta) \right] \qquad \text{(VII-9)}$$

S U M M A R Y

In Chapter I density and viscosity measurements of six aqueous solutions, viz., $Ca(NO_3)_2$-H_2O, $Mg(NO_3)_2$-H_2O, $MgCl_2$-H_2O, $NiCl_2$-H_2O, $Na_2S_2O_3$-H_2O, and $NaNO_3$-H_2O were made as functions of temperature and concentration. The concentration was varied from low value upto nearly the concentration of saturation (saturation point) of each solute in water at room temperature ($\sim$20°C). Density has been found to be linear functions of temperature and molar concentration, but varies non-linearly with molal concentration. The non-Arrhenius temperature dependence of viscosity has been analyzed in terms of the three-parameter Vogel-Tammann-Fulcher (VTF) equation. In each electrolytic solution the ideal glass transition temperature, one of the parameters of the VTF equation, has been found to vary linearly with the molal concentration. Such a variation of T_o with concentration has been attributed to the ion-solvent interactions (hydration) taking place within the electrolytic solution. Quantitative expressions have been obtained to account for the concentration dependences of the other two parameters of the VTF equation by introducing the empirical temperature dependence of heat capacity in the Adam-Gibbs equation for transport property. A three-parameter

isothermal equation has been derived from the VTF equation by substituting in it the concentration dependences of its three parameters. This isothermal equation has been found to be successful in explaining the concentration dependence of viscosity of electrolytic solutions in the entire experimental range of concentration. Other expressions used in the literature for describing the concentration dependence of viscosity have been shown to be the special cases of the newly derived isothermal equation. In each electrolytic solution studied a structural transition appears to take place at some critical concentration the value of which depends upon the system considered.

In Chapter II the conductances of the above six electrolytic solutions were measured as functions of temperature and concentration. The experimental range of concentration was the same as in the case of viscosity study. The temperature dependence of equivalent conductance has been described by the VTF equation. A three-parameter isothermal equation similar to that used in the case of viscosity describes the concentration dependence of equivalent conductance in the experimental range of concentration. Specific conductance isotherms of all the solutions studied pass

through maxima. The value of the concentration (m_{max}) at which the conductivity of an electrolytic solution becomes maximum has been found to be obtainable from the three-parameter isothermal equation also. An attempt has been made to correlate the m_{max} value of an electrolytic solution with the hydration number of its solute. The activation energies for conductance and viscous flows were calculated. Both the activation energy isotherms appear to pass through broad minima. The Walden product isotherm of each solution has also been found to pass through a minimum. A three-parameter isothermal equation has been obtained for describing the concentration dependence of the Walden product and this equation satisfactorily accounts for the minima observed in the Walden product isotherms. However, at low concentrations deviation from this isothermal equation has been observed. The necessity of taking into account the ion-ion interactions also, especially at low concentrations, has been highlighted. The conductance study also envisaged the occurrence of a structural transition at some concentration in the case of each electrolytic solution. This transition appears to take place over a concentration range instead of occuring at a definite concentration. The transition has

been speculated to be a change-over from a primitive structure to a quasi-crystalline structure.

The analyses of the concentration dependences of viscosity and conductances of the six electrolytic solutions under consideration were improved in Chapter III by incorporating in the above mentioned three-parameter isothermal equations the contributions to transport property from ion-ion interactions also. The measurements of density, viscosity, and conductance of the six solutions were extended to still lower concentrations. The modified isothermal equations have been found to be applicable in the concentration range from the extended low value upto the saturation point. From the improved isothermal equation for conductance the equivalent conductance of each solution at infinite dilution has been estimated fairly accurately. An improved isothermal equation has also been obtained for describing the variations in the Walden product with concentration which has been found to reproduce satisfactorily the values of the Walden product of all the solutions under consideration at low as well as high concentrations. An attempt has been made to correlate this isothermal equation for the Walden product with the Wishaw-Stokes equation. Such a correlation enabled us to estimate the ion-size parameter for the different aqueous

systems. In the case of $NaNO_3$ solution the calculated value of the ion-size parameter was found to be comparable with the reported value whereas in the rest of the solutions meaningful values were obtained for this parameter.

In Chapter IV it has been shown that in molten salt systems also the VTF equation may be derived by introducing in the Adam-Gibbs equation the empirical nature of the temperature dependence of heat capacity of molten salts. Such a derivation of the VTF equation provided an expression for describing the concentration dependence of its preexponential parameter in molten salt systems. The validity of this equation has been justified by using it successfully to explain the concentration dependences of the reported pre-exponential parameters for several binary molten mixtures containing hydrated salts. This expression, however, failed to explain the concentration dependence of the preexponential parameter reported for the molten mixture of calcium nitrate tetrahydrate and potassium thiocyanate. In order to find a plausible explanation for such an unexpected behaviour of this molten mixture, its density measurement was made as functions of temperature and composition. The analysis of the density data revealed that in this particular molten mixture the intrinsic volume is the key parameter and controls the

properties of the melt. This observation also provided an explanation for the unusual behaviour of the preexponential parameter of the VTF equation in calcium nitrate tetrahydrate and potassium thiocyanate melt. A two-parameter isothermal equation has been obtained for describing the concentration dependence of transport properties of binary melts. The applicability of this equation has been verified using the reported fluidity and conductance data for several melts containing hydrated salts.

In the last chapter of the thesis, Chapter V, density, viscosity, and conductivity of molten $0.3\,[xKSCN-(1-x)NaSCN]-0.7\,Ca(NO_3)_2 \cdot 4.06\,H_2O$ system were measured as functions of temperature and composition with a view to examine the presence of mixed-alkali effect. The temperature dependence of fluidity and conductivity has been described in terms of the VTF equation. Mixed-alkali effect has been observed for fluidity and conductivity at relatively higher temperatures. A three-parameter isothermal equation similar to that employed in aqueous solutions has been successfully used for the first time to represent the concentration dependence of fluidity and conductivity of ternary systems exhibiting the mixed-alkali effect. The mixed-alkali

effect for conductivity has also been found to exist at isofluidity condition. The time-scale for detecting the mixed-alkali effect appears to depend upon the system under interest unlike the universal time-scale criterion suggested by others. A probable mechanistic interpretation has been given to the observed mixed-alkali effect. This interpretation is based on the view that the paired-cations form the mobile species and the concentration of such species appears to govern the conductivity of the ternary system studied.